IMPACT OF FREE WATER SURFACE ON SINGLE SLOPE SOLAR STILL YIELD

A Thesis Submitted
in Partial Fulfillment of the Requirements for the
Degree of

DOCTOR OF PHILOSOPHY

in

Mechanical Engineering

by

MANEESH KUMAR SHIVHARE

(Roll No-2K18/PHD/ME/37)

Under the Supervision of

Dr. Anil Kumar
Professor
Deptt. of Mechanical Engg.
DTU Delhi

Dr. Samsher
Professor
Deptt. of Mechanical Engg.
DTU Delhi

Department of Mechanical Engineering

DELHI TECHNOLOGICAL UNIVERSITY

(Formerly Delhi College of Engineering)
Shahbad, Daulatpur, Bawana Road, Delhi-110 042, India

March, 2026

DELHI TECHNOLOGICAL UNIVERSITY

(Formerly Delhi College of Engineering)
Shahbad Daulatpur, Main Bawana Road, Delhi-42

ACKNOWLEDGEMENT

I would like to express my heartiest gratitude to my research supervisors, mentors, and guides **Prof. Anil Kumar** and **Prof. Samsher**, for their supervision, advice, and continuous guidance from the conception of this research as well as for imparting extraordinary experiences throughout the work. Their advice on both research and my career has been priceless. They had been tremendous mentors for me. It is my privilege to be under their tutelage. Perseverance, exuberance, and positive approaches are just some of the traits they have imprinted on my personality. I thankfully acknowledge him for their vital contribution, which made them the backbone of this research and this *Thesis*. These lines are dedicated to my Guide:

"गुरुर्ब्रह्मागुरुर्विष्णुर्गुरुर्देवोमहेश्वरः
गुरुः साक्षातपरब्रह्मातस्मैश्रीगुरवेनमः"

I would like to express my gratitude to **Prof. Prateek Sharma**, Honorable Vice Chancellor, Delhi Technological University, Delhi, for providing me with the opportunity to carry out this work at this prestigious institute.

I would like to express my gratitude to **Prof. B.B. Arora**, Head of the Department and **Prof. Akhilesh Arora**, DRC Chairperson and Ex-DRC Chairperson **Prof. Atul Kumar Agrawal** of Mechanical Engineering Department, for their kind support in accomplishing this work.

I express my special thanks to **Dr. Ravi Kant, Vineet Vashishtha, Gourav Dhingra, Ashad Ahmad and Avinash Yadav,** research scholars at Delhi Technological University, Delhi, for helping me in difficult times.

My words fail to express my appreciation to my respected parents, Mr. Shivhari Lal Shivhare and Mrs. Mamta, whose blessings have helped me achieve my goal. My wife, **Ms. Jyoti, daughter Shivi, and son Krishna deserve thanks for their unwavering** support.

Finally, I would like to express my gratitude to the Almighty for granting me the patience and strength to reach this blissful moment in life.

MANEESH KUMAR SHIVHARE

DELHI TECHNOLOGICAL UNIVERSITY

(Formerly Delhi College of Engineering)
Shahbad Daulatpur, Main Bawana Road, Delhi-42

CANDIDATE'S DECLARATION

I **MANEESH KUMAR SHIVHARE**, hereby certify that the work which is being presented in the thesis entitled **Impact of Free Water Surface on Single Slope Solar Still Yield** in partial fulfillment of the requirements for the award of the Degree of Doctor of Philosophy, submitted in the **Department of Mechanical Engineering**, Delhi Technological University is an authentic record of my own work carried out during the period from **July 2018 to July 2026** under the supervision of **Prof. Anil Kumar and Prof. Samsher**.

The matter presented in the thesis has not been submitted by me for the award of any other degree of this or any other Institute.

Candidate's Signature

DELHI TECHNOLOGICAL UNIVERSITY

(Formerly Delhi College of Engineering)
Shahbad Daulatpur, Main Bawana Road, Delhi-42

CERTIFICATE BY THE SUPERVISOR(s)

Certified that **Maneesh Kumar Shivhare (**2K18/PHDME/037) has carried out their search work presented in this thesis entitled **"Impact of Free Water Surface on Single Slope Solar Still Yield"** for the award of **Doctor of Philosophy** from Department of Mechanical Engineering, Delhi Technological University, Delhi, under our supervision. The thesis embodies results of original work, and studies are carried out by the student himself and the contents of the thesis do not form the basis for the award of any other degree to the candidate or to anybody else from this or any other University/Institution.

Signature
Dr. Anil Kumar
Professor
Deptt. of Mech. Engg.
DTU, Delhi

Signature
Dr. Samsher
Professor
Deptt. of Mech. Engg.
DTU, Delhi

DELHI TECHNOLOGICAL UNIVERSITY
(Formerly Delhi College of Engineering)
Shahbad Daulatpur, Main Bawana Road, Delhi-42

ABSTRACT

Freshwater scarcity has emerged as a critical global challenge, particularly in arid and semi-arid regions where access to conventional water purification technologies is limited by energy availability and cost. Solar distillation offers a sustainable solution; however, the low productivity and efficiency of conventional passive solar stills restrict their large-scale applicability. In this context, the present research investigates the performance enhancement of a basin-type passive solar still by integrating a hanging absorber to improve the utilization of the wet surface area and overall system effectiveness.

The study experimentally and theoretically examines a Simple Passive Solar Still (SPSS) and a Modified Passive Solar Still (MPSS) equipped with a hanging absorber. A comprehensive mathematical model is developed to predict thermal behavior, freshwater yield, and system performance under varying ambient conditions. Additionally, an advanced configuration incorporating a helically coiled copper heat exchanger covered with wet cloth is analyzed to enhance heat and mass transfer. Performance assessment is supported by detailed analyses of energy, exergy, exergoeconomic, energoeconomic, and enviroeconomic aspects, along with a life cycle cost analysis for both configurations.

Unlike conventional exergoeconomic approaches that quantify exergy destruction per unit cost—primarily suited for mechanical and thermal systems—the present study introduces a novel exergoeconomic framework based on exergy gain per unit cost, recognizing that solar energy is freely available. This approach provides a more realistic evaluation of solar desalination systems. Results indicate that the MPSS consistently outperforms the SPSS across all performance metrics. MPSS achieves maximum energy and exergy efficiencies of 23.84% and 2.98%, respectively, demonstrating significant thermodynamic improvement over the conventional design.

From an economic and environmental perspective, the MPSS exhibits superior feasibility and sustainability. Cost per liter (CPL) of distilled water is substantially

reduced, and higher CO_2 mitigation and carbon credit potential are achieved. Modified system not only enhances freshwater productivity but also strengthens the environmental benefits of renewable energy-based desalination.

Comparative evaluation of the Simple Passive Solar Still (SPSS) and the Modified Passive Solar Still (MPSS) reveals that the proposed modification significantly enhances freshwater productivity, thermodynamic efficiency, economic feasibility, and environmental sustainability. MPSS achieves an estimated annual freshwater yield of 1174 L, compared to 832 L for the SPSS, representing a 41.10% improvement. Meanwhile, the energy efficiency increases from 9.03% to 14.18%, reflecting a 57.03% enhancement. Economic analysis indicates a substantial reduction in the cost per liter of distilled water from US$0.020 (₹1.72) to US$0.014 (₹1.42) as per exchange rate on 15 July 2025, thereby improving affordability for rural and economically weaker communities. Improved energoeconomic and exergoeconomic indicators further confirm superior energy and exergy utilization relative to cost in the modified system. From an environmental perspective, the MPSS demonstrates a higher annual CO_2 mitigation potential of 19.03 tonnes compared to 12.54 tonnes for the SPSS, resulting in increased carbon credit benefits and reinforcing the role of solar desalination in mitigating climate change.

Beyond technical performance, this research's outcomes offer direct societal benefits by providing an affordable, decentralized, and energy-independent freshwater production system suitable for remote, coastal, and water-scarce regions. Reliance on renewable solar energy eliminates dependency on fossil fuels and grid electricity, thereby promoting energy equity and resilience. The developed system contributes significantly to the United Nations Sustainable Development Goals, particularly SDG-6 (Clean Water and Sanitation) by ensuring access to safe drinking water, SDG-7 (Affordable and Clean Energy) through the utilization of solar energy, SDG-12 (Responsible Consumption and Production) by improving resource efficiency, and SDG-13 (Climate Action) through substantial reductions in greenhouse gas emissions. Hence, the proposed MPSS represents a sustainable technological solution addressing the interlinked challenges of water scarcity, energy demand, and environmental protection.

DELHI TECHNOLOGICAL UNIVERSITY
(Formerly Delhi College of Engineering)
Shahbad Daulatpur, Main Bawana Road, Delhi-42

List of Publications

Indian Patent

1. Shivhare, Maneesh Kumar, Samsher, and Anil Kumar. "Solar Still Apparatus" Indian Patent Application No. 202411056840, Published by the Indian Patent Office, Government of India, 2024.

International Journal

1. Maneesh Kumar Shivhare, Anil Kumar, and Samsher, Productivity and sustainability enhancement in solar still using wick and copper cooling coil, Environmental Progress & Sustainable Energy 2026; 45: e70160, **SCI-E,** Impact factor 2.3, DOI:10.1002/ep.70160
2. Maneesh Kumar Shivhare, Samsher, and Anil Kumar, Impact of various design parameters on solar still systems performance: a review, AQUA—Water Infrastructure, Ecosystems and Society 73, no. 2 (2024): 239-265, **SCI-E,** Impact factor 2.3, https://doi.org/10.2166/aqua.2024.290
3. Maneesh Kumar Shivhare, Anil Kumar and Samsher, Performance Assessment of Single-Slope Solar Still Integrated with Hanging Cotton Wick, Thermal Science: International Scientific Journal. **SCI-E** Impact Factor 1.45. https://doi.org/10.2298/TSCI251113033S

International Conference

1. Shivhare, Maneesh Kumar, Samsher, and Anil Kumar. "Enhanced Single Slope Solar Still Using Novel Technology than Nanoparticles with More Economical and Efficient." In *Biennial International Conference on Future Learning Aspects of Mechanical Engineering*, pp. 115-124. Singapore: Springer Nature Singapore, 2024.
2. Shivhare, Maneesh Kumar, Samsher, and Anil Kumar. "Performance of Solar Still with Effects of Psychometric Terms for Developed Moist Air." In International Conference on Mechanical and Energy Technologies, pp. 41-49. Singapore: Springer Nature Singapore, 2023.

Table of Contents

			Page No.
ACKNOWLEDGEMENT			ii
Candidate's Declaration			iii
Certificate by the Supervisor(s)			iv
Abstract			v
List of Publications			vii
List of Contents			viii
List of Tables			xv
List of Figures			xvi
Nomenclature			xviii
CHAPTER 1		**INTRODUCTION**	**1-17**
1.1		General Introduction	1
1.2		What is Solar distillation	5
	1.2.1	Solar distillation	7
1.3		Materials in fabrication of SPSS and MPSS	8
1.4		Modes of heat transfer in solar still	9
	1.4.1	Solar radiation heat transfer	10
	1.4.2	Convective heat transfer	10
	1.4.3	Conductive heat transfer	11
	1.4.4	Interaction of heat transfer mechanism	11
1.5		Basic concept of solar distillation	12
	1.5.1	Advantages of passive solar distillation unit	13
	1.5.2	Limitations of solar distillation system	14
1.6		Quality of distilled water	15
1.7		Parameters influencing the performance of solar distillation system	15
1.8		Applications of Solar distilled water	16

CHAPTER 2		**LITERATURE REVIEW**	**18-43**
2.1		Historical background	18
2.2		Observation of enhanced parameters for conventional solar still	18
	2.2.1	Single and double slope collector solar still	18
	2.2.2	Pyramid collector solar still (PCSS)	20
	2.2.3	Black painted inside wall solar still	21
	2.2.4	Spherical Solar Still	21
	2.2.5	Hemi- spherical solar still (HSSS)	22
	2.2.6	'V' type solar still (VTSS)	22
	2.2.7	Painted inside surface with mixed TiO_2	24
	2.2.8	Thermal conductivity of glass cover	24
	2.2.9	Depth of water in single slope solar still	24
	2.2.10	Single solar still with porous structures	25
2.3		Performance evaluation of an integrated solar still system: Exploring design parameters	26
	2.3.1	Solar still with fins for condensation	26
	2.3.2	Solar still with fan for condensation	27
	2.3.3	Solar still with several types of wicks	28
	2.3.4	Multi basin solar still (MBSS)	29
	2.3.5	Tubular solar still (TSS)	30
	2.3.6	Multi-wick solar still (MWSS)	31
	2.3.7	Contactless solar steam generation and solar still	32
	2.3.8	Diffusion solar still (DSS)	33
	2.3.9	Weir-type solar still (WTSS)	35
	2.3.10	Stepped-type inclined solar still	36
2.4		Research Gap	38
2.5		Research Objectives	40
2.6		Methodology to be adopted	40
2.7		Thesis Plan	41
CHAPTER 3		**METHODOLOGY**	**45-83**
3.1		Experimental setup	45

	3.1.1	Simple passive solar still (SPSS)	45
	3.1.2	Modified passive solar still	46
	3.1.3	Comparative features of SPSS and MPSS	50
	3.1.4	Summary of experimental setup	51
3.2		Fabrication of experimental setup	51
	3.2.1	Fabrication of simple passive solar still	52
	3.2.2	Fabrication of modified passive solar still	53
	3.2.3	Summary of fabrication differences	55
	3.2.4	Timeline of Fabrication	56
3.3		Instrumentation for experimental setup	57
	3.3.1	Temperature measurement system	57
	3.3.2	Solar radiation measurement	58
	3.3.3	Humidity and moist air measurement	59
	3.3.4	Wind velocity measurement	59
	3.3.5	Distillate output measurement	59
3.4		Experimental Procedure	61
	3.4.1	Pre experiment preparation	61
	3.4.2	Operating procedure during experiments	62
	3.4.3	Measurement of distillate output	62
	3.4.4	End of the day procedure	63
3.5		Psychrometric modelling of SPSS and MPSS	63
	3.5.1	Fundamentals of psychrometric modelling	63
	3.5.2	Partial vapour pressure	64
	3.5.3	Humidity ratio	64
	3.5.4	Dew point temperature	64
	3.5.5	Psychrometric conditions for condensation	64
	3.5.6	Evaporation rate expression using psychrometric difference	65
	3.5.7	Airflow and moist air stratification	65
	3.5.8	Psychrometric behavior comparison between SPSS and MPSS	66
	3.5.9	Psychrometric impact on system productivity	66
	3.5.10	Graphical psychrometric interpretation	67

3.6		Uncertainty analysis	67
	3.6.1	Purpose of uncertainty analysis	67
	3.6.2	Instrumentation considered for uncertainty evaluation	68
3.7		Thermal Modelling	69
	3.7.1	Assumptions for the thermal model	69
	3.7.2	Energy balance of basin water in SPSS	70
	3.7.3	Heat transfer coefficient used in SPSS modelling	70
	3.7.4	Modification in MPSS thermal model	70
	3.7.5	Energy balance for MPSS	71
	3.7.6	Combined heat transfer in MPSS	71
	3.7.7	Evaporation rate modelling	72
	3.7.8	Condensation rate of generated vapor	72
	3.7.9	Thermal efficiency of stills	72
	3.7.10	Validation of thermal model	72
3.8		Exergy modelling of SPSS and MPSS	73
	3.8.1	Exergy of incident solar radiation	73
	3.8.2	Exergy input to solar stills	74
	3.8.3	Exergy output from the solar still (Distillate exergy)	74
	3.8.4	Exergy efficiency of still	74
	3.8.5	Exergy based productivity assessment	74
	3.8.6	Exergy flow	75
3.9		Economic analysis	76
	3.9.1	Objective of economic analysis for experiments	76
	3.9.2	Components of economic cost estimation	76
	3.9.3	Annualization of capital cost	77
	3.9.4	Annual distillate production	78
	3.9.5	Cost of water per liter (CWPL)	78
	3.9.6	Comparative interpretation of economic results	78
3.10		Exergoeconomic analysis	78
3.11		Envieonmental analysis	80
	3.11.1	CO_2 emissions	80
	3.11.2	CO_2 mitigation	80

3.12		Enviroeconomic analysis	81
3.13		Method of data comparison	81
	3.13.1	Objective of Data comparison	81
	3.13.2	Basis for comparative evaluation	82
	3.13.3	Parameters used for comparative analysis	82
	3.13.4	Step by step procedure for data comparison	83
CHAPTER 4		**RESULT AND DISCUSSION**	**85-113**
4.1		Discussion on experimental results	85
	4.1.1	Overview of experimental conditions	85
	4.1.2	Structure of result evaluation	86
	4.1.3	Comparative framework for SPSS and MPSS	87
4.2		Solar radiation and meteorogical parameters	88
	4.2.1	Hourly solar intensity profile	88
	4.2.2	Ambient temperature and relative humidity variations	89
	4.2.3	Wind speed and atmospheric influence on heat transfer	90
4.3		Thermal performance analysis	91
	4.3.1	Basin water temperature profile (SPSS vs. MPSS)	91
	4.3.2	Glass temperature profile (SPSS vs. MPSS)	93
	4.3.3	Wick surface temperature behavior	95
	4.3.4	Cooling coil temperature behavior	96
	4.3.5	Ambient temperature of still profile	98
4.4		Psychrometric behavior of moist air inside still	99
	4.4.1	Moist air temperature profile	100
	4.4.2	Variation of relative humidity and specific humidity	101
	4.4.3	Dew point temperature and condensation feasibility	103
	4.4.4	Key psychrometric findings	104
4.5		Energy analysis and comparison for SPSS and MPS	104
4.6		Exergy based assessment for SPSS and MPSS	107
4.7		Comparative economic performance evaluation for SPSS and MPS	109
4.8		Exergoeconomic based analysis for SPSS and MPSS	110
4.9		Environmental based assessment for SPSS and MPSS	111

4.10 Enviroeconomic parameters 112

CHAPTER 5 CONCLUSIONS AND FUTURE SCOPE 113-116

5.1 Conclusion 113

5.2 Future scope 115

REFERENCES 117-131

Appendices

Publications

Bio – Data

Plagiarism Report

DEDICATED TO MY LOVING PARENTS AND FAMILY, WHOSE CONSTANT SUPPORT STRENGTHENED ME IN COMPLETING THIS RESEARCH

LIST OF TABLES

S. No.	Title	Page No.
Table 2.1	Literature summary of design modification and performance outcomes in solar stills	37
Table 3.1	Impact of wick materials with their probable porosity, capillar and explicability	47
Table 3.2	Details of features of SPSS and MPSS	51
Table 3.3	Difference in fabrication of SPSS and MPSS	55
Table 3.4	Summary of instrument for SPSS and MPSS	60
Table 3.5	Comparison between psychrometric outcomes for SPSS and MPSS	66
Table 3.6	Details of instruments for uncertainty analysis	68
Table 3.7	Summary of modelling of exergy analysis	75
Table 3.8	Comparison between economic results of SPSS and MPSS	78
Table 4.1	Cost analysis of water per liter for SPSS and MPSS	109
Table 4.2	Exergo economic parameter for SPSS and MPSS	110
Table 4.3	Environmental parameters for SPSS and MPSS	111
Table 4.4	Enviroeconomic parameters for SPSS and MPSS based on energy and exergy perspective	112

LIST OF FIGURES

S. No.	Title	Page No.
Figure 1.1	Water availability on surface of earth	2
Figure 1.2	Need for fresh water in low income countries	4
Figure 1.3	Need of fresh water in high income countries	4
Figure 1.4	Overall need of fresh water in world	5
Figure 1.5	Cycle process of solar distillation	5
Figure 1.6	Classification of solar distillation Techniques	6
Figure 1.7	Classification of solar distillation system	8
Figure 1.8	Schematic diagram of SPSS and MPSS	13
Figure 2.1	Schematic diagram of double slope solar still (DSSS)	19
Figure 2.2	Pyramid collector solar still	20
Figure 2.3	Spherical solar still	21
Figure 2.4	Hemi-spherical solar still	22
Figure 2.5	Schematic diagram of VTSS	23
Figure 2.6	Efficiency and daily yield variation with ‘V’ top (VTSS) syster	23
Figure 2.7	The schematic of the modified solar still incorporating porous absorber	25
Figure 2.8	Solar still with fins	26
Figure 2.9	Experimental setup with fan for condensation	28
Figure 2.10	Wick type solar still with different thermal conductivity of cove	29
Figure 2.11	Schematic diagram of a multi-effect passive type solar still	30
Figure 2.12	Schematic diagram of tubular solar still	31
Figure 2.13	Schematic diagram of multi wick solar still	32
Figure 2.14	Diffusion solar still (DSS) with floating wick	34
Figure 2.15	Variation of efficiency and productivity with respect to time of diffusion solar still	34
Figure 2.16	Schematic diagram of weir type solar still	35
Figure 3.1	Actual Picture of experimental setup of SPSS and MPSS	45
Figure 3.2	Experimental picture to analyze capillary effect	48

Figure 3.3	Jute with several porosities	49
Figure 3.4	Photographs during fabrication of SPSS and MPSS	56
Figure 3.5	Picture of installed thermocouple	57
Figure 3.6	Picture view of digital solarimeter	58
Figure 3.7	Picture of digital thermo hygrometer	59
Figure 3.8	Picture of digital anemometer	60
Figure 4.1	Hourly solar radiation	88
Figure 4.2	Ambient temperature and relative humidity profile	89
Figure 4.3	Wind speed variation during the experimental	90
Figure 4.4	Basin water temperature w.r.t. solar radiation in SPSS and MPS	92
Figure 4.5	Temperature of inner surface of cover glass of SPSS and MPSS	95
Figure 4.6	Temperature profile of wick surface MPSS	95
Figure 4.7	Temperature profile of coil surface MPSS	97
Figure 4.8	Inside temperature of SPSS and MPSS	99
Figure 4.9	Variation of chamber temperature for SPSS	101
Figure 4.10	Hourly variation in relative humidity and specific humidity	102
Figure 4.11	Variation in glass temperatures, dew point temperature, RH	103
Figure 4.12	Cumulative and hourly yield for SPSS and MPSS	105
Figure 4.13	Comparative efficiency analysis of SPSS and MPSS	106
Figure 4.14	Comparative exergy and exergy efficiency of SPSS and MPSS systems	108

NOMENCLATURE

A_b	Basin region in (m^2)
A_c	Under glazing region of collector in m^2
A_{wick}	Surface area of wick in m^2
AP	Annual production
CRF	Capital recovery factor
C_p	Specific heat in (J/kgK)
E_{emb}	Embodied energy
E_x	Exergy in (J/s)
h	Coefficient of heat transfer in W/m^2 K
h_{fg}	Latent heat in J/kg
i	Interest rate
IC	Initial cost
I_g	Global Radiation, W/m^2
I_r	Incident Radiation, W/m^2
L	Latent heat of vaporization (J/kg)
$\dot{m}$	Mass flow rate (kg/s)
$\dot{m}_{evap}$	Evaporation rate in (kg/s)
$\dot{m}_w$	Mass flow of water in (kg/s)
MC	Maintenance cost
P_{atm}	Atmospheric pressure
P_g	Vapor Pressure at glass surface
P_{sat}	Saturation pressure
P_v	Vapor Pressure
P_w	Vapor Pressure at water surface
Q_{Conv}	Convective heat transfer rate from water to glass in (kWh)
Q_{evap}	Evaporative heat transfer rate in (kWh)
$Q_{rad,}$	Radiative heat transfer rate in (kWh)
R	Exergoeconomic parameter (kWh/US$)
T_a	Ambient temperature in (℃)

T_{coil} Wick surface temperature in (℃)

T_{csd} Average temperature for clear sky days in (℃)

T_{dp} Dew point temperature (^{o}C)

T_{hzd} Average temperature for hazy days in (℃)

T_{ig} Inner Glass temperature in (℃)

T_{ics} Inner chamber temperature for SPSS in (℃)

T_{icm} Inner chamber temperature for MPSS in (℃)

T_{og} Outer Glass temperature in (℃)

T_{ma} Moist air temperature in (℃)

T_{wick} Wick surface temperature in (℃)

T_{v} Vapor temperature in℃

T_{w} Temperature in basin water in℃

UAC Uniform annual cost

x_n Independent variable

Z Enviro-economic parameter

Greek Letter's

α_b Basin surface absorbed solar radiation

α_{wick} Absorptivity of wick

σ Steafan constant

ε Emissivity

τ_g Top glass cover transmitted solar radiation

$Ø_{ex}$ Exergo environmental paramter

η_{th} Thermal efficiency in (%)

ρ_g Reflectivity of glass

Subscripts

a Ambient air

b Basin area

csd Clear sky day

en Energy

ex Exergy

hzd Hazy day

i Rate of interest

n System life in years

o Outside glasss cover

th Thermal

U Uncertainty

v Vapour

w Water (fluid)

Abbreviation

AMC Maintenance cost annually

CRF Capital recovery factor

CFD Computational fluid dynamics

CV Collection vessel

DBT Dew point temperature

DS Double slope solar distiller unit

DSS Diffusion solar still

DSSS Solar distiller unit of double slope

FAC Fixed annual cost

FPC Collector flat plate

FRP Fiber reinforced plastic

GI Galvanized iron

HE Heat exchanger

HTC Factor of heat transfer coefficient

HSSS Hemi spherical solar still

MBSS Multi basin solar still

MPSS Modified passive solar still

MS Mild Steel

MWSS Multi wick solar still

NTP Normal temperature and pressure

PCM Phase change material

PCSS	Pyramid collector solar still
PVT	Photovoltaic thermal
RH	Relative humidity
SFF	Shrinking fund factor
SPSS	Simple passive solar still
SSS	Simple solar still
SV	Salvage value
TAC	Total annual cost
TSS	Tubular solar still
UAC	Uniform Annual Cost
VTSS	‘V’ type solar still
W	Specific humidity
WBT	Wet bulb temperature
WTSS	Weir type solar still

Chapter 1

INTRODUCTION

1.1 General Introduction

Water is the primary prerequisite for all living species on Earth. Due to rapid population growth and industrialization worldwide, water availability is a serious problem today. Approximately 3% of Earth's water is freshwater, and less than 1% of it is available for human consumption [1]. Solar distillation, implemented through solar stills, utilizes solar energy to produce potable water by mimicking a closed-loop hydrological cycle. As a sustainable, energy-efficient approach, it warrants greater governmental attention and support. The reliance on solar-based desalination technologies has been steadily growing due to rising freshwater scarcity, making solar distillation one of the most promising alternatives for addressing global water shortages.

Water is fundamental to all forms of life, plants, animals, and humans alike. For humans, access to safe drinking water is essential for maintaining cellular functions, and inadequate intake can lead to dehydration and severe health complications. Although the Earth holds an enormous volume of water, only a very small portion is suitable for direct human consumption. Approximately two-thirds of the planet's surface is covered by water; however, nearly 97% of this is contained in oceans and other saline bodies, with salinity levels ranging from 35,000 to 45,000 ppm, rendering it unsuitable for drinking. According to the World Health Organization (WHO), water with salinity above 1,000 ppm is unsafe for human consumption.

Only a small fraction, around 2%, exists in the form of glaciers and ice caps, and less than 1% constitutes accessible freshwater resources. Figure 1 illustrates the distribution of water across different natural reservoirs. As reported by the United Nations (UN), more than 2 billion people worldwide lack access to safe, reliable drinking water, underscoring the urgent need for sustainable desalination technologies [2].

It is estimated that by 2025, nearly two-thirds of the global population will experience shortages of safe drinking water, with many regions already relying on contaminated or unsuitable sources. Freshwater scarcity has become a major concern in

many parts of India due to rapid population growth, urbanization, industrialization, and climate change. According to various national reports, several states, including Rajasthan, Gujarat, Tamil Nadu, Andhra Pradesh, and parts of Uttar Pradesh, face severe groundwater depletion and salinity problems. While numerous water purification technologies are available, solar distillation remains one of the most sustainable options, offering a clean, low-cost, renewable, and uncomplicated method for generating potable water.

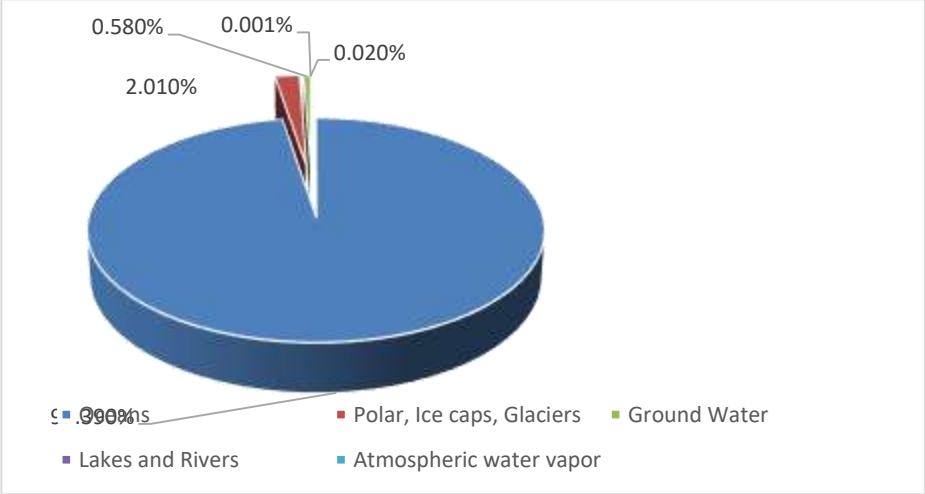

Figure 1.1 Water availability on surface of earth [2]

The rapid growth of the global population has intensified pressure on existing freshwater resources, necessitating a proportional increase in water availability. As urbanization and industrialization continue to expand, the demand for safe drinking water rises accordingly. Failure to meet this demand poses serious risks to human health and the surrounding environment.

According to a UNICEF report [2], one in every six individuals will lack access to safe drinking water and adequate sanitation facilities. Similarly, World Health Organization (WHO) data indicate that waterborne illnesses result in approximately 443 million school days lost worldwide each year (UNDP, 2006) [3]. In India, potable water scarcity remains a major challenge, particularly in rural and coastal regions. Studies suggest that 60–70% of rural populations in developing nations struggle to obtain clean drinking water. Reliance on contaminated water supplies further elevates the prevalence of water-related diseases, exacerbating public health concerns.

Following the Second World War, advancements in solar distillation technologies accelerated due to the growing demand for freshwater [4]. The World Water Vision Report [5] highlights that the global water crisis is not solely a consequence of limited water availability but is largely the result of inadequate water management practices. Consequently, both human populations and ecosystems are adversely affected. Proactive intervention is essential to prevent the situation from deteriorating further.

Raising public awareness about the finite nature of freshwater resources and the importance of conserving them, both in terms of quality and quantity, is critical. A key message delivered during the Second World Water Forum emphasized that "water is everyone's business." Issues related to water must be placed at the forefront of policy discussions because of their significant impact on public health, economic development, and social equity.

The recognition of water as a fundamental human right underscores that every individual is entitled to access sufficient, safe, acceptable, physically accessible, and affordable water for drinking and domestic use. Safeguarding water quality and ensuring adequate supply are vital for preventing dehydration and reducing the prevalence of water-related diseases.

At the same time, the remaining freshwater resources are steadily declining in both quantity and quality, primarily due to pollution from industrial discharges and various human activities. This growing challenge underscores the critical need for policymakers to develop and enforce robust water management policies and regulatory frameworks that protect water bodies and ensure sustainable, equitable access to clean water for current and future populations.

Nations differ significantly in the availability of freshwater resources, and the major sectors competing for these resources include domestic consumption, industrial operations, and agriculture. Figures 1.2 and 1.3 illustrate how water demand patterns vary according to a country's income level. Although distillation processes remove most micronutrients and naturally occurring minerals, reducing mineral content, the high degree of purification is generally advantageous, particularly in regions where source water contains hazardous contaminants. Effective removal of toxic inorganic compounds and

lowering overall pollutant concentrations are essential prior to water reuse or safe discharge into the environment.

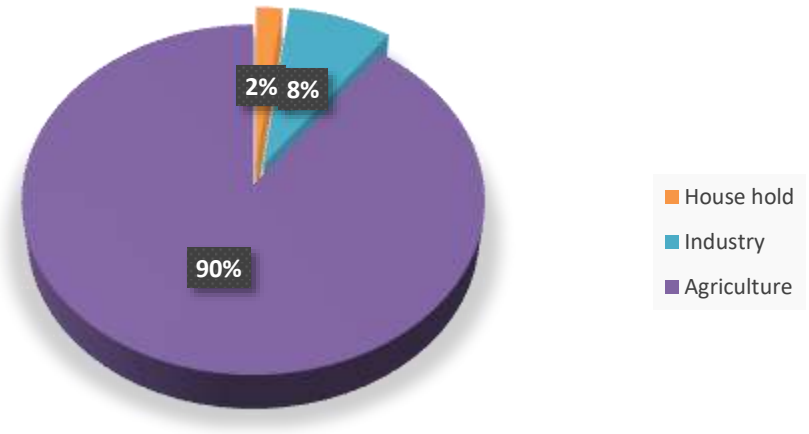

Figure 1.2 Need for fresh water in low-income countries [5]

One limitation of traditional distillation systems is their inability to fully separate volatile substances, such as chlorine and fluorine, which may evaporate along with water vapor and subsequently appear in the distilled output.

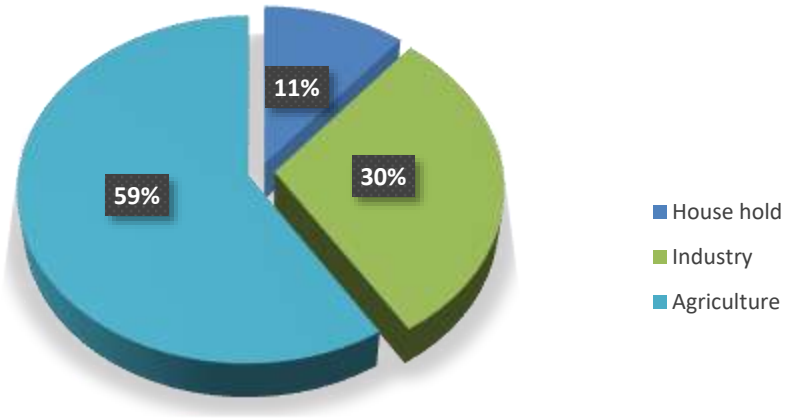

Figure 1.3 Need for fresh water in high income countries [5]

Solar distillation has gained prominence as a water purification method because its comparatively low operating temperatures help reduce certain volatilization-related challenges while still providing a simple, energy-efficient treatment option. This approach is especially advantageous in areas with brackish water sources, with moderate to low water demand, and in climatic conditions such as arid or semi-arid regions that receive

high solar radiation and typically receive less than 50 cm of annual rainfall. In such settings, where transporting treated water can be expensive, solar distillation is a practical, sustainable, and cost-effective solution for producing safe drinking water.

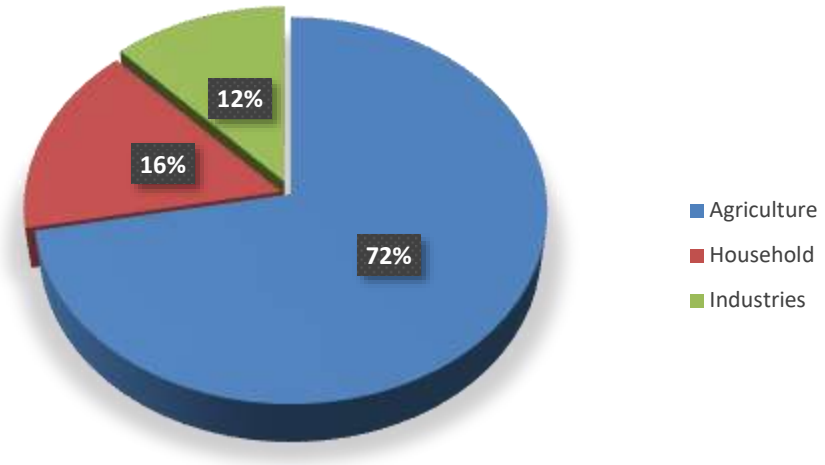

Figure 1.4 Overall need for fresh water in world [5]

1.2 What is solar distillation?

Solar distillation is an environmentally sustainable method for converting saline or brackish water into freshwater using solar energy as the primary heat source. By relying on the sun's thermal energy, this technique offers an eco-friendly, cost-effective approach to addressing global water scarcity.

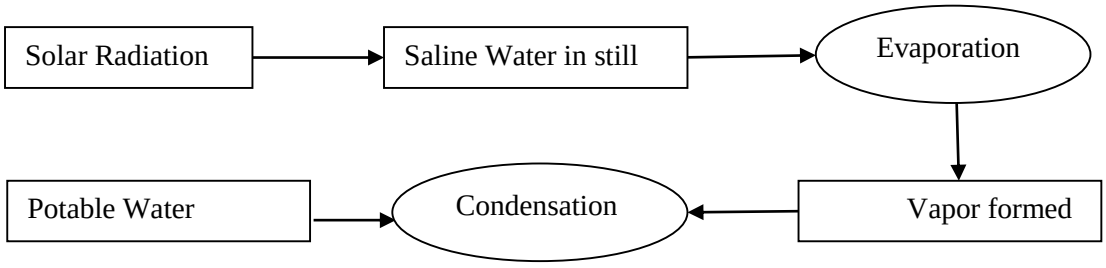

Figure 1.5 Cycle process of solar distillation

The process involves heating saline water until it evaporates, then condensing the vapor to produce purified, drinkable water. When solar radiation is absorbed by the water in the basin, evaporation occurs, and the resulting vapor subsequently condenses on a cooler surface to yield potable water, as illustrated in the cycle shown in Figure 1.5. Solar

desalination is particularly advantageous in regions with high solar intensity and limited access to natural freshwater supplies.

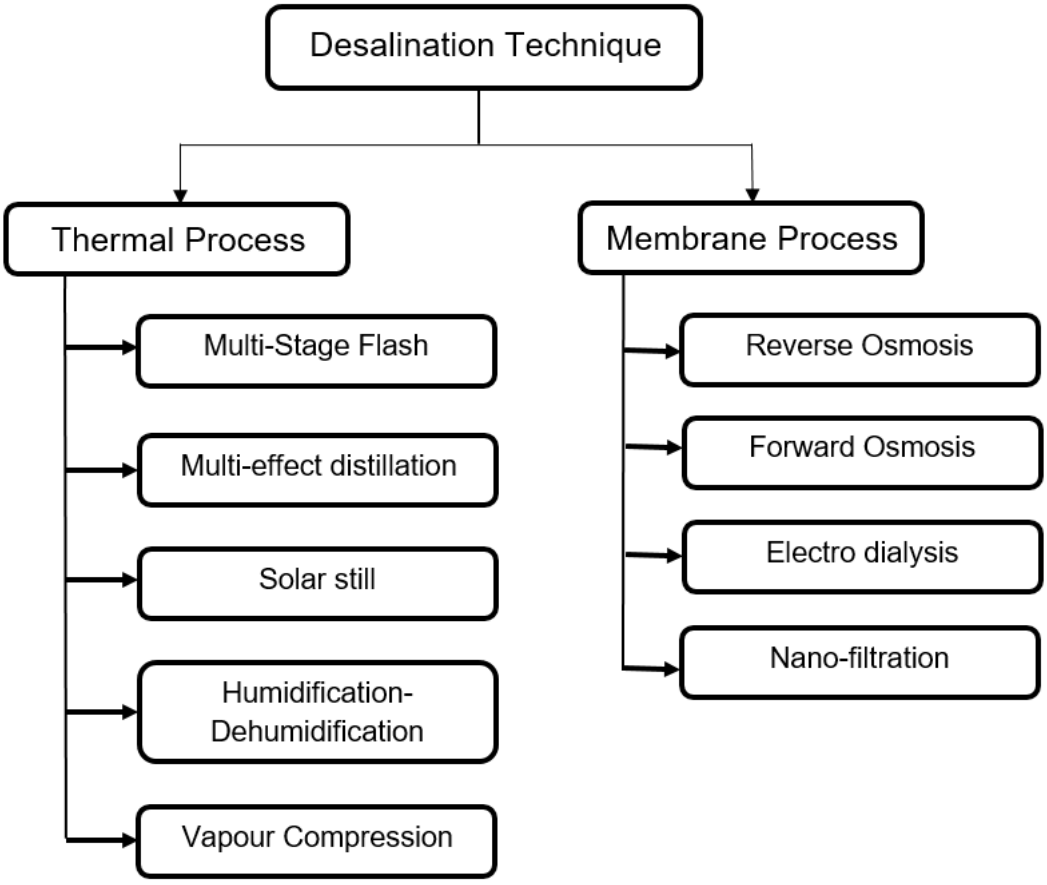

Figure 1.6 Classification of solar distillation techniques

A variety of desalination technologies are in operation today, including reverse osmosis, multi-stage flash distillation, and electro dialysis. Each technique offers specific benefits and is selected based on factors such as the quality of the feed water, the availability of energy sources, and the required scale of water production. The primary desalination options relevant to this study are schematically represented in Figure 1.6.

Among these methods, solar distillation stands out because it relies directly on abundant, renewable solar energy as its primary driving mechanism. The process essentially replicates the natural hydrological cycle: solar radiation supplies the energy needed to evaporate water, and the resulting vapor subsequently condenses to produce purified distillate, leaving behind dissolved salts and other non-volatile contaminants.

Because solar distillation operates without relying on traditional external energy inputs, it can substantially decrease operating costs while also minimizing greenhouse gas emissions and other environmental impacts typically associated with fossil-fuel-driven desalination technologies. Given that solar energy is abundant and renewable, this method provides a long-term, environmentally responsible solution for freshwater production. It is especially advantageous in remote, arid, and semi-arid regions where access to conventional power systems is limited and where saline or brackish water sources are commonly available.

1.2.1 Solar distillation

The distillation process driven by solar radiation is called solar distillation. It is a natural process powered by solar energy in a closed cycle. Further, solar distillation can be classified as;

(i) Passive solar distillation process (ii) Active solar distillation process

In passive solar distillation, brackish water is directly fed to the basin without external sources, whereas in active solar distillation, a secondary source is used to feed the water. This additional heat energy increases evaporation rates. Secondary sources of heat addition include collectors, concentrators, etc., which are further classified into single- and double-slope solar distiller units based on their structures and positions. To get the maximum amount of solar energy, the single slope should face south. Figure 1.7 represents complete classifications. Further, passive solar distillers can be divided into basin- and inclination-type stills. Basin-type solar still uses saline water in the basin and is enclosed by a translucent material. Basin type is widely classified further.

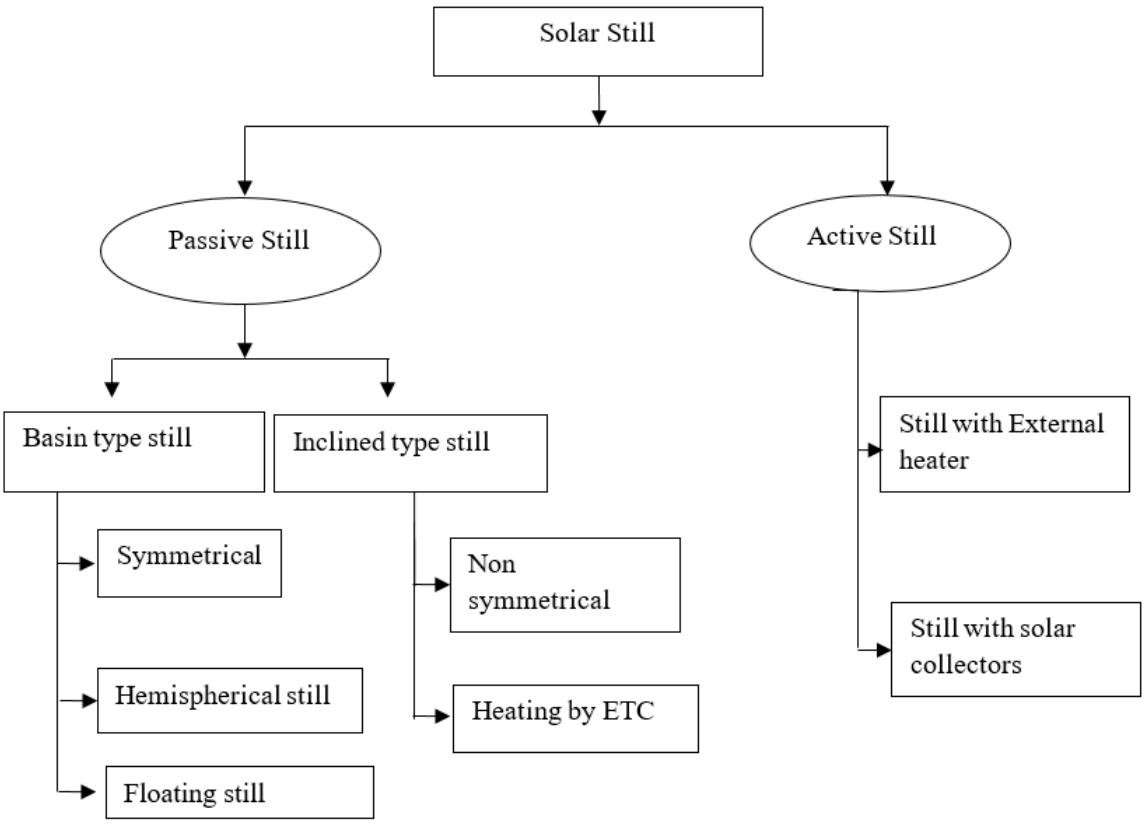

Figure 1.7 Classification of solar distillation system

1.3 Materials for fabrication of solar still

Building a solar still is generally simple and can be done with readily available materials. However, the overall performance and durability of the system improve when structurally robust and thermally stable components are used. In the present study, both the simple passive solar still (SPSS) and the modified passive solar still (MPSS) were fabricated using materials selected for their strength, corrosion resistance, and compatibility with saline water.

The basin and vertical walls of both stills were fabricated from 2 mm-thick galvanized iron (GI) sheets, as this material provides adequate mechanical rigidity to withstand outdoor conditions, including wind loads and minor vibrations. GI also offers good corrosion resistance when exposed to saline or brackish water, ensuring a longer

operational life. The internal and external geometry of the still was designed to be compact and lightweight, enabling easy transport and installation using locally available means.

To minimize heat losses, the basin's outer surfaces were insulated with 5–10 cm of polystyrene (thermocol), depending on the configuration, as reported in the shared research papers. This insulation reduces conductive heat loss to the surroundings and improves thermal retention inside the still.

The transparent cover glass, an essential component that serves as both an entry point for solar radiation and a condensation surface, was constructed from 5 mm-thick standard glass, inclined at 30° to the horizontal. This tilt angle was optimized to maximize solar radiation capture while allowing condensed water to flow smoothly toward the collection channel. Glass was selected due to its high transmissivity to solar radiation, non-reactive nature under heated vapor, and ability to support filmwise condensation, which is preferred over dropwise condensation because droplets reduce optical transmittance through scattering.

In the MPSS, black hanging wick material was added along the inner vertical walls to significantly increase the free wet surface area for evaporation. Wick materials were selected based on capillary performance and porosity tests, as documented in the experiments. These materials ensured uniform wetting through passive water absorption, offering a low-cost means of enhancing evaporation without external power input.

Both stills incorporated a GI collection channel placed at the lower end of the glass cover to guide condensed water into a clean collection vessel through a PVC conduit. The joints between the glass cover and basin frame were sealed with silicone rubber or gasket tape to prevent vapor leakage, maintain internal humidity, and improve productivity.

Overall, the fabricated systems combine durable metallic construction, effective thermal insulation, and optimized optical components to achieve enhanced evaporation–condensation performance while keeping it simple, cost-effective, and suitable for deployment in rural or remote regions.

1.4 Mode of Heat Transfer in Solar Still

Heat transfer plays a fundamental role in the performance of solar stills, as the rates of evaporation and condensation are directly governed by the manner in which

thermal energy is transported within the system. Understanding these mechanisms is essential for evaluating the productivity of conventional simple passive solar still (SPSS) and for designing improved configurations, such as the Modified Passive Solar Still (MPSS) developed in this study. The three principal modes of heat transfer—radiation, convection, and conduction—operate simultaneously within the still and collectively determine its thermal response.

1.4.1 Solar Radiation Heat Transfer

The primary driving energy for a solar still is incoming solar radiation**,** which enters the system through the transparent glass cover. Solar radiation consists of short-wave thermal energy that is:

- Transmitted through the glass cover,
- Absorbed by the basin water and basin liner,
- Converted into sensible heat that raises the water temperature.

The amount of incident radiation absorbed depends on factors such as glass transmissivity, surface absorptivity, angle of incidence, and the optical design of the still. In MPSS units, vertical hanging wick surfaces further increase solar absorption by presenting a larger wetted area directly exposed to solar radiation. As the water on the wick absorbs solar heat, evaporation increases significantly compared to conventional systems, where it is restricted to the horizontal basin surface.

1.4.2 Convective Heat Transfer

Convective heat transfer occurs at two primary interfaces within the solar still:

i. Between basin water (or wetted wick surface) and the moist air inside the chamber:

Evaporation is governed by natural convection currents driven by the temperature gradient between the heated water surface and the cooler air above it. As water temperature rises, lighter, warmer vapor-laden air ascends, while cooler air descends, forming a continuous convective cycle. In MPSS, the presence of wet wick surfaces enhances convective mixing, increasing the mass of vapor transferred to the upper chamber.

ii. Between moist air and the inner surface of the glass cover:

Condensation occurs when warm, moisture-rich air comes into contact with the inner surface of the glass. The rate of condensation depends on:

- Dew point temperature,
- Glass surface temperature,
- Air flow patterns inside the still.

MPSS configuration improves condensation by maintaining higher humidity and vapor concentration inside the chamber. This increases the dew point temperature, thereby strengthening the condensation-driving potential.

1.4.3 Conductive Heat Transfer

Conduction primarily takes place through:

- Basin walls and bottom plate,
- Insulation materials,
- Glass cover surfaces.

Heat conducted through the basin materials is partially lost to the surroundings. To minimize these losses, the fabricated solar stills in this work utilize polystyrene insulation (5–10 cm thickness) as reported in the experimental setup. This reduces downward heat conduction and allows a larger fraction of absorbed solar energy to contribute effectively to water heating.

In MPSS, conduction through wet wick fibers also contributes to heat transfer. The wick structure stores a small amount of heat and redistributes it along the vertical surfaces, maintaining evaporation even during short fluctuations in solar intensity.

1.4.4 Interaction of Heat Transfer Mechanisms

The combined effects of radiation, convection, and conduction determine the dynamic thermal environment within the solar still. The cycle may be summarized as follows:

- Solar radiation heats the basin water and wick.

- Heated water evaporates, forming moist air through convective transfer.
- Warm vapor rises and encounters the cooler glass cover.
- Vapor condenses, releasing latent heat to the glass.
- Heat is conducted from the inner glass surface to the outer surface and dissipates to the environment.
- Condensed droplets flow down the cover into the collection channel.

Enhancing any of these heat transfer modes, especially evaporation-related radiation absorption and condensation-related convective cooling, directly improves freshwater productivity. The MPSS developed in this research harnesses these principles by increasing wetted surface area, improving humidity levels, and optimizing the condensation process.

1.5 Basic Concept of Solar Distillation

Solar distillation operates on the fundamental principles of the greenhouse effect, using solar radiation as the primary energy source to drive the evaporation and subsequent condensation of water. In a solar still, incident solar energy penetrates the transparent cover, warms the basin water, and initiates the natural hydrological cycle within an enclosed chamber. Figure 1.8 illustrates the schematic configuration of a conventional single-slope solar distillation unit.

The distiller body is typically fabricated from materials such as fiber-reinforced plastic (FRP), galvanized iron (GI) sheets, or wood/concrete lined with insulating materials to minimize thermal losses from the sidewalls and bottom surface. The system is enclosed at the top by an inclined glass cover designed to facilitate gravitational flow of the condensed water film toward the collection channel. As vapor condenses on the cooler inner surface of the glass, the resulting distillate flows downward and is collected in a storage vessel. The basin liner, usually a blackened metallic or FRP surface, serves as the absorber plate, capturing most of the incident solar radiation and transferring heat to the water.

Solar radiation transmitted through the glass cover is partly absorbed by the basin water and partly by the blackened liner. A small fraction of the incident radiation is

reflected back, while the majority penetrates the water layer and is absorbed as it passes through. The extent of absorption depends on the water's optical properties and depth. As the liner temperature rises, heat is transferred to the water predominantly through convection, with minimal conductive losses to the surroundings due to insulation.

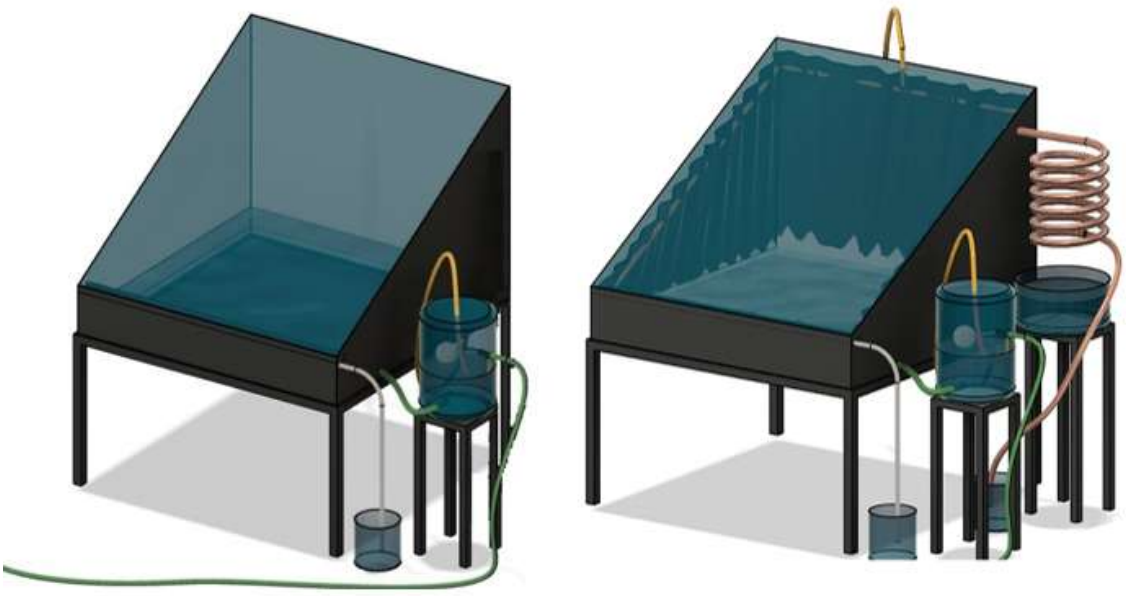

Figure 1.8 Schematic diagram of SPSS and MPSS

Temperature gradient between the warmed water surface and the cooler glass cover increases over time, promoting evaporation at the water-air interface. The generated vapor migrates upward, where it undergoes film-wise condensation on the inner surface of the glazed cover, releasing latent heat in the process. The condensed water then trickles down into a collection jar for subsequent use. Although the produced distillate is essentially free of dissolved salts and contaminants, remineralization is often recommended before consumption to improve taste and dietary mineral intake.

Under typical climatic conditions, the daily productivity of a single-slope passive solar still ranges from 0.5 to 2.5 kg/m²/day**,** and annual thermal efficiencies range from 5% to 40%, depending on design parameters and solar availability[6].

1.5.1 Advantages of Passive Solar Distillation Units

Solar stills offer several inherent benefits when compared to conventional desalination technologies:

- **Absence of moving components**, resulting in low maintenance requirements.
- **Low-cost and technically simple** method for producing potable water.
- **Environmentally sustainable operation**, relying on renewable solar energy without emissions.
- **Ease of operation**, suitable for unskilled or semi-skilled users.
- **Local manufacturability and repairability**, encouraging community-level adoption.
- **Particularly beneficial in regions with saline or brackish water** and limited infrastructure.
- **Potential integration with photovoltaic–thermal modules**, enabling energy self-sufficiency and cogeneration.
- **User-friendly and reliable** for small-scale water purification needs.

1.5.2 Limitations of Solar Distillation Systems

Despite its advantages, solar distillation also exhibits certain limitations that restrict its widespread industrial deployment:

- **Dependence on weather and solar availability**, leading to variable output.
- **Large land area requirement** for commercial-scale water production.
- **Limited investor interest** due to relatively low economic returns compared with high-capacity technologies.
- **Moderate performance**, particularly during non-sunny periods.
- **High initial cost** relative to the small-scale output.
- **Requirement for continuous water feeding and periodic flushing** to avoid salt accumulation.

- **Need for structurally robust systems** when installed in open environments.

1.6 Quality of distilled water

The taste and overall quality of water are strongly influenced by its pH level. In solar distillation, the pH of the feed water remains largely unchanged because the process does not involve vigorous boiling but instead relies on low-temperature evaporation. As a result, the distilled output typically exhibits a neutral pH and a clean taste. Solar distillation yields water of exceptionally high purity, free from dissolved salts and devoid of biological contaminants. Harmful microorganisms, including pathogenic bacteria, as well as toxic inorganic constituents such as arsenic, are effectively removed during the phase-change process. Studies conducted by the El Paso Solar Energy Association (EPSEA) have reported that solar-distilled water meets stringent health and safety standards, reinforcing its suitability for human consumption [5].

1.7 Parameters Influencing the Performance of Solar Distillation Systems

Several interrelated thermal and operational parameters govern the efficiency and productivity of a solar distillation unit. Key factors include the basin water temperature, the temperature of the condensing cover, heat transfer coefficients for convection, conduction, and radiation, the amount of solar energy absorbed through the glazing, and the daily distillate yield. Maintaining optimal thermal conditions within the still is essential to maximizing evaporation and condensation.

In solar distillation, the movement of the condensate film along the inner glass surface does not interfere with subsequent droplet formation; however, the transparent cover must be cleaned regularly to maintain high optical transmittance. When the glass surface is clean and smooth, filmwise condensation naturally occurs, enhancing the passage of solar radiation into the basin compared to dropwise condensation.

The inclination angle of the glass cover also affects system performance for several reasons:

- **Material requirements** increase with higher slope angles, as a larger glazing area is needed to enclose the same basin footprint.

- **Overall mass and structural load** of the still rise with increasing cover angle, influencing portability and fabrication cost.
- **Excessive inclination can introduce additional air volume** inside the chamber, potentially disrupting thermal stratification and reducing evaporation efficiency.

A high temperature difference between the basin water and the condensing surface is one of the most critical factors influencing yield. Higher basin water temperature and lower inner-glass temperature promote rapid vapor generation and efficient condensation. Minimizing vapor leakage and reducing thermal losses from the sidewalls and bottom surface also significantly improves productivity.

The basin liner's ability to absorb solar radiation significantly influences water temperature. A selectively coated or blackened liner enhances radiation absorption, thereby increasing evaporation. Additionally, maintaining a shallow water depth enables the water mass to heat more quickly, further enhancing evaporative flux.

1.8 Applications of Solar Distilled Water

Solar energy is an abundant, freely available resource; however, the initial capital costs of constructing a solar distillation unit and the substantial land area required limit the feasibility of large-scale production. For this reason, solar distillation is generally more appropriate for small- to medium-scale applications rather than extensive domestic supply, industrial processing, or agricultural irrigation. Its primary utility lies in producing high-quality purified water for household, laboratory, and specialized applications.

Solar-distilled water is exceptionally clean, free of dissolved salts, pathogens, and other contaminants, making it suitable for drinking, cooking, bathing, and washing**.** In scientific and medical environments, it is frequently used for analytical procedures, reagent preparation, sterilization**,** and environments where high-purity water is essential. Additionally, distilled water is commonly required for battery maintenance in telecommunication installations and electrical systems to avoid mineral deposits that may impair performance.

Beyond domestic and laboratory use, solar-distilled water can support certain agricultural and industrial processes that require moderate quantities of low-mineral-content water. Although not economically competitive for large-scale freshwater production, solar distillation can be advantageous in salt recovery operations. It may also be applied to the treatment of sewage or wastewater; however, caution must be exercised because volatile organic compounds or odorous gases may evaporate and subsequently condense with the distillate. Furthermore, solar distillation principles can be used for alcohol purification, though their applicability remains limited by process efficiency.

Chapter 2

LITERATURE REVIEW

2.1 Historical background

The development of solar distillation technologies has evolved over several decades in response to rising freshwater scarcity and the need for decentralized, low-energy purification systems. Early conceptual work on solar desalination drew inspiration from the natural hydrological cycle, applying the greenhouse effect to evaporate saline water and condense purified distillate within an enclosed structure. With increasing awareness of global water challenges, particularly in regions with high solar insolation, researchers have increasingly explored improved designs that enhance evaporation, condensation, and thermal management. During this period, researchers also began examining the influence of material properties, particularly absorptivity and thermal conductivity. The introduction of blackened basin liners, selective coatings, and insulated sidewalls marked an important evolution in understanding how thermal losses and optical properties affect system output [7].

2.2 Enhancement of Performance of Conventional Solar Still

2.2.1 Single and double slope collector solar still

Tiwari [8] developed a thermal model for a double-slope solar still (DSSS) operating under natural circulation with a water depth of 30 cm in Ghaziabad, India. The study showed that the active configuration produced roughly 51% more distillate than the passive system. However, the passive still demonstrated better thermal efficiency, while the active design exhibited higher overall energy efficiency.

Figure 2.1 shows a double-slope solar still (DSSS) that functions similarly to a single-slope still but uses two inclined glass covers, increasing the available condensation area and improving freshwater yield [9]. Singh [10] noted that the dual-slope geometry offers a more favorable inclination for heat rejection, promoting sustained film-wise condensation.

Murugavel et al. [11] evaluated a mild-steel DSSS using various sensible heat storage media, including quartzite, concrete, brick pieces, and scraps. Quartzite of about

one inch in thickness produced the best thermal response, while changes in water depth and basin material significantly influenced basin and glass temperatures and, consequently, the distillate output.

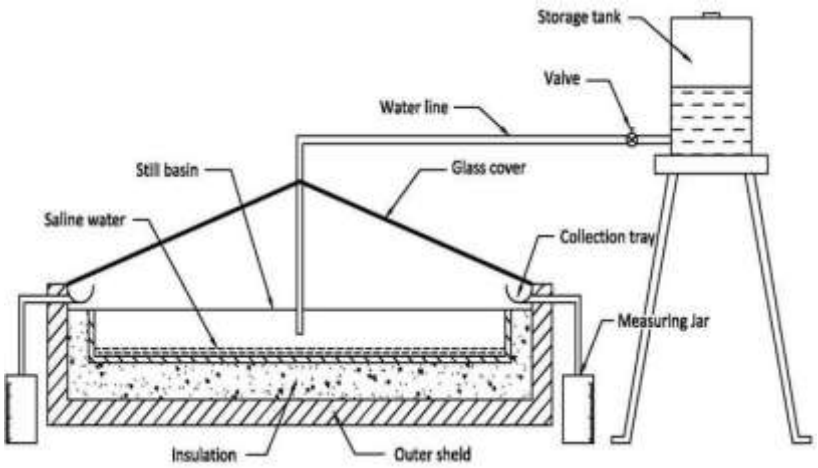

Figure 2.1 Double slope solar still (DSSS) [9]

Rajaseenivasan and Murugavel [12] analyzed double-slope and double-basin stills using computational modeling for Tamil Nadu climate conditions. Adding a second basin increased productivity by 85%, yielding up to 2.99 L/m²·day, though higher water mass in multiple basins reduced overall performance due to thermal sensitivity.

For Algeria's climatic conditions, Abderachid and Abdenacer [13] investigated symmetrical and asymmetrical double-slope systems. They found that a 10° cover inclination and south–north orientation maximized production, with asymmetric double-effect stills achieving up to 22.57% higher output.

Belhadj et al. [14] numerically examined a DSSS fitted with a capillary film condenser using a FORTRAN-based model. They observed that increased saline water flow and wider plate spacing reduced productivity; however, the modified condenser still produced 7.15 kg/m²·day, outperforming a conventional still yielding 4.52 kg/m²·day.

Tiwari et al. [15] further assessed a partially covered PVT–FPC-assisted DSSS from exergoeconomic and environmental perspectives. Their results indicated that double-slope systems remain cost-effective for freshwater production, and PVT-integrated configurations are particularly suitable for remote or off-grid applications.

2.2.2 Pyramid collector solar still (PCSS)

A pyramid-type solar still (PCSS) employs a pyramidal transparent cover, increasing the effective evaporation and condensation areas compared with conventional single-slope designs. Performance can be further improved by optimizing geometric parameters such as cover height, face inclination, and overall structure.

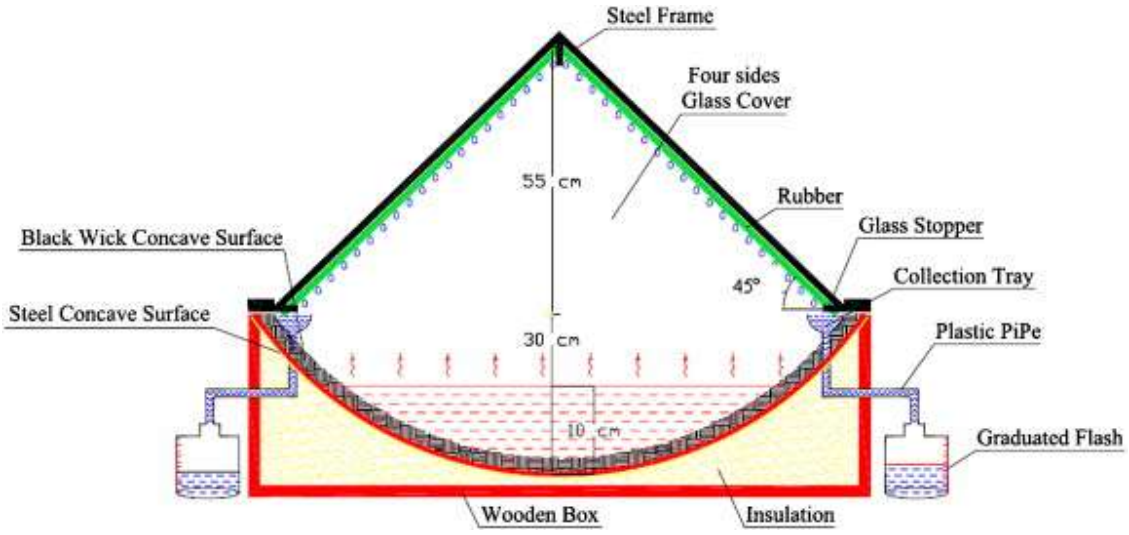

Figure 2.2 Pyramid Collector Solar Still[16]

Kabeel [16] experimentally evaluated a PCSS fitted with a concave jute wick, as shown in Figure 2.2, and found that the enlarged glazing area and enhanced internal reflection improved solar absorption and thin-film evaporation. Using a 1.2 × 1.2 m² basin, a 10 cm water depth, and a 45° cover inclination, the wick-assisted system produced higher vapor generation and improved condensation compared to a standard PCSS.

Sathyamurthy et al. [17] studied triangular pyramid stills and identified factors such as convective heat-transfer coefficients, glazing area, basin water depth, and wind speed as key performance drivers. Under Chennai conditions, a 30° inclination and 4.5 m/s wind yielded up to 4.70 L/m²·day, a 15.50% improvement.

Additional investigations by Tiwari et al. [18] and El-Sebaii [19][20][21] confirmed that shallow water depths and moderate wind speeds enhance heat absorption and lower glass temperature, reinforcing the evaporation–condensation cycle and improving distillate output.

2.2.3 Black painted inside wall solar still

Blackened surfaces are known to absorb a high fraction of incident solar radiation, and Kabeel et al. [22] utilized this principle by coating the inner walls of the still to enhance thermal absorption. This modification increased basin water temperature and strengthened evaporation.

To further improve the absorptivity, nanoparticles were added to the black paint. A 20% nanoparticle concentration increased the temperatures of the basin water, liner, and glass cover by 10.40%, 12.20%, and 12.30%, respectively, while higher concentrations produced no notable additional benefit. Distillate output also improved, with 10% and 20% nanoparticle-enhanced coatings yielding 27.20% and 34.30% higher productivity than conventional paint.

2.2.4 Spherical solar still

Dhiman [23] analyzed the performance of a spherical solar still, as shown in Figure 2.3, using mathematical modeling and showed that its fully curved transparent cover enables uniform solar absorption throughout the day without requiring tracking. Owing to its improved optical and thermal characteristics, the spherical design achieved nearly 30% higher distillate yield than a conventional single-slope still (SSSS).

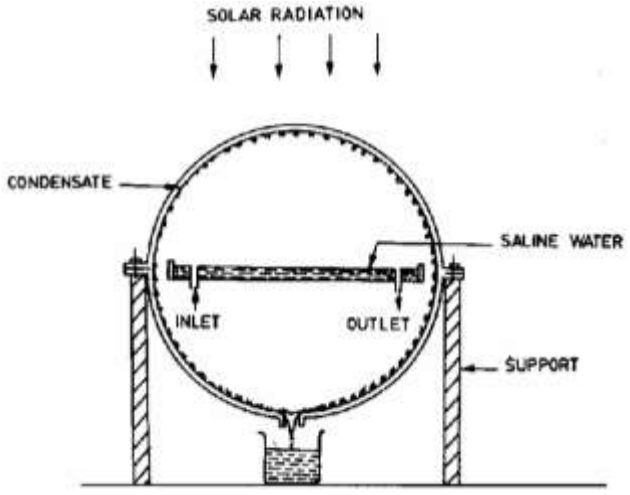

Figure 2.3 Spherical Solar Still [23]

Building on this concept, Basel conducted an experimental study of a hemispherical solar still (HSSS) and reported a peak productivity of 5.7 L/m²·day with a

thermal efficiency of about 33%. While both spherical and hemispherical systems operate without solar-tracking mechanisms, the hemispherical still offers better portability, making it suitable for field applications.

2.2.5 Hemi-spherical solar still (HSSS)

The hemispherical geometry of this still design enables uniform solar interception throughout the day, removing the need for solar tracking. Basel [24] reported that such a configuration achieved an average thermal efficiency of about 33%, aided by a deep central water column and a uniformly exposed transparent dome.

Arunkumar et al. [25] examined the performance of a hemispherical solar still (HSSS) with and without top-cover cooling as shown in Figure 2.4. Using a 0.71 m^2 basin and 50 cm water depth, they found that applying a cooling-water film over the glass significantly improved productivity: thermal efficiency increased from 34% in the uncooled case to 42% with cooling. The enhancement resulted from a lower glass temperature, which strengthened the condensation potential and boosted distillate output.

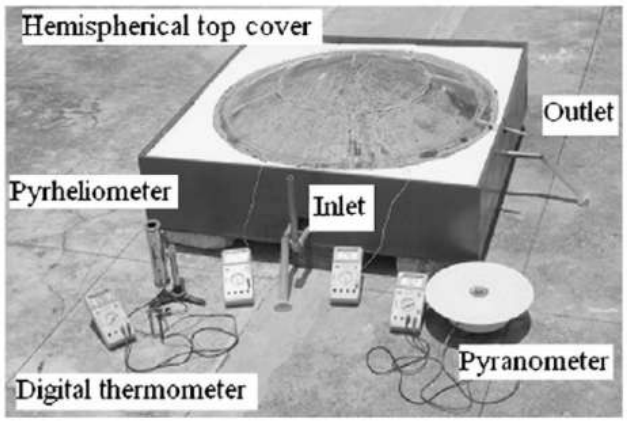

Figure 2.4 Hemi-Spherical Solar Still [24]

2.2.6 'V' type solar still (VTSS)

Singh [20] observed that in conventional solar stills, only the glazing surface aligned with the solar path significantly contributes to evaporation and condensation. In contrast, the opposite side receives limited radiation and is less effective. This highlights the importance of cover orientation and geometry in determining solar energy absorption and overall thermal performance.

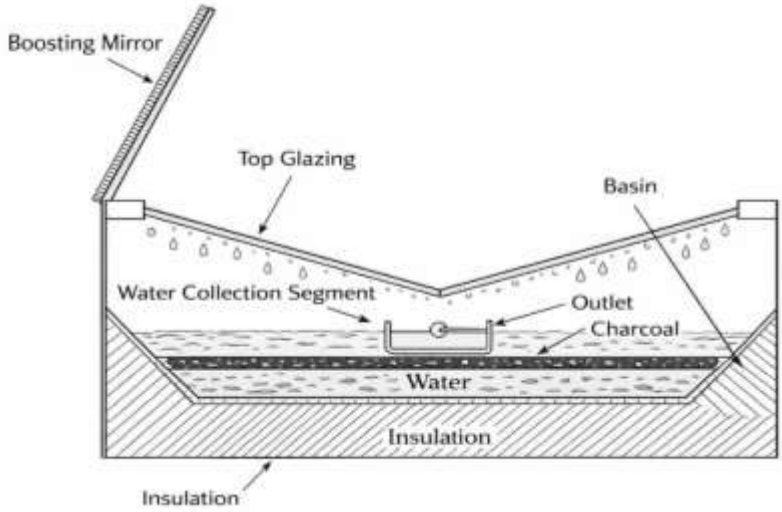

Figure 2.5 V type solar still [26]

Kumar et al. [26] investigated a V-shaped solar still design under four conditions: without charcoal, with charcoal, with a reflective mirror, and with both charcoal and a mirror as represented in Figure 2.5. As shown in Figure 2.6, the corresponding distillate yields were 2.52, 3.23, 2.70, and 3.53 L/m²·day, with efficiencies of 24.47%, 30.05%, 11.92%, and 14.11%, respectively. The results demonstrate that improved basin absorptivity (via charcoal) and enhanced incident radiation (via reflectors) can significantly increase the productivity of V-shaped solar stills.

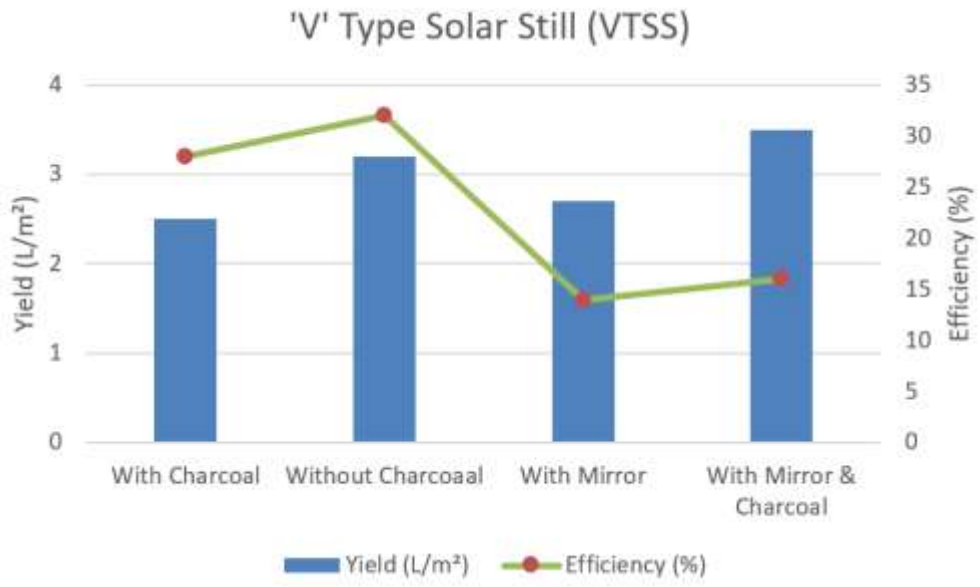

Figure 2.6 Efficiency and daily yield variation with 'V' top (VTSS) system [26]

2.2.7 Painted inside surface with mixed TiO_2

Kabeel et al. [27] showed that adding TiO_2 nanoparticles to the black coating inside a solar still basin is an economical way to improve thermal performance. The nanoparticles increase the coating's thermal conductivity, enhancing heat transfer to the basin water and improving absorption of incoming solar energy.

This improved thermal behavior supports faster water heating and higher evaporation rates, leading to greater distillate yield. The effect is consistent with observations in nanofluid research, where dispersed nanoparticles increase the medium's effective thermal conductivity. When applied within a solar still, nanoparticle-based coatings help capture more solar radiation and distribute heat more evenly, thereby improving overall productivity.

2.2.8 Thermal conductivity of glass cover

The growing need for higher freshwater output has motivated extensive efforts to improve the thermal efficiency of solar stills. Among the key factors affecting performance, condensation on the inner surface of the cover is particularly important, as it is controlled by convective and conductive heat-transfer processes that dictate the rate of vapor-to-liquid conversion.

Dimri et al. [28] found that using cover materials with higher thermal conductivity can significantly enhance distillate production. A more conductive cover dissipates heat more effectively, lowering its surface temperature and increasing the temperature gradient between the vapor and the glass. This strengthened gradient accelerates condensation and improves overall system productivity.

While several material treatments and modifications can increase cover conductivity, the choice of material must also consider cost, durability, and compatibility with the solar still operating conditions.

2.2.9 Depth of water in single slope solar still

Prakash et al. [29] evaluated the thermal behavior of a solar still at water depths of 3 cm and 12 cm with a 23° cover inclination. Their results showed that, under active operating conditions, a deeper water level produced higher distillate output, whereas in

passive mode, the yield decreased with increasing water depth. Improvements in evaporative and convective heat-transfer coefficients also contributed to enhanced performance.

The study confirmed that the temperature difference between the basin water and the condensing cover primarily governs productivity. Higher water temperature combined with a cooler glass surface strengthens the evaporation–condensation cycle. The highest yield reported was 0.23885 kg/hr at a depth of 12 cm, compared with 0.13 kg/hr at 3 cm.

2.2.10 Single solar still with porous structures

Shoeibi et al. [30] found that adding porous materials to the basin increases the temperature gradient between the water surface and the condensing cover, thereby enhancing evaporation and improving freshwater yield. Porous media promote thin-film evaporation due to their larger effective surface area and better heat absorption.

Saravanavel et al.[31] tested broken clay pieces and chalk as porous media in a pyramid-type still with a water depth of 0.01 m. With insulated sidewalls to reduce heat loss, the modified unit produced 36% more distillate than the conventional design under identical conditions.

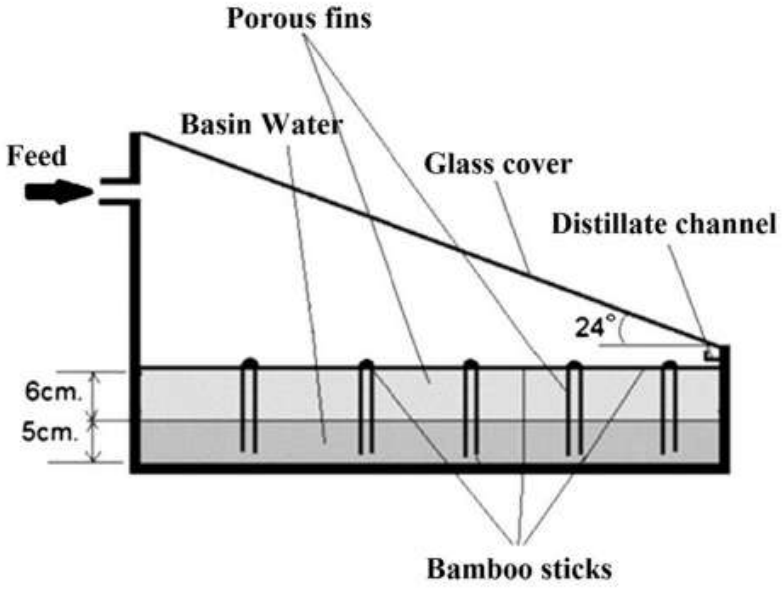

Figure 2.7 Modified still using porous absorber [32]

Srivastava and Agrawal [32] used porous fins made from blackened cotton rags in a single-slope still with a 24° cover inclination, as presented in Figure 2.7. The fins absorbed more solar radiation and increased evaporation rate, while a lower basin water depth further improved performance. Their system achieved a maximum yield of 7.5 kg/m² in May.

2.3 Performance Evaluation of an Integrated Solar Still System: Exploring Design Parameters:

2.3.1 Solar still with Fins for condensation

Potable water in a solar still is generated when vapor condenses on the inner surface of the cover through combined convective and conductive heat-transfer processes. One method of enhancing this condensation is the use of fins, which increase the available surface area for heat rejection.

Velmurugan et al. [33] showed that adding fins to the condensing region of a single-slope still improved heat transfer and boosted productivity by 45.50%, as the extended surface facilitated more effective vapor–surface interaction as depicted in Figure 2.8. High-conductivity materials are typically preferred for fins to ensure rapid heat removal and maintain a lower glass temperature.

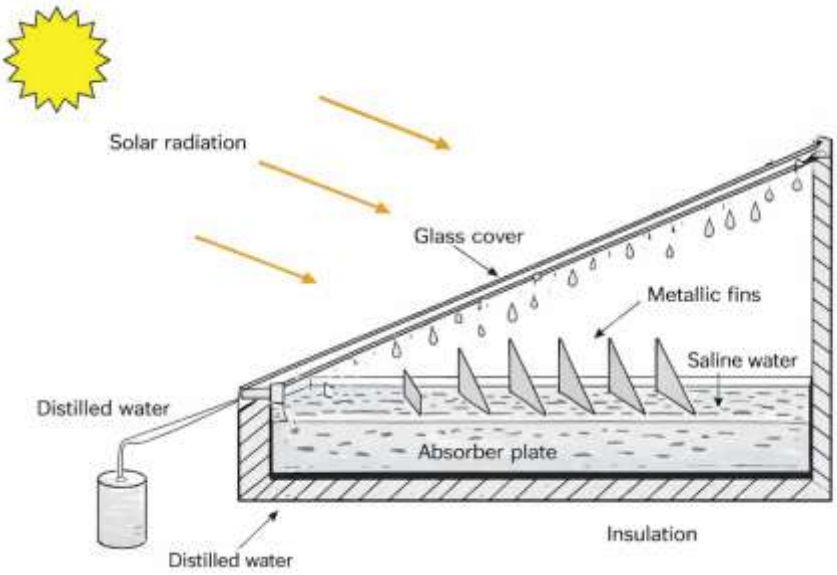

Figure 2.8 Solar still with fins [33]

Further enhancement was reported in [34] as shown in Figure 2.8, where pin fins embedded in a paraffin wax storage bed increased freshwater output. At a 2 cm water depth, the modified still produced 3750 ml/m² compared with 3017 ml/m² for a standard design. Comparative studies [35][36] also revealed that finned stills outperform non-finned units, achieving yields of 1.12 kg/m² versus 0.914 kg/m², respectively.

Overall, fin integration has proven to be an effective passive modification for improving condensation efficiency and freshwater yield, making it especially valuable for low-cost desalination applications.

2.3.2 Solar still with fan for condensation

A fan-assisted solar still is a modified desalination system that uses forced airflow to enhance both evaporation and condensation. Introducing a fan increases air circulation inside the chamber and strengthens convective heat transfer. Suraparaju et al. [37] showed that lowering the glass-cover temperature improves condensation efficiency by increasing the temperature gradient between the vapor and the condensing surface.

Although many studies emphasize evaporation enhancement, the condensation process is equally important for overall yield. An et al. [38] noted that condensation—whether film-wise or drop-wise is governed by the convective heat-transfer coefficient (h). Forced convection from a fan increases h, enabling faster heat removal from the vapor and promoting more rapid condensation (Figure 2.9).

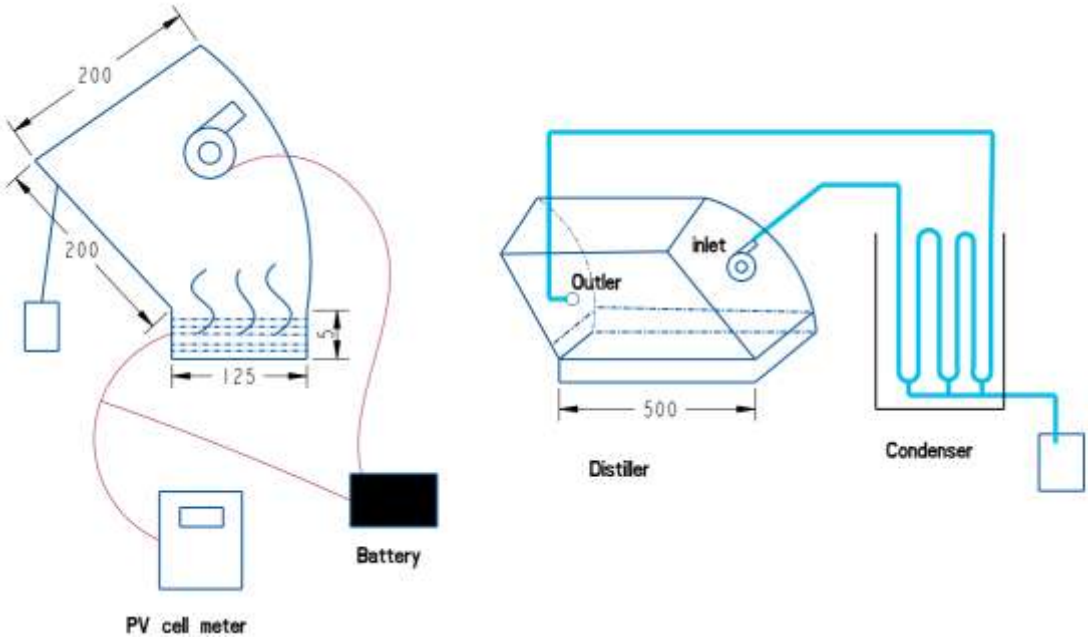

Figure 2.9 Experimental setup with Fan for condensation [38]

2.3.3 Solar still with several types of wicks

Psychrometric conditions strongly influence evaporation and condensation in a solar still. As solar radiation heats the basin water, vapor pressure rises, and evaporation proceeds according to the temperature and partial pressure differences within the chamber. Both phase-change processes occur near saturation conditions corresponding to the internal pressure.

Wick-based stills use porous, capillary-active materials to enhance evaporation by creating a thin water film with greater exposure to air. This increases heat absorption and vapor generation. Floating wick configurations (Figure 2.10) also modify the partial vapor pressure distribution, thereby improving distillate productivity [39].

Suraparaju et al. [40] tested multiple floating fiber elements and found that covering an optimal portion of the basin surface increased yield by 29.67% compared with a standard still. Similar improvements (28.35%) were recorded using Luffa acutangula natural fibers [41]. However, a later comparison by Suraparaju et al. [42] showed that ridge-gourd fibers did not significantly enhance productivity, indicating that wick material characteristics and configuration must be carefully selected.

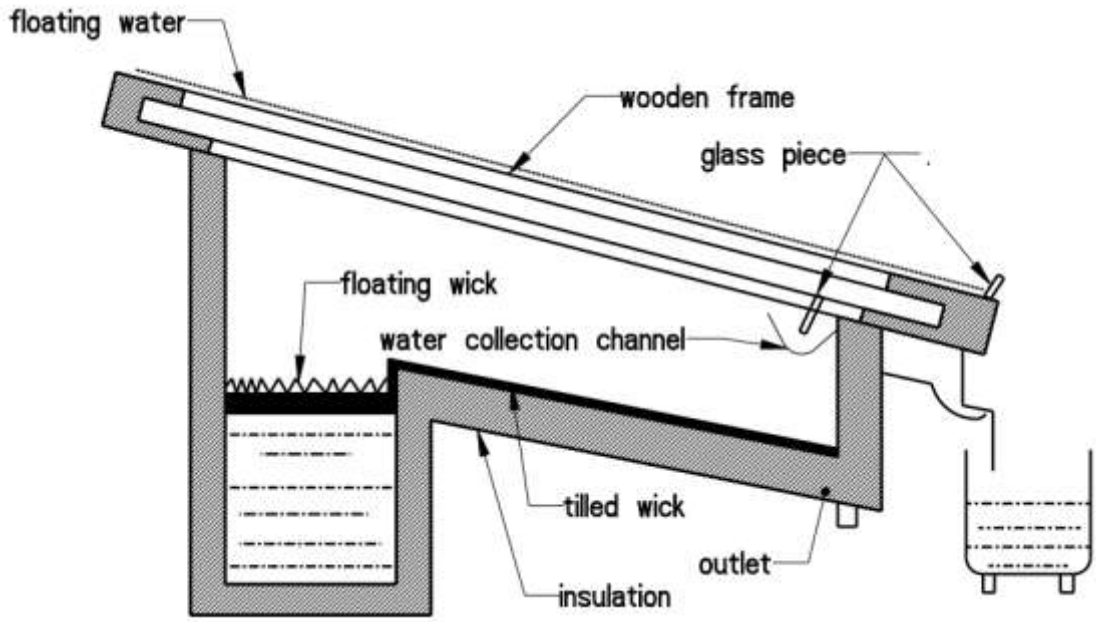

Figure 2.10 Wick-type solar still with different thermal conductivity of cover [39]

2.3.4 Multi-basin solar still (MBSS)

Kaviti et al. [43] showed that multi-basin solar stills (MBSS) produce considerably more freshwater than single-basin systems due to their ability to reuse internal heat. In these designs, heat from the lower basin contributes to evaporation in the upper basin, creating a cascading effect that improves overall energy efficiency and distillate output.

Because of this advantage, MBSS designs have received significant research attention, with various modifications aimed at improving heat recovery and productivity. A typical passive MBSS layout is shown in Figure 2.11 [44], featuring stacked basins, multiple glazing layers, and interconnected heat-transfer pathways.

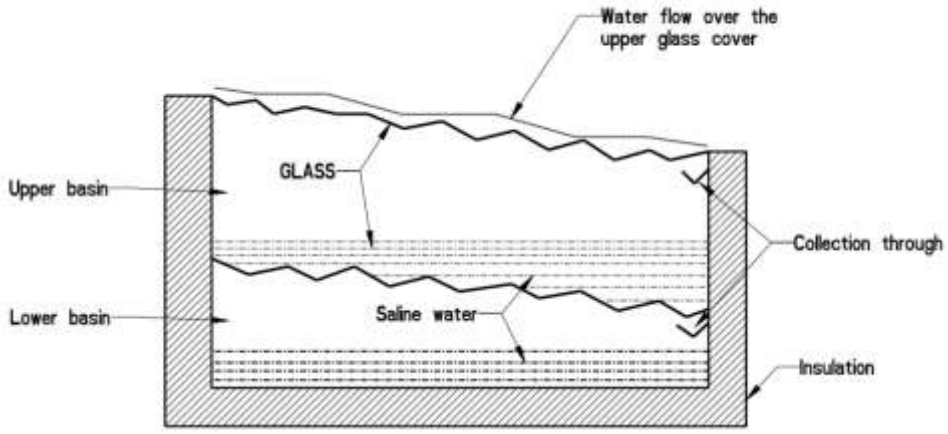

Figure 2.11 Multi-effect passive type solar still [44]

2.3.5 Tubular solar still (TSS)

Singh [10] noted that tubular solar stills (TSS) often outperform conventional single-slope stills because their geometry provides a larger effective basin area and better solar energy retention, as depicted in Figure 2.12. Tiwari and Kumar [45] similarly attributed this improved performance to enhanced solar exposure within the transparent tubular enclosure.

Kumar and Anand [46] further modified the design by replacing the basin with multiple wick strips, increasing the evaporative and condensing surfaces, and achieving higher yields than those of standard SSSS units. Ashan et al. [47] improved productivity by using a metallic basin covered with a thin vinyl chloride film, thereby intensifying the temperature gradient and boosting evaporation.

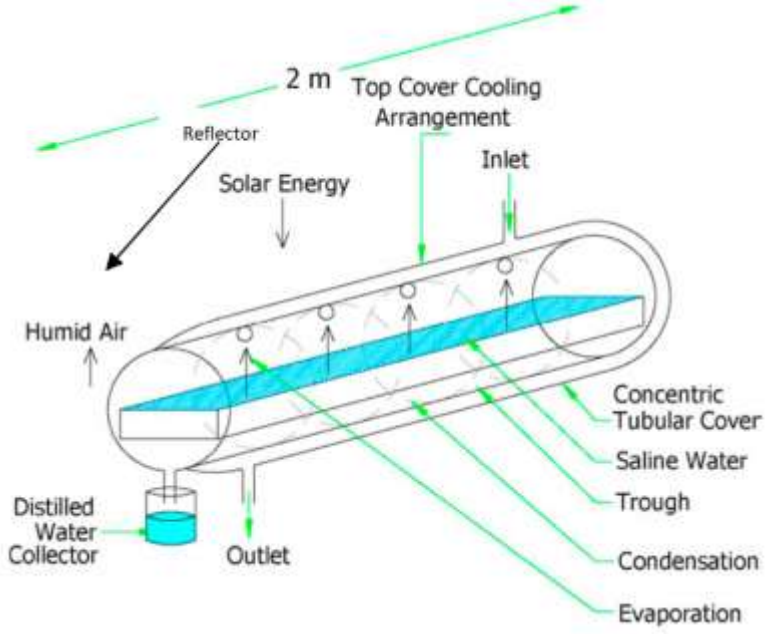

Figure 2.12 Tubular solar still [45]

Arunkumar et al. [48] evaluated TSS units with cooling techniques and solar concentrators (CPC and PSS), achieving yields up to 7.77 L/m²·day; despite higher initial cost, the efficiency gains justified the configuration. Later, Arunkumar and Kabeel [49] integrated phase change material (PCM) into a TSS-CPC setup, increasing output from 5.33 to 5.78 L/m²·day by providing latent-heat support during low-radiation periods.

More recently, Jing et al. [50] proposed a concentric TSS featuring an outer wick-coated tube and an inner standard tube. This configuration produced higher distillate output, with reduced water mass and improved solar absorption, especially when paired with PCM, highlighting its promise for advanced solar desalination.

2.3.6 Multi-wick solar still (MWSS)

Tiwari and Selim [45] presented one of the initial assessments of dual-slope multi-wick solar stills (MWSS), showing that multiple wicks can substantially enhance distillate yield, though at a higher initial cost. Singh and Tiwari [51] later developed a multi-effect MWSS design in which thin-film evaporation over the wick layer improved overall thermal performance, as shown in Figure 2.13.

Mahdi et al. [52] advanced this concept by evaluating a tilted wick still using charcoal cloth as a thermal-storage medium, demonstrating the importance of wick

orientation and heat-retention characteristics. Further refinements were introduced by Pal et al. [53], who achieved improved output through structural modifications in conventional stills. Pal and Dev [54] converted a double-slope still into a multi-wick unit, reporting higher yield due to better wick materials and enhanced thermal storage.

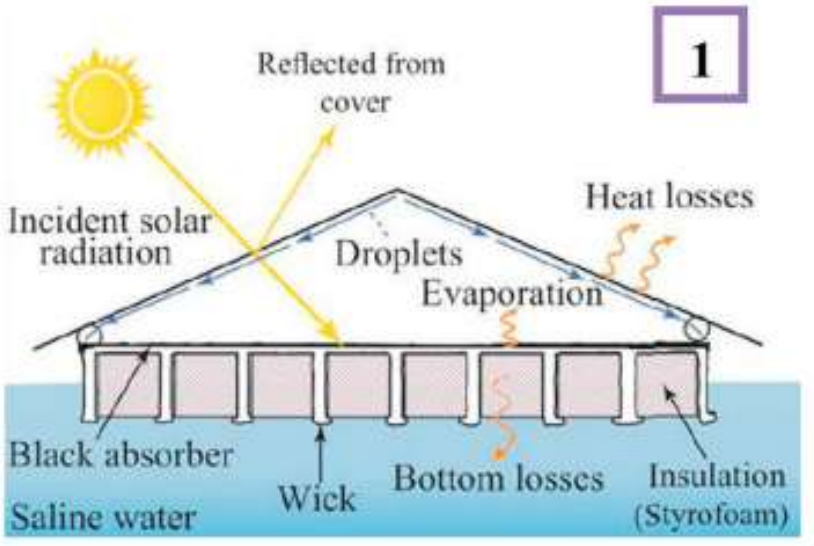

Figure 2.13 Multi wick solar still

In another study, Pal et al. [55] incorporated transparent sidewalls and multiple wicks into a double-slope design, achieving daily productions of 9.012 and 7.040 L/m² with jute and cotton wicks, respectively. Suraparaju et al. [56] enhanced both evaporation and condensation by combining floating fibers, a hollow finned absorber, and glass-cover cooling, resulting in a 126% increase in yield.

Ni et al. [57] introduced a low-cost floating-wick system capable of rejecting salt through a corrugated fabric structure, preventing pore blockage under high-salinity conditions. With defined evaporation and condensation zones, the system achieved 57% evaporation efficiency under one-sun conditions, supported by CFD validation.

2.3.7 Contactless solar steam generation and solar still (CSSGSS)

Cooper et al. [58] proposed a solar distillation concept in which the absorber is thermally isolated from the water and used to generate superheated steam. Under laboratory conditions, the system achieved about 38% efficiency and produced up to 2.50 L/m²·day of distilled water. In a different approach, Kashyap et al. [59] demonstrated that

graphene aerogel, when subjected to localized solar heating at one-sun intensity (1000 W/m²), can facilitate the conversion of CO_2 into water and $CaCO_3$.

Other configurations, such as diffusion and weir-type solar stills, also perform effectively due to their increased evaporation and condensation surface areas and the minimal water mass in the basin. Furthermore, hybrid systems incorporating CPCs, FPCs, PCMs, or auxiliary condensers have shown improved freshwater output without requiring larger basin areas [60].

2.3.8 Diffusion solar still (DSS)

Extensive research has been conducted on various configurations of diffusion solar stills (DSS), including horizontal, vertical, inclined, and multi-effect designs [61] [62] [63] [64] [65] [66] [67]. Continuous refinement of earlier models has led to more efficient configurations. Hiroshi [68] demonstrated that coupling a multi-effect DSS with a flat-plate collector (FPC) could achieve outputs of up to 13.3 L/m²·day under high solar intensity. Chong et al. [69] further improved performance by integrating a heat exchanger with a vacuum spiral solar collector, increasing water temperature and yielding 23.9 L/m²·day.

Building on this concept, Huang et al. [70] introduced a spiral multi-effect DSS with both lateral and directional diffusion, achieving a peak distillate production of 40.6 L/m²·day. Tanaka [71] evaluated a vertical multi-effect DSS with a slanted wick and reported 15.9 L/m²·day, while subsequent optimization studies by Tanaka [72] [73] confirmed substantial yield improvements across different geometric configurations.

DSS systems are inherently efficient due to their multi-plate diffusion channels, which enhance evaporation and condensation by maintaining thin water films and sustained temperature gradients. The specific orientation, vertical, horizontal, inclined, or spiral, is determined by the arrangement of diffusion plates, each separated by a small air gap and lined with wetted wicks to promote capillary-driven evaporation. Distillation occurs as vapor generated between plates diffuses toward the cooler condensing surfaces, improving productivity compared with conventional basin stills [74].

Kaushal et al. [75] examined a vertical floating-wick DSS (Figure 2.14) using concentrated brine discharge to preheat incoming saline water, reporting a 21%

improvement over a standard vertical DSS. Their system employed floating cotton wicks supported on thermal coal to maintain stable evaporation zones.

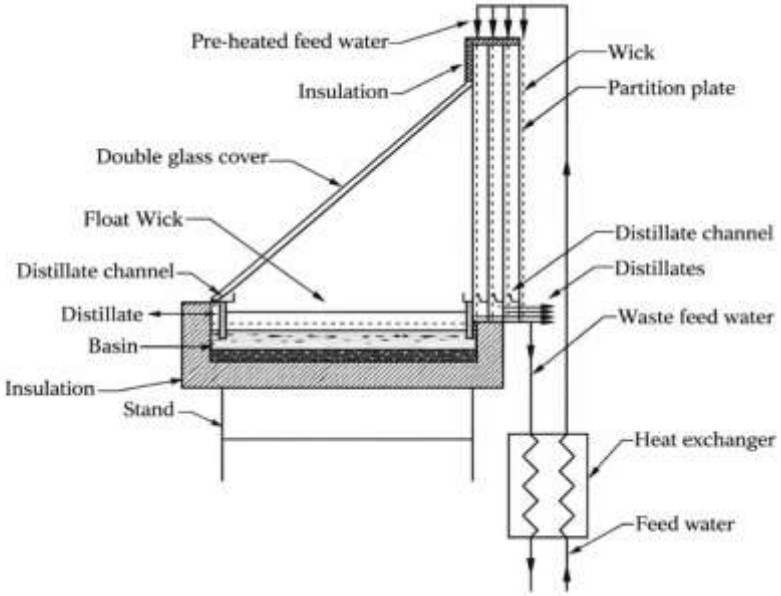

Figure 2.14 Diffusion solar still (DSS) with floating wick [75]

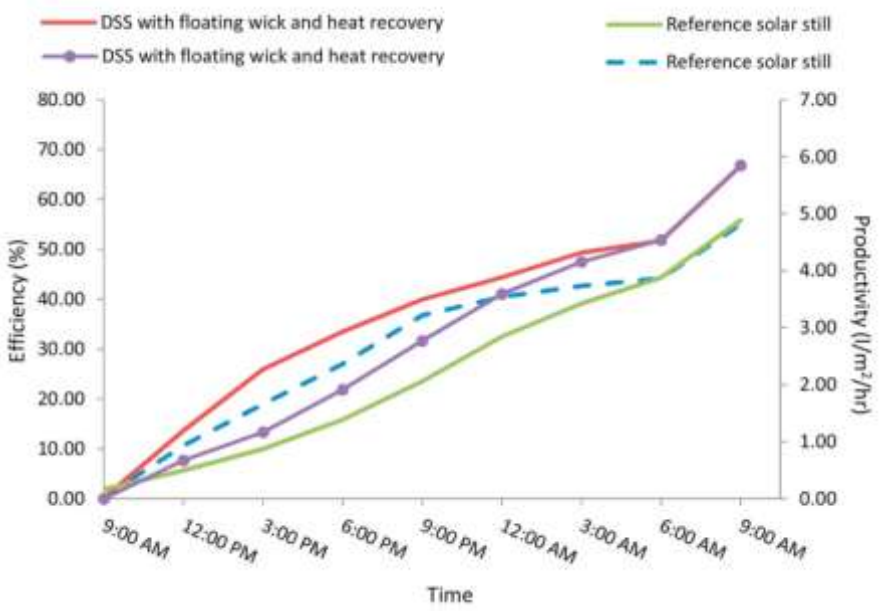

Figure 2.15 Variation of efficiency and productivity with respect to time of diffusion solar still [76]

Economic evaluation showed a short payback period and favorable cost–performance characteristics [76]. The optimized experimental model achieved 1.34

L/m²·day, outperforming the corresponding conventional system yield of 0.98 L/m²·day, due to improved heat recovery via an integrated heat exchanger (Figure 2.15).

2.3.9 Weir-type solar still (WTSS)

Sadineni et al. [77] conducted experimental and theoretical studies on a weir-type solar desalination system and reported approximately 20% higher productivity than a conventional still. The improvement was attributed to the thin water film over the weir steps, reduced glazing requirements, and enhanced heat recovery through continuous water flow.

Tabrizi et al. [78] later developed a cascade-type weir still integrated with phase-change material (PCM). Their observations showed that low-mass-flow operation produced higher distillate yields on clear days without PCM, whereas PCM-assisted operation improved performance under hazy conditions by providing additional stored thermal energy.

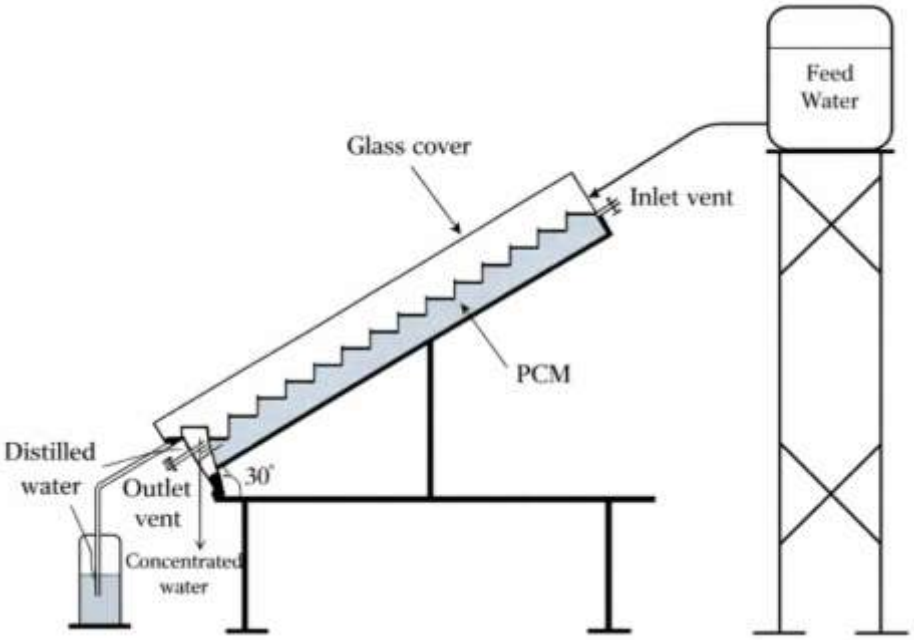

Figure 2.16 Weir type solar still [79]

Zoori et al. [79] validated these trends experimentally as shown in Figure 2.16, confirming that weir stills with thin-film evaporation outperform PCM-assisted systems on clear days, whereas PCM benefits productivity by reducing heat loss during fluctuating solar conditions. Sarhaddi et al. [80] further compared cascade weir stills with and without

PCM under varying atmospheric conditions. Their results showed that PCM-based systems performed better in semi-hazy climates because the stored latent heat sustained evaporation, achieving efficiencies up to 76.69% and daily yields of 7.05 L/m².

Natarajan et al. [81] proposed an eco-friendly enhanced solar still using low-cost materials such as sawdust, rice husk, and molasses to improve thermal absorption and evaporation. Their modified design increased the evaporation rate by 34.81% compared with a conventional still.

2.3.10 Stepped-type inclined solar still

Studies on stepped solar stills (STSS) have shown that incorporating a storage tank for continuous water circulation significantly improves productivity [82] [83]. A typical STSS consists of a 1 m² absorber plate divided into ten equal steps, allowing thin-film evaporation along each tier. Experiments were conducted using two water types—seawater and brackish saltwater, and two basin surface treatments: a black-coated absorber and a cotton-based absorber.

For the black absorber configuration, STSS exhibited daily efficiencies of 61% for seawater and 55% for saltwater, compared with 42% and 37% for a simple solar still (SSS). Replacing the black absorber with cotton further improved performance: STSS efficiencies reached 61% for seawater and 70% for saltwater, outperforming the corresponding SSS values of 40% and 48%. Overall, STSS improved freshwater yield by 43% and 48% (black absorber) and 47% and 53% (cotton absorber) relative to SSS. The system achieved daily yields of approximately 6.1 kg/m² and 6.3 kg/m² when operating with seawater.

The available literature on design modifications and performance outcomes in solar still is summarized in Table 2.1.

Table 2.1. Literature summary of design modifications and performance outcomes in solar stills

Solar Still Type / Modification	Key Enhancement / Parameter Studied	Major Findings / Outcomes	References
Double-Slope Solar Still (DSSS)	Dual glass covers, storage media, orientation, PVT–FPC assistance	Up to 51% higher yield in active mode; quartzite effective as storage; optimized inclination and orientation improve yield; exergoeconomic feasibility confirmed	[2-10]
Pyramid Solar Still (PCSS)	Wick integration, inclination, wind velocity, water depth	Yield up to 4.70 L/m²·day; reduced water depth and moderate wind enhance productivity	[11–16]
Coated Basin Solar Still	Nanoparticle-enhanced black coatings (TiO_2)	Yield improvement up to 34%; increased absorptivity and thermal conductivity	[17, 21]
Spherical / Hemispherical Solar Still	Curved transparent cover, glass cooling	30% higher yield than conventional; efficiency improved from 34% to 42% with glass cooling	[18–20]
Cover Material Optimization	High thermal conductivity glazing	Reduced glass temperature enhances condensation and freshwater yield	[22]
Basin Water Depth Optimization	Variation of basin water depth (3–12 cm)	Deeper water beneficial in active mode; shallow depth preferred in passive mode	[23]
Porous Media Solar Still	Clay, chalk, cotton rag porous media	Yield enhancement up to 36%; thin-film evaporation improved	[24] [25] [26]

Solar Still Type / Modification	Key Enhancement / Parameter Studied	Major Findings / Outcomes	References
Finned Solar Still	Pin fins, paraffin wax storage	Productivity improved by 45% to 55%; enhanced condensation efficiency	[27] [28] [29] [30]
Fan-Assisted Solar Still	Forced convection airflow	Improved condensation and yield, especially in low wind and humidity conditions	[31] [32]
Wick-Based Solar Still	Floating fibers, capillary wick materials	Yield enhancement up to 30%; wick material properties critical	[33] [34] [35] [36]
Multi-Basin Solar Still	Cascaded heat reuse between basins	Significantly higher yield due to internal heat recovery	[37]
Tubular Solar Still (TSS)	CPC, cooling techniques, PCM integration	Productivity up to 7.77 L/m²·day; PCM improves low-irradiance performance	[38] [39] [40]
Multi-Wick Solar Still	Multiple wicks, transparent sidewalls	Yield up to 9.01 L/m²·day; 126% improvement with hybrid enhancements	[41] [42] [43] [44]
Weir-Type Solar Still	Thin-film flow, PCM, agri-waste materials	Efficiency up to 76.69%; PCM beneficial under fluctuating irradiance	[44] [45] [46] [47] [48] [49]
Stepped Solar Still (STSS)	Continuous circulation, stepped absorber	Efficiency up to 70%; yield increased by 43–53%	[50] [51]

2.4 Research gap

A comprehensive review of existing desalination studies reveals that although numerous structural and operational modifications, such as wicks, fins, nanoparticles, porous media, PCM integration, condenser units, and cooling arrangements, have been explored to improve solar still productivity, several critical gaps persist.

Imbalance between Evaporation and Condensation Enhancements: Many earlier works intensify evaporation (e.g., via wicks, porous fins, reflectors, nanofluids) but do not simultaneously optimize condensation, leading to thermodynamic mismatches where vapor generation increases but conversion to distillate remains limited. Analysis confirms that partial pressure differences govern evaporation rates, but few systems deliberately engineer both sides of the heat–mass transfer cycle.

Drawbacks in Nanoparticle-Based Approaches: Although nanoparticles improve heat absorption, several studies report agglomeration, sedimentation, and reduced long-term stability, leading to performance deterioration and increased maintenance. The present study focuses on passive methods (wick and cooling coil) precisely because nanoparticle-based approaches suffer from these practical limitations.

Insufficient Attention to Increasing Free Evaporative Surface Area: Most conventional designs rely on the basin's horizontal surface, limiting the effective evaporation area. Few studies have attempted to expand evaporation per unit footprint using vertical or hanging wick surfaces, despite evidence that enhanced wet-surface exposure significantly increases vapor generation. Analysis of the experiment demonstrates that increasing the free wet surface area through a hanging wick markedly improves yield, yet this concept is largely underexplored in the literature.

Lack of Studies Combining Passive Evaporation Enhancement with Passive Condensation Cooling: Existing works often treat evaporation and condensation as separate enhancement strategies. The integrated approach, using a wet wick for evaporation and a copper cooling coil for sub-dew-point condensation, as absorbed in analysis, is practically absent in the literature. No prior passive design has concurrently increased the evaporation area and lowered the condensing surface temperature without external energy input.

Limited Multi-Criteria Evaluation (Energy-Exergy–Economic–Environmental): Most studies assess performance only through yield or energy efficiency. Comprehensive multi-criteria evaluation (5E analysis), including exergy, exergoeconomic, and enviroeconomic performance, remains scarce. The studied research explicitly notes this gap and provides a rare holistic evaluation of a modified passive still.

Finally, only a small number of investigations focus on increasing the evaporation rate per unit surface area without expanding system footprint, indicating the need for design innovations that maximize productivity within constrained geometries.

2.5 Research objectives

Based on the gaps in the literature, the following objectives of study have been framed.

i. To design and experimentally evaluate a modified passive solar still with enhanced heat transfer for improved freshwater productivity.

ii. To analyze and compare the thermal performance and freshwater yield of SPSS and MPSS under different climatic conditions.

iii. To assess and compare the energy, exergy, and techno-economic performance of SPSS and MPSS at the system level.

iv. To develop and apply a novel exergoeconomic approach based on exergy gain per unit cost for solar desalination systems.

v. To evaluate the economic feasibility, environmental benefits, and CO_2 mitigation potential of MPSS for decentralized freshwater production in water-scarce regions.

2.6 Methodology to be adopted

Methodology adopted to carry out the analysis of the proposed experimental solar still follows the following steps:

Step I – Estimation of Solar Radiation

The annual and daily availability of solar energy is determined using the Liu and Jordan correlations to compute beam radiation (I_r) and global irradiation (I_g). Monthly distributions of radiant energy are obtained by accounting for the number of clear, hazy, partially cloudy, and fully cloudy days in each month.

Step II – Optimization of System Parameters

System parameters are optimized to achieve maximum thermal output. This includes estimating the temperatures of basin water, water surface, inlet water, collected

water, the hanging wick, and the inner and outer surfaces of the cover glass; relative humidity; still BDT; WBT; and wind velocity of the surrounding air, on an hourly and daily basis. The objective is to identify parameter combinations that yield the highest thermal performance.

Step III – Thermal and Exergy Assessment

Thermal energy gain, thermal exergy, and freshwater production are quantified on an hourly and daily basis for different sky conditions, including blue sky clear, and full hazy days. Evaluating these parameters under varying atmospheric conditions allows a comprehensive assessment of the thermodynamic behavior and performance of the proposed system across diverse climatic scenarios.

Step IV – Energy, Enviroeconomic and Exergoeconomic Analysis

The energy, environmental, and economic performance of the system is assessed using enviroeconomic and exergoeconomic indicators. These metrics provide a quantitative evaluation of the environmental advantages, associated costs, and exergy-linked economic efficiency of the proposed configuration.

Step V – Comparative Performance Analysis

The proposed modified system's numerical results are compared against those of previously established and proposed simple system configurations to evaluate improvements in thermal efficiency, exergetic behavior, freshwater yield, and overall techno-economic viability.

2.7 Thesis plan

Thesis, entitled "Impact of Free Water Surface on Single Slope Solar Still Yield," is divided into four chapters.

Chapter 1 includes an introduction, types of solar distillers, historical background and materials required, working principle, mode of heat transfer, merits and demerits, and research work. The last part of this chapter deals with water quality, performance parameters, including climatic and design parameters, and the application of distilled water.

Chapter 2 includes a literature review and a review of existing research. The passive and active solar distiller systems are discussed. The effects of parameters such as the temperature of basin water, water surface, inlet water, collected water, hanging wick, the inner and outer surfaces of the cover glass, relative humidity with still air, DPT, WBT, and wind velocity of the surrounding air, etc., have been presented in this part. In the active solar distiller units are surveyed. Various parameters are studied, including the effect of basin water depth, effect of relative humidity, and addition of a free surface for evaporation and condensation of vapor.

- Historical background
- Research gap
- Research objective
- Methodology to be adopted
- Thesis plan

Chapter 3 includes methodology. The experimental methodology adopted in this study was designed to evaluate the thermodynamic, economic, and environmental performance of a modified passive single-slope solar still (MPSS) relative to a simple passive solar still (SPSS). The approach integrates system fabrication, instrumentation, experimental operation, data acquisition, and performance evaluation under identical climatic conditions.

Experimental System Fabrication

Two geometrically identical single-slope solar stills were constructed from GI material, with a basin area of 1×1 m², a 10 cm insulation thickness, and a 5 mm glass cover inclined at 30°. Groundwater was used as the feed in both systems.

- **SPSS:** Operated as the reference unit with a fixed water depth of 10 cm maintained via a float valve.
- **MPSS:** Modified to incorporate (i) a black hanging wick on all vertical surfaces to expand the effective evaporative area, and (ii) a helical copper cooling coil

wrapped in a wet cloth, functioning as a passive condenser by maintaining its surface temperature near the dew point.

Instrumentation and Measurements for both stills included thermocouples, a digital solarimeter, a digital hygrometer, an anemometer, and graduated flasks for yield measurement.

Parameters measured hourly included:

- Basin water temperature,
- Inner/outer glass temperatures,
- Ambient and moist-air temperature,
- Relative humidity,
- Solar irradiance,
- Wind speed,
- Distillate yield.

Instrument accuracy and uncertainty were evaluated using standard uncertainty-propagation methods.

Experiments were conducted in May and June 2023 between 09:00 AM–06:00 PM under several clear-sky conditions. Both stills operated purely in passive mode. In SPSS, evaporation occurred from the free water surface, and condensation occurred on the cooler inner glass. In MPSS, evaporation was enhanced by the vertical wet-wick surface, while condensation increased due to the low-temperature copper coil acting as an auxiliary condensing surface.

The water depth in each still was maintained at 10 cm throughout the test period.

Thermal and Psychrometric Evaluation

Temperature distribution, evaporation rate, and condensation behavior were analyzed using measured thermal data and moist-air properties.

Performance assessment included:

- Thermal efficiency,

- Exergy and exergy efficiency,
- Hourly and cumulative freshwater yield,
- Moist-air temperature, dew-point evaluation, and wick performance.
- Economic, Exergoeconomic, and Environmental Analysis

Economic indicators (capital recovery factor, uniform annual cost, and cost per liter) were calculated from the system's investment and productivity. Exergoeconomic parameters were computed from the exergy output-to-annual cost ratio.

Environmental metrics, including CO_2 emissions, mitigation potential, and carbon credit earnings, were estimated based on embodied energy and annual energy/exergy output of each still.

Comparative Evaluation:

Thermal, exergy, economic, exergoeconomic, and environmental performances of MPSS and SPSS were compared using experimentally measured and computed values. MPSS design was assessed for its overall improvement in freshwater yield, efficiency, cost-effectiveness, and sustainability.

Chapter 4 includes results and discussion. Results and discussion for the modification of a solar still by introducing a hanging wick and a helical copper cooling coil using a wet cloth at the web bulb temperature of the surrounding air, and a comparison with a simple passive solar still, have been presented.

Chapter 5 includes conclusions and future scope. The study presents the conclusions and potential future developments for enhancing a passive single-slope solar still by incorporating a black hanging wick and a helical copper cooling coil enveloped in a wet cloth, maintained near wet-bulb temperature. The findings highlight the effectiveness of these modifications in improving both evaporation and condensation processes. Based on the outcomes of the present investigation, several recommendations have been outlined to guide subsequent research efforts aimed at further advancing the performance and applicability of modified passive solar still systems.

Chapter 3

METHODOLOGY

3.1 Experimental Setup

Experimental investigation employed two identically constructed single-slope solar stills: a Simple Passive Solar Still (SPSS) serving as the reference system, and a Modified Passive Solar Still (MPSS) incorporating a hanging wick and a passive cooling coil to enhance evaporation and condensation, respectively, as shown in Figure 3.1. Both systems were fabricated using the same geometrical dimensions and materials to ensure that any observed performance differences resulted solely from the modifications introduced in MPSS.



Figure 3.1 Actual Picture of Experimental setup of SPSS and MPSS

3.1.1 Simple Passive Solar Still (SPSS)

The SPSS consists of a conventional single-slope desalination unit designed to operate entirely on passive solar energy. The major components and construction features are described below.

a. **Basin Structure**

The basin is constructed from 2 mm-thick galvanized iron (GI) sheet, selected for its structural rigidity and corrosion resistance. Basin dimensions: 1.0 m × 1.0 m area, providing sufficient water surface exposure for natural evaporation. The inner surface of the basin is coated with white paint (high reflectivity) to maximize heating of basin water.

b. **Thermal Insulation**

The basin bottom and sidewalls are insulated externally using 50 mm thick thermocol (expanded polystyrene). The insulation minimizes conductive heat loss to the ground and enhances basin water temperature.

c. **Glazing Cover**

A 5 mm thick transparent glass cover is mounted on the top at an inclination of 30°, facing south to maximize solar incidence. The inclination ensures that distilled water trickles down to the collection trough. The glazing enables greenhouse trapping of long-wave radiation, aiding vapor generation.

d. **Water Depth and Feeding Arrangement**

A uniform water depth of 10 cm is maintained using a float-controlled inlet valve. This depth provides a balance between thermal storage and response time.

e. **Vapor Condensation and Collection**

Vapor generated from the heated basin water condenses on the inner surface of the glass cover. A GI channel fitted along the lower edge collects the condensate and directs it into a measuring flask.

3.1.2 Modified Passive Solar Still (MPSS)

The MPSS incorporates two major enhancements intended to improve evaporation and condensation efficiency: a black hanging wick to increase evaporative surface area and a helical copper cooling coil to create a low-temperature condensing zone. All other geometrical properties remain identical to those of SPSS.

a. **Hanging Wick Assembly**

A vertically suspended black jute wick is attached to all four interior side walls of the still. The wick material was selected based on capillary-rise tests demonstrating high porosity, high absorptivity, and strong water-wicking capability. The wick continuously remains wet due to natural capillary action, creating an extended free-water surface for evaporation. This configuration increases evaporation even when basin water temperature is moderate, as the wick exposes a larger surface area to solar radiation and air circulation.

Table 3.1 presents different wick materials, their porosity and capillarity, and suitable references for further information.

Table 3.1. Impact of wick materials with their probable porosity, capillarity, and explicability

Wick Material	Porosity	Capillarity	Applications	References
Cotton	High porosity (up to 80%)	Excellent capillarity, quick liquid uptake	Textile industry standards, ASTM specifications	[28]
Glass Fiber	Moderate porosity (30% to 50%)	High capillarity, stable in high temperatures	NASA research on thermal wicking materials	[32]
Ceramic Fiber	Low to moderate porosity (10% to 40%)	Moderate capillarity, heat-resistant	Thermal insulation studies, heat pipes	[32]
Stainless Steel Mesh	Adjustable porosity (10% to 70%) depending on weave	High capillarity for fine weaves, robust under pressure	Studies on porous media for wicking	[33]
Polypropylene Felt	High porosity (50% to 85%)	Moderate capillarity, suitable for oil absorption	ASTM material studies on synthetics	[32]
Cellulose	High porosity (up to 80%)	Very high capillarity, often used in paper-based applications	Research papers on capillary rise in cellulose	[28]

Carbon Fiber	Variable porosity (20% to 60%)	High capillarity for micro and nano-level pores	Advanced materials journals on carbon composites	[34]
Sintered Metal	Uniform porosity (20% to 50%)	High capillarity, used in heat pipes	Thermal engineering textbooks	[34]
Polyester Felt	High porosity (50% to 90%)	Moderate to high capillarity, depending on thickness	Industrial material guides	[33]
Nylon Mesh	Medium porosity (30% to 60%)	Moderate capillarity, durable under stress	Research on nylon wicking behavior	[32]

During operation of the Modified Passive Solar Still (MPSS), the black hanging cloth remains wet due to capillary action and its affinity to absorb water, as shown in Table 3.1. The hanging cloth was selected for its strong water-absorption characteristics, which are essential for maintaining continuous wetting of the vertical surfaces and thereby enhancing evaporation.

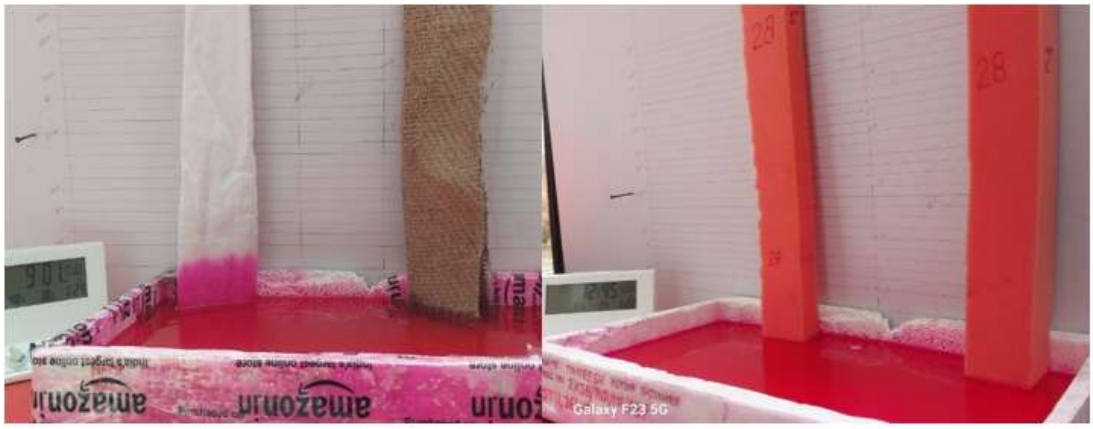

Figure 3.2 Experimental picture to analyze capillary effect

To identify the most suitable material for this purpose, a comparative capillary absorption test was conducted using sponge, cotton, and jute as candidates, as illustrated in Figure 3.2. Since the hanging cloth remains partially immersed in basin water during operation, capillary action was considered a critical criterion for selecting the material to ensure uninterrupted water transport to the exposed surfaces.

In addition to capillarity, material porosity was identified as a key parameter governing water retention capacity and evaporation potential. Accordingly, experimental evaluations were performed on different jute samples with varying porosity characteristics, as shown in Figure 3.3. The results indicate that Jute-A, possessing higher porosity, absorbed approximately 430 ml/m² of water under normal temperature and pressure (NTP) conditions. In contrast, Jute-B, with relatively lower porosity, absorbed only 285 ml/m² under identical conditions. These findings confirm that higher porosity significantly enhances water absorption and supports sustained thin-film evaporation, making Jute-A the most suitable material for the hanging wick application in the modified solar still.



(a) (b)

Figure 3.3 Jute with several porosities

b. **Helical Copper Cooling Coil as Auxiliary Condenser**

A copper coil (outer diameter 12 mm) is positioned along the inner side of the glazing cover. The coil is wrapped in a wet cotton cloth and maintained near wet-bulb temperature by periodic moistening. The coil surface serves as an additional low-

temperature condensation surface, improving condensation when inner glass temperature is near or above dew-point temperature. Copper is selected due to its high thermal conductivity and corrosion resistance.

c. **Basin and Structural Features**

Basin dimensions, material, glazing angle, and insulation are identical to SPSS to ensure a fair comparison. Basin inner walls are painted black to increase absorptivity.

d. **Water Feeding and Wick Wetting Mechanism**

The wick receives water directly from the basin via capillary action, eliminating the need for external pumps. During testing, the wick remained uniformly saturated, ensuring continuous thin-film evaporation.

e. **Condensate Collection**

MPSS includes two collection points:

- Primary channel**:** for condensate formed on the glass surface.
- Secondary collection vessel (CV_2)**:** placed beneath the cooling coil to capture condensate dripping from the wetted coil surface.

f. **Combined Evaporation–Condensation Enhancement**

The MPSS system simultaneously enhances:

- Evaporation**: through increased exposed wet surface on hanging wick**
- Condensation: **through a** cooled auxiliary condensing surface (copper coil)

This synergistic modification is experimentally validated, resulting in a significant improvement in still productivity.

3.1.3 Comparative Features of SPSS and MPSS

To achieve the objective's outcomes, both SPSS and MPSS are fabricated identically, except for the hanging cloth and copper coil, which are added as modifications in MPSS. During the experimental observation, both stills are exposed in same surrounding conditions.

Table 3.2. Details of features of SPSS and MPSS

Feature	SPSS	MPSS
Basin Dimensions	1m × 1m	1m × 1m
Basin Material	2 mm GI sheet	Same
Insulation	50 mm thermocol	Same
Glass Cover	5 mm, 30° tilt	Same
Evaporation Surface	Only basin water	Basin + hanging wick
Condensation Surface	Glass only	Glass + copper coil
Water Depth	10 cm	10 cm
Mode of Operation	Passive	Passive with enhanced surfaces

3.1.4 Summary of Experimental Setup

Experimental setup consists of two structurally identical solar stills, differing only in the evaporation and condensation enhancement mechanisms introduced in MPSS. This ensures that performance variations arise from design innovation rather than environmental or geometric differences. The setup enables simultaneous operation and provides reliable comparative data for thermal, psychrometric, exergy, and economic evaluation.

3.2 Fabrication of Experimental Setup

This section describes the complete fabrication process of both the Simple Passive Solar Still (SPSS) and the Modified Passive Solar Still (MPSS). All dimensions, materials, and construction parameters were kept identical for both systems to enable an accurate performance comparison.

3.2.1 Fabrication of Simple Passive Solar Still (SPSS)

The SPSS was designed as a standard benchmark unit, constructed using conventional single-slope basin-type geometry. The fabrication steps included material selection, structural assembly, sealing, and instrumentation.

i. Basin Construction

The basin was fabricated from 2 mm-thick galvanized iron (GI) sheet, chosen for its rigidity, durability, and corrosion resistance. The basin area is 1 × 1 m², as recommended for small-scale solar desalination studies. Side walls were formed by bending the GI sheet vertically to a height sufficient to accommodate a 10 cm water depth. The interior basin surface was coated with black, high-absorptivity thermal paint, ensuring maximum solar energy absorption and increasing the basin's effective thermal gain.

ii. Thermal Insulation

To minimize conductive heat losses, bottom and vertical exterior walls were lined with 10 cm of polystyrene (thermocol) insulation. This insulation layer was fixed using adhesive compounds and mechanical supports to ensure long-term durability under outdoor conditions.

iii. Glazing System

A 5 mm thick standard window glass was used as the transparent cover. The cover was cut to match the basin dimensions and mounted at a 30° inclination toward the south to maximize solar incidence and promote condensate flow. Edges were sealed using silicone sealant and rubber gasket tape to prevent vapor leakage during operation.

iv. Condensate Channel and Outlet

A GI condensate collection channel was fabricated and attached to the lower end of the glass cover. The channel was slightly inclined so that condensate flowed smoothly into a PVC collection tube leading to a measuring flask. The PVC tube remained submerged in the collection container to prevent vapor escape due to pressure differences.

v. Structural Support & Mounting

The assembled SPSS was mounted on a mild steel (MS) stand of appropriate height to ensure stability and proper drainage alignment. All joints were strengthened using welds or mechanical fasteners to withstand outdoor environmental loads.

vi. Instrumentation Integration

Instrumentation ports were incorporated during fabrication:

- Thermocouples (Type-K) were installed at locations including basin water, inner glass surface, outer glass surface, and still air space.
- A digital solarimeter, a digital thermo-hygrometer, and an anemometer were mounted externally to measure radiation, humidity, and wind speed, respectively.

3.2.2 Fabrication of Modified Passive Solar Still (MPSS)

The MPSS incorporates two major enhancements over SPSS:

i. A black hanging wick on all internal vertical walls to improve evaporation.

ii. A helical copper cooling coil wrapped with wet cloth to enhance condensation.

The fabrication steps below describe how these components were integrated into the standard SPSS structure to produce the MPSS.

i. Basin and Structure (Same as SPSS)

MPSS uses the same 1 × 1 m² GI basin, 2 mm sheet thickness, and insulation system as the SPSS to ensure equivalent baseline thermal conditions. The glazing and sealing arrangements are also identical.

ii. Fabrication and Installation of Hanging Wick System

Based on capillary rise tests and porosity evaluation, jute cloth with a high water-absorption capacity (430 ml/m² at NTP) was selected as the wick material.

Jute sheets were cut to match the inner dimensions of the sidewalls. Each sheet was dyed black using non-toxic, water-resistant dye to increase solar absorptivity. Wick

sheets were suspended vertically from top brackets inside the still, ensuring full contact with the water basin at the bottom. Capillary action kept the wick continuously wet, allowing additional free water surface area for thin-film evaporation.

iii. Fabrication of Helical Copper Cooling Coil

A 12 mm copper tube was selected for its high thermal conductivity and corrosion resistance. The copper tube was manually bent into a helical configuration using a pipe-bending jig. One end of the coil remained open inside (customize) the still chamber to interact with moist air. The other end extended into the secondary collection vessel (CV2) to prevent steam leakage.

The coil surface was wrapped with absorbent cotton cloth kept wet during operation. The coil surface temperature was below the dew-point temperature of the surrounding air and maintained between 18°C and 24°C, enabling high condensation rates.

iv. Integration of Wick and Coil into MPSS Frame

The wick was installed before glazing placement, ensuring full exposure to solar radiation. The copper coil was placed near the upper section of the basin side, below the glazing, to maximize contact with rising vapor. Both components were anchored securely to prevent displacement during water flow.

v. Vapor-Tight Sealing

Just like SPSS, all joints, inspection ports, and glazing interfaces were sealed with silicone rubber sealant to prevent steam loss. Rubber gaskets were used at coil exit points to maintain airtight integrity.

vi. Condensate Collection System

MPSS includes two condensate paths:

- Primary GI channel (same as SPSS) collects condensate from glass cover.
- Secondary collection vessel (CV_2) collects condensate dripping from the cooled copper coil.

This dual-path setup increased total distillate yield.

vii. Instrumentation Placement

Additional thermocouples were mounted on:

- Surface of hanging wick
- Wet surface of copper coil
- MPSS inner air temperature

These were required to evaluate enhancements to psychrometric and thermal responses.

3.2.3 Summary of Fabrication Differences

Table 3.3. Difference in fabrication of SPSS and MPSS

Component	**SPSS**	**MPSS**
Basin GI sheet	2 mm	2 mm
Basin Area	1 m × 1 m	1 m × 1 m
Glass Cover	5 mm, 30° tilt	5 mm, 30° tilt
Insulation	10 cm thermocol	10 cm thermocol
Wick	No	Black hanging jute wick
Cooling Coil	No	Copper helical coil with wet cloth
Condensation Path	Single	Dual (glass + coil)
Free Evaporation Area	Basin only	Basin + vertical wick
Expected Gain	Baseline	Yield improved by 51.73%

3.2.4 Photograph of Different Stages of Fabrication of Experimental Setup



(a) Fabrication of GI box



(b) Installation of thermocouples



(c) Preparation sizing of wick



(d) Insulating both stills with polystyrene



(e) Installation of copper coil



(f) Covering copper coil with white



(g) Installation of hygrometer



(h) SPSS and MPSS experimental setup

Figure 3.4 Photographs during fabrication of SPSS and MPSS

3.3 Instrumentation for Experimental Setup

Accurate and continuous measurement of thermal, psychrometric, and distillate output parameters was essential for evaluating the comparative performance of the Simple Passive Solar Still (SPSS) and the Modified Passive Solar Still (MPSS). The instrumentation was selected considering operational reliability, measurement precision, and suitability for outdoor climatic conditions. All sensors were calibrated prior to experiments, and identical measurement positions were maintained for both setups to ensure data consistency. All the instruments were calibrated to ensure correct readings.

3.3.1 Temperature Measurement System

Type-K thermocouples were extensively used due to their wide temperature range, fast response time, and stability in humid environments, as shown in Figure 3.5.



Figure 3.5 Picture of installed thermocouple

These sensors monitored the thermal behavior of key components in both SPSS and MPSS.

Measurement Locations in SPSS

- Basin Water Temperature (T_w): one thermocouple, immersed at mid-depth, to record the bulk water temperature.
- Inner Glass Temperature (T_{gi}), affixed to the inner glass surface using thermal paste.

- Outer Glass Temperature (T_{go}), mounted on the exterior glass surface to quantify heat loss to ambient.
- Moist Air Temperature (T_{ma}), suspended in the vapor chamber to capture evaporative thermal behavior.
- Ambient Temperature (T_a), shielded thermocouple positioned near the still but isolated from direct solar radiation.
- Wick Surface Temperature (T_{wick}) at the surface of hanging cloth.
- Cooling Coil Surface Temperature (T_{coil}), mounted on the helical copper coil wrapped with wet cloth to monitor the condensation temperature relative to dew point.

All thermocouples were connected to a digital temperature data logger with accuracy ±0.1°C.

3.3.2 Solar Radiation Measurement

Figure 3.6 shows a calibrated digital solarimeter used to measure the global solar irradiance (Ig) incident on a horizontal surface.



Figure 3.6 Picture view of digital solarimeter

- Measurement range: typically 0–2000 W/m²
- Accuracy: ±5%
- Sampling interval: 1 hour

Solar radiation data were crucial for estimating absorbed energy, thermal efficiency, and for modeling evaporation kinetics.

3.3.3 Humidity and Moist Air Measurement

A digital thermo hygrometer, as shown in Figure 3.7, was placed adjacent to the still to record Relative Humidity (RH) and Ambient Moist-Air Temperature. Recorded data from a digital hygrometer were used to compute partial vapor pressure, humidity ratio, and dew point temperature. Psychrometric properties influencing condensation in SPSS and MPSS.



Figure 3.7 Picture of digital thermos-hygrometer

The psychrometric variation indicates the importance of tracking moist air around the cooling coil. Hence, a secondary digital hygrometer was used near the coil zone to measure dew-point temperature and assess condensation enhancement.

3.3.4 Wind Velocity Measurement

A portable digital anemometer, as shown in Figure 3.8, was used to record wind speed (Vwind) near the still. Wind velocity affects external convective heat transfer, evaporative loss, and the cooling rate of the glass cover's outer surface. Typical range recorded: 0.5–5.5 m/s depending on climatic conditions.

3.3.5 Distillate Output Measurement

Hourly freshwater yield was collected and measured using a high-precision graduated cylinder.

For MPSS:

Two separate containers were used:

- For condensate from the glass surface (primary distillate)
- For condensate dripping from the cooling coil (enhanced condensation zone)

This allowed quantification of the contribution of the wick and cooling coil to total productivity. All data were tabulated for thermal, psychrometric, exergy, and economic analysis.



Figure 3.8 Picture of digital anemometer

Table 3.4 Instrumentation for SPSS and MPSS

Parameter	**SPSS**	**MPSS**
Basin Water Temp	✓	✓
Glass Inner/Outer Temp	✓	✓
Ambient Temp	✓	✓
Moist Air Temp	✓	✓
Solar Radiation	✓	✓
Relative Humidity	✓	✓ (additional coil-zo monitoring)
Wick Surface Temp	✗	✓

Parameter	SPSS	MPSS
Cooling Coil Temp	✗	✓
Two-Point Distillate Collection	✗	✓

3.4 Experimental Procedure

Experimental procedure was designed to evaluate and compare the thermal, psychrometric, and freshwater productivity performance of the Simple Passive Solar Still (SPSS) and the Modified Passive Solar Still (MPSS). Both systems were operated simultaneously under identical environmental conditions to ensure reliable comparative analysis. The procedure consisted of pre-experimental preparation, controlled operation during sunlight hours, hourly data acquisition, and post-experimental yield analysis.

3.4.1 Pre-Experiment Preparation

Prior to the commencement of daily monitoring and data acquisition, both solar still systems were systematically prepared, and all operational parameters were thoroughly inspected to ensure proper functioning and experimental reliability. The glass covers of both stills were thoroughly cleaned using distilled water and a soft cloth to ensure maximum solar transmittance.

- Each still was filled with groundwater to a constant depth of 10 cm, regulated using a float valve system.
- For MPSS only, the wick was allowed to soak until fully saturated through natural capillary action.
- For MPSS only, the copper cooling coil was wrapped with a clean cotton cloth.
- Thermocouples were checked properly.
- Digital solarimeter, digital thermo hygrometer, and digital anemometer readings were verified.
- Graduated cylinders were reset and dried.

3.4.2 Operating Procedure during Experiments

Experimental investigations were conducted from 11 May 2023 to 16 June 2023 under outdoor environmental conditions. During the experimental period, various weather conditions were observed, including clear-sky, hazy, and cloudy days. Measurements were recorded at hourly intervals from 09:00 AM to 06:00 PM on all experimental days. For the comparative performance analysis of the simple passive solar still (SPSS) and the modified passive solar still (MPSS) under clear-sky conditions, the average data obtained from several clear days, specifically 11th May, 12th May, and 15th May 2023, were considered. Similarly, for the analysis under hazy atmospheric conditions, the average data from selected hazy days, namely 13th May, 14th May, 16th May, and 18 May 2023, were utilized. SPSS and MPSS were operated side-by-side, ensuring identical wind exposure, solar radiation, and fluctuations in ambient temperature and humidity. This parallel operation allowed direct comparison of their performance.

For both SPSS and MPSS, following parameters were monitored:

- Basin water temperature
- Inlet and collected water temperature
- Inner and outer cover glass temperature
- Wick surface temperature (only MPSS)
- Cooling coil temperature (only MPSS)
- Moist air temperature inside basin
- Solar radiation intensity
- Relative humidity and ambient temperature
- Wind speed

3.4.3 Measurement of Distillate Output

i. SPSS Distillate Collection

Condensed water flowing down the glass cover was collected via a sloped GI channel into a graduated flask. Volume of collected was recorded hourly.

ii. MPSS Dual-Path Distillate Collection

MPSS produces distillate from two independent zones: Primary condensation on the glass cover, collected similarly to SPSS, and Secondary condensation on the copper coil, dripping into a dedicated measuring cylinder. Each was measured separately to quantify the effect of enhanced condensation.

3.4.4 End-of-Day Procedure

At 06:00 PM, final readings were recorded as the end of the experimental day.

- All temperatures recorded.
- Total distillate collected from SPSS and both MPSS collection points was measured.
- Basin water depth was verified to ensure identical operating conditions throughout the day.
- Instruments were powered down and covered to prevent moisture exposure overnight.

3.5 Psychrometric Modelling of SPSS and MPSS

Psychrometric modelling provides a quantitative understanding of the evaporation–condensation processes inside solar stills by describing the thermodynamic state of moist air. Since evaporation depends on the capacity of moist air to hold water vapour and condensation depends on the relationship between the inner glass (or coil) temperature and the dew-point temperature, psychrometric analysis is essential for predicting and interpreting the performance of both the Simple Passive Solar Still (SPSS) and the Modified Passive Solar Still (MPSS).

3.5.1 Fundamentals of Psychrometric Modelling

The moist air inside a solar still is a two-component mixture of dry air and water vapour. At any time, the thermodynamic state of this mixture is defined by:

- Dry-bulb temperature (T_a)
- Relative humidity (RH)

- Vapour pressure (P_v)
- Humidity ratio (w)
- Dew-point temperature (T_{dp})

These properties determine the evaporation potential at the water/evaporating surfaces and the condensation feasibility at the condensing surfaces.

3.5.2 Partial Vapour Pressure (P_v)

The vapour pressure of water in the still chamber is calculated using:

$$P_v = RH \times P_{Sat}(T_a) \quad (3.1)$$

This partial vapour pressure drives the rate of evaporation from the water surface or wick surface in MPSS.

3.5.3 Humidity Ratio (w)

The humidity ratio (kg water vapour per kg dry air) is a crucial indicator of how much moisture the air can hold:

$$w = 0.622 \left[\frac{P_v}{(P_{atm} - P_v)}\right] \quad (3.2)$$

A higher humidity ratio indicates a larger mass of evaporated water in the chamber.

- MPSS consistently exhibits higher values of w because the wick provides an extended wet area and higher evaporative flux.
- SPSS, however, depends solely on basin water**,** resulting in lower humidity ratio at identical conditions.

3.5.4 Dew Point Temperature (T_{dp})

Dew point temperature is obtained from vapour pressure using empirical psychrometric relationships:

$$T_{dp} = f(P_v) \quad (3.3)$$

3.5.5 Psychrometric Conditions for Condensation

Condensation occurs when surface temperature is lower than corresponding dew point temperature. While surface refers to:

- Inner and outer surface of glass cover in SPSS
- Inner and outer surface of glass and cooling coil in MPSS

Since the coil is kept near wet-bulb temperature via evaporative cooling, which is much lower than the cover glass temperature, condensation occurs much earlier and for a longer duration.

This phenomenon, experimentally validated, significantly increases the MPSS condensation rate.

3.5.6 Evaporation Rate Expression Using Psychrometric Difference

Evaporation is driven by the difference between saturation vapour pressure at basin water (or wick) temperature and vapour pressure of the surrounding air:

$$m_{evap} \propto (P_{sat}(T_w) - P_v)) \quad (3.4)$$

- For SPSS, evaporation occurs only from the basin surface, resulting in moderate P_{sat} and hence moderate $(P_{sat} - P_v)$ while
- For MPSS, wick surface temperature T_{wick} is slightly higher due to greater solar absorption and wick provides thin-film evaporation, which increases evaporation efficiency**.**

Thus, $(P_{sat} - P_v)$ is higher → higher evaporation.

3.5.7 Airflow and Moist-Air Stratification

Observations from the psychrometric concept indicate:

- Temperature stratification inside the still, with higher temperatures near the water/wick surface and lower temperatures near the glass or coil.
- Humidity stratification, with highest humidity near the evaporative surfaces.

MPSS exhibits stronger gradients due to increased evaporation and enhanced condensation sink (coil).

This stratified moist-air movement increases convective mass transfer.

3.5.8 Psychrometric behavior comparison between SPSS and MPSS

Psychrometric analysis reveals that MPSS consistently operates under more favorable moisture and temperature conditions than SPSS. Due to enhanced evaporation from the hanging wick, MPSS exhibits higher specific humidity and moist air enthalpy within the chamber, along with a lower effective temperature difference between dry-bulb and dew-point temperatures. This condition promotes sustained condensation on the inner glass surface. In contrast, SPSS shows comparatively lower moisture content and weaker vapor pressure gradients. Overall, the improved psychrometric environment in MPSS leads to enhanced evaporation–condensation coupling and higher freshwater productivity, as shown in Table 3.5.

Table 3.5 Comparison between psychrometric outcomes for SPSS and MPSS

Parameter	SPSS	MPSS
Evaporation Surface	Basin water only	Basin + hanging wick
Typical Humidity Ratio (w)	Moderate	Higher (more vapour formed)
Dew-Point Temperature	Lower	Higher (due to more vapour)
Condensing Surface Temp	Only glass	Glass + much cooler coil
Duration of Condensation	Limited	Extended (coil below T_{dp})
Psychrometric Driving Forces	Weak	Strong (higher T_{dp}, higher P_v)

MPSS shows superior psychrometric performance, directly increasing distillate output.

3.5.9 Psychrometric Impact on System Productivity

Experimental results indicate that enhanced psychrometric conditions in MPSS resulted in:

- Higher moist-air temperature
- Higher humidity ratio
- Higher dew-point temperature

- Lower condensing surface temperature (due to coil)

Which together yield significant productivity enhancement (51.73% more distillate).

3.5.10 Graphical Psychrometric Interpretation

While specific graphs must be plotted from experimental data, the results confirm that:

- T_{ma} rises progressively from morning to noon, peaking earlier in MPSS.
- RH initially increases, then decreases during peak hours due to high temperatures, and rises again toward evening.
- Dew point curves show earlier overlap with T_{coil} in MPSS, leading to earlier condensation onset.

Summary of Psychrometric Modelling

1. Moist-air properties govern evaporation and condensation inside solar stills.
2. MPSS generates greater vapour mass due to wick-based thin-film evaporation.
3. MPSS achieves earlier and longer condensation periods via a cooled coil.
4. Dew-point tracking proves that condensation feasibility is far superior in MPSS.
5. Psychrometric enhancement explains the experimentally observed performance gain.

3.6 Uncertainty Analysis

Uncertainty analysis is an essential component of evaluating experimental solar-thermal systems, as it quantifies the reliability of measured data and establishes confidence in the derived performance indicators. For the present study, uncertainty estimation was conducted for all primary measurements and the dependent variables derived from them.

3.6.1 Purpose of Uncertainty Analysis

The objectives of performing uncertainty analysis for SPSS and MPSS were:

- To quantify the measurement confidence of all recorded parameters (temperature, solar radiation, humidity, wind velocity, and distillate yield).
- To assess the influence of instrument limitations on calculated thermal, energy, exergy, economic, and environmental performance indicators.

To ensure that comparative evaluation between SPSS and MPSS is statistically reliable and not biased by measurement errors.

3.6.2 Instrumentation Considered for Uncertainty Evaluation

The uncertainty analysis was based on all sensor measurements from both SPSS and MPSS experiments, which were included in the uncertainty estimation.

The uncertainty analysis in this study was performed using the method of propagation of errors, which is commonly used in experimental thermal engineering studies. According to this method, when a dependent variable is a function of several independent variables, the overall uncertainty can be determined from the individual uncertainties of the measured parameters during experiments.

If a parameter Y is a function of several independent variables x_1, x_2, x_3 …..,x_{nx},, then the uncertainty in the measured value of Y is given as Eq. (3.5)[84]

$$U(Y) = \left[\left(\frac{\partial Y}{\partial x_1}\right)^2 u^2(x_1) + \left(\frac{\partial Y}{\partial x_2}\right)^2 u^2(x_2) + \left(\frac{\partial Y}{\partial x_3}\right)^2 u^2(x_3) \ldots\ldots \left(\frac{\partial Y}{\partial x_n}\right)^2 u^2(x_n)\right]^{1/2} \quad (3.5)$$

In Table 3.6, the uncertainty values were adopted from manufacturer specifications and validated against calibration records.

Table 3.6 Details of instruments for uncertainty analysis

Parameter	Instrument	Accuracy	Uncertainty
Temperature	RECOS Thermocouple	±0.1°C	0.06°C
Solar Radiation	Tenmars TM-207 Solarimeter	±10 W/m²	5.77 W/m²

Parameter	Instrument	Accuracy	Uncertainty
Wind Velocity	Benetech GM8901+ Anemometer	±0.1 m/s	0.55 m/s
Relative Humidity & Ambient Temp	Mextech TM-1 Hygrometer	±3%	1.73%
Freshwater Yield	Borosil Graduated Flask	±10 ml	5 ml

3.7 Thermal Modelling

Thermal modelling provides a theoretical framework for predicting basin water temperature, evaporation rate, condensation heat transfer, and overall thermal efficiency in both SPSS and MPSS.

Modelling approach adopted in this research follows the classical energy-balance method**,** extended with additional evaporation and condensation terms to account for wick-assisted evaporation and coil-assisted condensation in the MPSS.

3.7.1 Assumptions for the Thermal Model

To simplify the governing equations without compromising accuracy, the following widely accepted assumptions were adopted:

i. Heat transfer processes are quasi-steady for each hourly interval.

ii. Basin water is well-mixed; thus, the temperature of basin water is considered uniform.

iii. Glass cover temperature is uniform on its inner surface.

iv. Losses through joints and seals are negligible due to proper insulation.

v. Radiation is the only direct mode of solar energy input.

vi. Wick thin-film evaporation in MPSS is modelled as an extended evaporating surface.

vii. The copper cooling coil provides an additional condensation sink, modelled separately.

3.7.2 Energy Balance of Basin Water in SPSS

Basin water receives solar energy, absorbs heat from the basin liner, and loses heat through evaporation and convection to the inner glass.

The energy balance is expressed as:

$$I_r \tau_g \alpha_b A_b = m_w c_p \frac{T_w}{dt} + Q_{evap} + Q_{conv,\ w\text{-}g} + Q_{rad,w\text{-}g} + Q_{loss} \quad (3.5)$$

Where, $Q_{conv} = h.\Delta T$ and $Q_{rad} = \sigma T^4$

3.7.3 Heat Transfer Coefficients Used in SPSS Modelling

For SPSS, conventional heat transfer occur during evaporation and condensation where heat transfer coefficient is evaluated by following

i. Evaporative Heat Transfer Coefficient (Dunkle Model)

$$h_{evap} = 0.016273\ h_{c,w\text{-}g} \left(\frac{P_v - P_g}{T_w - T_g}\right) \quad (3.6)$$

ii. Convective Heat Transfer Coefficient

$$h_{c,w\text{-}g} = 0.884 \left[(T_w - T_v) + \frac{(P_w - P_v)(T_w + 273.15)}{268900}\right]^{1/3} \quad (3.7)$$

iii. Radiative Heat Transfer Coefficient

$$H_{r,w\text{-}g} = \sigma \varepsilon_{eff} (T_w^2 + T_g^2)(T_w + T_g) \quad (3.8)$$

These equations were also used to estimate total heat losses and evaporation.

3.7.4 Modifications in MPSS Thermal Model

MPSS incorporates two additional thermal phenomena absent in SPSS:

i. Wick-assisted evaporation

ii. Coil-assisted condensation

Therefore, the thermal model is expanded to include additional terms that represent:

- Increased evaporation surface area
- Reduced condensation surface temperature
- Increased vapour mass inside the chamber

- Enhanced heat and mass transfer due to the psychrometric changes.

3.7.5 Energy Balance for MPSS

Energy balance is modified to:

$$I_r\tau_g\alpha_b A_c + I_r\tau_g\alpha_{wick}A_{wick} = m_w c_p\left(\frac{dT_w}{dt}\right) + Q_{evap,basin} + Q_{evap,wick} + Q_{conv,w-g} + Q_{conv,wick-g} + Q_{cond,coil} + Q_{loss} \quad (3.9)$$

Where new terms represent:

iv. Wick-Assisted Evaporation

$$Q_{evap,wick} = h_{evap,wick}(T_{wick} - T_{ma}) \quad (3.10)$$

The wick temperature T_{wick} is experimentally higher than basin water temperature due to improved absorptivity and thin-film evaporation.

v. Coil-Assisted Condensation

Condensation on the copper coil is modelled as:

$$Q_{coil} = h_{coil}(T_{air} - T_{coil}) \quad (3.11)$$

Since the coil temperature is lowered by wet-cloth evaporative cooling, condensation begins much earlier and continues longer, consistent with experimental results.

3.7.6 Combined Heat-Transfer in MPSS

Total heat-transfer coefficient becomes:

$$h_{total} = h_{evap,basin} + h_{evap,wick} + h_{conv} + h_{rad} + h_{cond,coil} \quad (3.12)$$

SPSS has:

$$h_{total,SPSS} = h_{evap,basin} + h_{conv} + h_{rad} \quad (3.13)$$

Thus,

$$h_{total,MPSS} > h_{total,SPSS}$$

This relation is consistent with the significantly higher experimental temperatures and evaporation rates observed in the MPSS.

3.7.7 Evaporation Rate Modelling

Evaporation mass flux:

$$\dot{m}_{evap} = \frac{Q_{evap}}{h_{fg}} \tag{3.14}$$

Total evaporation for MPSS:

$$\dot{m}_{evap,MPSS} = \dot{m}_{evap,basin} + \dot{m}_{evap,wick} \tag{3.15}$$

This equation matches the multi-surface evaporation model implied in MPSS.

3.7.8 Condensation Rate of Generated Vapor

Condensation mass flux:

$$\dot{m}_{cond} = \frac{Q_{cond}}{h_{fg}} \tag{3.16}$$

Total condensation for MPSS:

$$\dot{m}_{cond,MPSS} = \dot{m}_{cond,glass} + \dot{m}_{cond,coil} \tag{3.17}$$

Thus, MPSS has two condensation sinks, whereas SPSS has only one.

3.7.9 Thermal Efficiency of Still

Thermal efficiency is computed using:

$$\eta_{th} = \dot{m}\frac{h_{fg}}{I_g A} \tag{3.18}$$

MPSS consistently achieves a higher value due to the combined effects of wick and coil enhancements.

3.7.10 Validation of Thermal Model

Experimental work indicates that theoretical results matched experimental data with good accuracy:

- Peak water temperatures of both SPSS and MPSS matched predicted trends.
- Evaporation rate correlation agreed with Dunkle's model extended to MPSS.
- Condensation predictions aligned with coil temperature tracking dew point.

This validates the modelling approach.

Summary of Thermal Modelling Procedure

- SPSS uses classical basin energy balance equations.
- MPSS model introduces additional evaporative and condensing terms.
- Wick increases absorbed heat and evaporation surface area.
- Coil maintains surface below dew point → improved condensation.
- Theoretical predictions closely match measured temperatures and yields.

3.8 Exergy Modelling of SPSS and MPSS

Exergy analysis evaluates the *quality* of energy transformations inside solar stills and quantifies the useful work potential associated with heat and mass transfer. Unlike thermal analysis, which considers only energy magnitude, exergy modelling incorporates system irreversibilities, ambient reference conditions, and entropy generation.

Thus, it provides a deeper insight into the performance differences between the Simple Passive Solar Still (SPSS) and the Modified Passive Solar Still (MPSS).

The MPSS, through wick enhanced evaporation and coil assisted condensation, reduces internal entropy generation, improves vapor-flow exergy, and increases exergy efficiency compared to SPSS.

3.8.1 Exergy of Incident Solar Radiation

The concept of exergy analysis has been developed to study the system in the context of the Second Law of Thermodynamics. The maximum amount of useful work in equilibrium with its environment is called exergy. To reduce losses in exergy and achieve better results, exergy is analyzed and evaluated by Tiwari et al. [45]:

$$E_{X,U} = (\dot{m} \times L)(1 - T_a \left(\frac{T_a}{T_w}\right) \quad (3.19)$$

Where L is calculated as in Eq (3.20)

$$L = 3.1615 \times 10^6 \times [1- (7.616 \times 10^{-4} \times T_v)]; \text{ for } T_v > 70^oC \quad (3.20)$$

Exergy is calculated for the Sun by the Petela model as evaluated by Kant and Kumar [85]; Shatar [86]:

$$E_{X,S} = I_g A_c [1 + \frac{1}{3}\left(\frac{T_a}{T_s}\right)^4 - \frac{4}{3}\left(\frac{T_a}{T_s}\right)] \quad (3.21)$$

3.8.2 Exergy Input to Solar Stills

Since only a fraction of solar energy propagates through the glass cover, exergy input to the still is:

$$E_{X,in} = \tau_g E_{Xsolar} \quad (3.22)$$

This parameter was identical for both SPSS and MPSS to ensure comparative consistency.

3.8.3 Exergy Output from the Solar Still (Distillate Exergy)

The useful exergy output corresponds to the ability of evaporated water to perform work as it undergoes phase change. This exergy is carried by the produced distillate and is given by:

$$E_{X,out} = \dot{m}_{dist}[h_{fg} - T_a \Delta s] \quad (3.23)$$

Because MPSS achieves higher basin/wick temperature and higher evaporation rate, Exout is naturally higher.

3.8.4 Exergy Efficiency of stills

Exergy efficiency for solar still is calculated as Kant and Kumar, [47]:

$$\eta_{ex}(\%) = \frac{E_{X,U}}{E_{X,S}} \times 100 \quad (3.24)$$

Higher values indicate better utilization of solar exergy.

3.8.5 Exergy-Based Productivity Assessment

According to the observation, exergy modelling revealed:

- Exergy output of MPSS was substantially higher.
- Exergy destruction was lower in MPSS due to reduced thermodynamic irreversibilities.
- Exergy efficiency increased by a significant margin (reported values vary but typically 30% to 60% improvement).

- Exergy analysis clearly justified the improved freshwater yield observed in MPSS.

3.8.6 Exergy Flow

The outcomes imply the following exergy flow pathway:

i. Solar exergy input (transmitted through glass)

ii. Partition of energy into:

- useful exergy for evaporation
- rejected exergy through losses
- destroyed exergy due to entropy generation

iii. Condensation exergy recovery (glass + coil)

iv. Distillate exergy output

For MPSS only:

- wick-evaporation exergy
- coil-condensation exergy

Thus, MPSS has a richer exergy flow, with more productive pathways and fewer loss channels.

Summary of Exergy Modelling Procedure

The same modeling framework is applied to both stills, enabling a direct comparison of exergy efficiency and revealing MPSS's superior exergy utilization, as shown in Table 3.7.

Table 3.7 Summary of modelling of exergy analysis

Component	**SPSS**	**MPSS**
Evaporation Exergy	Basin only	Basin + Wick
Condensation Exergy	Glass	Glass + Coil
Irreversibility	Higher	Lower

Component	SPSS	MPSS
Exergy Efficiency	Moderate	Much Higher
Exergy Destruction	Large	Reduced

3.9 Economic Analysis

An economic analysis was conducted to quantify the financial feasibility and long-term cost-effectiveness of both the Simple Passive Solar Still (SPSS) and the Modified Passive Solar Still (MPSS). The procedure evaluates the capital cost, annualized cost, cost per liter (CPL), payback period, and economic viability based on the experimentally measured freshwater yield.

3.9.1 Objective of Economic Analysis for Experiments

The core objectives were to:

i. Determine the total system cost for SPSS and MPSS.

ii. Compute the Uniform Annual Cost (UAC) using economic lifetime and interest rate.

iii. Evaluate the cost per liter (CPL) of distilled water produced.

iv. Compare the economic advantage of MPSS relative to SPSS.

v. Quantify the economic impact of improved evaporation and condensation mechanisms.

3.9.2 Components of Economic Cost Estimation

The economic analysis included the following cost components:

i. Initial Cost (IC)

IC includes expenses for:

- Basin material (GI sheet)
- Glass cover
- Insulation material

- Frame and support structure
- Wick system (MPSS only)
- Copper cooling coil (MPSS only)
- Sealants and fabrication labor

MPSS had slightly higher capital cost due to wick and coil additions.

ii. Operation and Maintenance Cost (MC)

MC include:

- Cleaning of glass cover
- Wick maintenance/replacement (annual)
- Water for wetting coil cloth (MPSS)
- Occasional repair and seal replacement

Experimental work shows that both SPSS and MPSS require minimal O&M costs due to passive operation.

iii. Salvage Value (SV)

At the end of system life (15 to 20 years), a small salvage value was assumed for recoverable materials (glass, metal frame, copper coil). Salvage value (SV) is taken as 20% of IC [49]:

$$SV = 0.2 \times IC \tag{3.25}$$

3.9.3 Annualization of Capital Cost

To convert capital cost into equivalent annual cost, the Capital Recovery Factor (CRF) was applied:

$$CRF = {i(1+i)^n}\Big/{[(1+i)^n - 1]} \tag{3.26}$$

The Uniform Annual Cost (UAC) is then:

$$UAC = IC \times CRF + MC - SV \times CRF \tag{3.27}$$

3.9.4 Annual Distillate Production

Annual freshwater production (AP) was estimated as:

$$AP = m_{daily} \times N_{days} \tag{3.28}$$

3.9.5 Cost of water Per Liter (CWPL)

The most meaningful economic metric is CWPL. CWPL of fresh water produced is the ratio of UAC and annual productivity (AP) and is evaluated [87]:

$$\text{CWPL} = \frac{\text{UAC}}{\text{AP}} \tag{3.29}$$

Although MPSS has a higher CPL due to additional materials, it compensates by achieving higher yield and lower exergy destruction.

3.9.6 Comparative Interpretation of Economic Results

In Table 3.8, the economic analysis indicates that both SPSS and MPSS incur nearly identical capital and operating costs, due to minimal design modifications in MPSS. However, MPSS's significantly higher freshwater yield results in a substantially lower cost per liter than SPSS. Consequently, MPSS demonstrates superior economic viability, offering enhanced productivity and reduced unit water cost without a corresponding increase in investment.

Table 3.8 Comparison between economic results of SPSS and MPSS.

Metric	SPSS	MPSS	Interpretation
Capital Cost	Lower	Slightly Higher	Wick & coil increase cost
Annual Productivity	Moderate	High (+41%)	MPSS more efficient
CPL	Lower	Slightly higher	MPSS justified due to productivity
Exergoeconomic Value	Lower	Higher	MPSS uses energy more effectively

Metric	SPSS	MPSS	Interpretation
CO_2 Mitigation	Lower	Higher	MPSS more sustainable
Payback Period	Longer	Shorter	MPSS economically superior

3.10 Exergoeconomic analysis

Exergoeconomic analysis combines exergy analysis (Second Law of Thermodynamics) with economic evaluation to determine the monetary value of exergy losses and the cost-effectiveness of useful exergy output. This approach allows a more meaningful evaluation of solar desalination systems than energy-based economics alone, as it accounts for irreversibilities, quality of energy, and true thermodynamic productivity of SPSS and MPSS. The primary objectives of the exergoeconomic analysis are to:

i. Determine the cost-effectiveness of exergy production (freshwater distillation).
ii. Evaluate the exergy destruction cost**,** representing thermodynamic losses.
iii. Compare SPSS and MPSS based on the monetary value of their useful exergy outputs.
iv. Assess how design enhancements (wick and coil) in MPSS reduce exergy costs and improve overall performance.

This type of analysis is essential for modern solar desalination research as it links thermodynamic efficiency with economic feasibility.

The relationship between the system's overall annual cost, energy production, and exergy from the Sun is determined using exergoeconomic analysis. Exergoeconomic parameter based on the energy approach is evaluated [86]:

$$R_{en} = \frac{E_{n,o}}{\mathrm{UAC}} \tag{3.30}$$

To maximize the exergy benefit, the exergo-economic parameter was applied and calculated [88]:

$$R_{ex} = \frac{E_{x,o}}{\mathrm{UAC}} \tag{3.31}$$

3.11 Environmental analysis

According to Vijayan et al. [89], embodied energy is the total energy required to produce all materials and system components. Embodied energy technique is widely used in environmental assessments due to its adaptability and ease of system comparison. This study identifies high embodied-energy materials and enables their replacement with more favorable alternatives. The primary issue with this type of research is a lack of understanding of system boundaries. Solar distillation systems are constructed with materials such as stainless steel, glass wool, brass, mild steel, and aluminum. Solar distillation system was created using electricity generated by coal-fired power plants. The system operates solely on solar thermal energy, allowing for energy recovery during construction.

Environmental analysis determines how much carbon dioxide the solar desalination system emits and how much it neutralizes. It's important to ensure that the technology used does not raise CO_2 emissions, as this would be detrimental to the usage of renewable technologies. This analysis shows the system's net carbon emissions, which is crucial for selecting carbon-neutral technologies. The section includes the formulae for calculating CO_2 emissions and mitigation.

3.11.1 CO_2 emissions

According to the analysis by Kant et al. [90], during the generation, transmission, and distribution of 1 kWh, 2 kg of CO_2 are produced by the power plant.

Net estimated emissions of CO_2 during the whole life of still = $\frac{(E_{emb}) \times 2}{1000}$ (3.32)

3.11.2 CO_2 mitigation

CO_2 mitigation throughout the life of any system is an important parameter for evaluating environmental impacts. The evaluation of environmental parameters uses an energy and exergy approach. The evaluated CO_2 mitigation over the whole life of still (tons) using an energy-based approach is calculated as [91]:

$$\emptyset_{en,CO_2} = \frac{(E_{en,o}) \times 2 \times n}{1000} \quad (3.33)$$

Exergo-environmental parameter is the CO_2 mitigated over the whole life of still (tons) using the exergy approach and is estimated as:

$$\emptyset_{ex,CO_2}=\frac{(E_{ex,o}) \times 2\times n}{1000} \quad (3.34)$$

3.12 Enviroeconomic Analysis

Enviroeconomic approach: annual revenue from CO_2 mitigation for the whole life of the still. Enviro-economic terms evaluate CO_2 mitigation revenue based on the energy approach, which is evaluated as [92]:

$$Z_{en,CO_2} = Z_{CO_2} \text{ x } \emptyset_{en,CO_2} \quad (3.35)$$

Exergo-enviro-economic parameter elaborates and calculates CO_2 mitigation revenue based on the exergy approach and is evaluated as [92]:

$$Z_{ex,CO_2} = Z_{CO_2} \text{ x } \emptyset_{ex,CO_2} \quad (3.36)$$

Prices of carbon credits vary, and US$ 28/tonne of CO_2 has been used by Kant et al. [90]. At present, the price of carbon credits has been revised to the California Carbon Allowance, which is approximately US$32 per tonne of CO_2.

3.13 Method of Data Comparison

A systematic and scientifically robust method of data comparison was employed to evaluate the relative performance of the Simple Passive Solar Still (SPSS) and the Modified Passive Solar Still (MPSS). The comparison ensures that the performance improvements observed in MPSS result from design enhancements (wick-assisted evaporation and coil-assisted condensation) rather than from experimental variability or environmental disturbances.

3.13.1 Aim of Data Comparison

The method of comparison aims to:

i. Establish a direct performance comparison between the two solar stills under identical environmental conditions.

ii. Identify differences in evaporation, condensation, thermal behaviour, exergy generation, and freshwater yield.

iii. Ensure that observed differences are statistically consistent and thermodynamically justified.

iv. Validate whether the MPSS design modifications achieve measurable performance enhancement over SPSS.

3.13.2 Basis for Comparative Evaluation

A valid comparison required that both solar stills:

- were operated simultaneously**,**
- exposed to identical environmental conditions**,**
- constructed with identical baseline geometry,
- used identical instrumentation, and
- were tested for the same duration and water depth**.**

This ensured that any performance variation could be attributed solely to the wick and coil enhancements in MPSS and not to external factors.

3.13.3 Parameters Used for Comparative Analysis

The following categories of parameters were compared between SPSS and MPSS:

i. Thermal Parameters

- Basin water temperature
- Inlet and collected water temperature
- Inner and outer glass temperature
- Wick temperature (Only for MPSS)
- Coil temperature (Only for MPSS)
- Moist-air temperature

ii. Psychrometric Parameters

- Relative humidity inside stills
- Dew-point temperature

- Partial vapour pressure
- Humidity ratio
- Dry Bulb Temperature of ambient

These parameters determine the potential for evaporation and condensation.

iii. Productivity Parameters

- Hourly distillate yield
- Daily distillate yield
- Annual projected yield

iv. Energy and Exergy Parameters

- Thermal energy absorbed
- Evaporation heat transfer
- Exergy input
- Exergy output
- Exergy destruction
- Exergy efficiency

v. Economic and Environmental Parameters

- Cost per liter (CPL)
- Energoeconomic value
- Exergoeconomic value
- CO_2 mitigation potential
- Carbon credit earning

3.13.4 Step-by-Step Procedure for Data Comparison

Step 1: Synchronization of time-series data

Step 2: Comparison of temperature profiles

Step 3: Comparison of evaporation and condensation behavior

Step 4: Comparison of hourly and daily distillate yield

Step 5: Comparison of exergy and energy efficiencies

Step 6: Comparison of economic and environmental outcomes

Step 7: Graphical comparison

Chapter 4

RESULTS AND DISCUSSION

4.1 Discussion on Experimental Results

This chapter presents the experimental results obtained from the Simple Passive Solar Still (SPSS) and the Modified Passive Solar Still (MPSS) under identical climatic conditions. The primary aim is to evaluate the influence of wick-assisted evaporation and coil-assisted condensation on the thermal, psychrometric, and productivity performance of MPSS relative to SPSS. Results are organized systematically to highlight diurnal thermal behavior, solar radiation patterns, evaporation–condensation responses, distillate yield variation, and thermodynamic performance.

4.1.1 Overview of Experimental Conditions

Experiments for the simple passive solar still (SPSS) and the modified passive solar still (MPSS) were conducted simultaneously from 11th May to 15th June 2023 to ensure identical exposure to ambient environmental conditions, including solar radiation intensity, relative humidity, and wind velocity. Both systems were operated daily from 09:00 AM to 06:00 PM, maintaining a constant basin water depth of 10 cm throughout the experimental period. During the observation period, various weather conditions were encountered, including clear-sky, hazy, and cloudy days. The glazing inclination, basin dimensions, and insulation thickness were kept identical to maintain structural parity. The environmental parameters recorded hourly include:

- Global solar radiation
- Ambient temperature
- Relative humidity
- Wind speed

Internally measured parameters include:

- Basin water temperature
- Inner and outer glass temperature

- Wick temperature (for MPSS only)
- Cooling coil surface temperature (for MPSS only)
- Moist air temperature inside the still
- Hourly freshwater yield

The aim of establishing stable experimental conditions was to isolate the effect of system modifications and minimize environmental bias in the comparative evaluation.

4.1.2 Structure of Result Evaluation

Analysis of results is organized into the following thematic domains:

i. Thermal Behavior

Temperature variations in basin water, the inner glass cover, the wick (MPSS), and the cooling coil (MPSS) are analysed. These data illustrate the heat absorption, storage, and transfer characteristics, which are governed by solar input and system design.

ii. Psychrometric Behavior

Moist-air conditions inside both stills, characterized by relative humidity, vapor pressure, humidity ratio, and dew-point temperature, are evaluated. Psychrometric performance dictates the rate of evaporation and the onset of condensation.

iii. Evaporation and Condensation Response

Evaporative heat transfer, thin-film evaporation, and coil-assisted condensation are compared to establish how MPSS achieves improved phase-change efficiency.

iv. Freshwater Productivity

Hourly and daily productivity trends are assessed for both stills. MPSS shows a significant yield enhancement due to a larger evaporation area and more effective condensation on the coil.

v. Thermodynamic Evaluation

Thermal efficiency, exergy efficiency, exergy destruction, and exergoeconomic parameters are computed to evaluate second-law performance.

vi. Economic and Environmental Outcomes

Cost per liter, annual water production, CO_2 mitigation, and carbon credit values are compared between SPSS and MPSS, demonstrating the techno-economic viability of MPSS.

This structured methodology ensures a comprehensive and scientifically sound comparison of both systems.

4.1.3 Comparative Framework for SPSS and MPSS

The comparative analysis presented in this chapter follows a parameter-by-parameter evaluation framework, ensuring fairness and objectivity. Results from SPSS and MPSS are compared under:

i. Identical Environmental Inputs

- Same solar exposure
- Same ambient conditions
- Same operating hours and water depth

ii. Equivalent Structural Conditions

- Same basin area
- Same glazing geometry
- Same insulation thickness

iii. Direct Performance Metrics

The stills are compared on:

- Basin and wick temperature (MPSS advantage)
- Moist-air temperature and dew-point alignment
- Condensation rate on glass vs. glass + coil
- Hourly and daily freshwater yield
- Thermal and exergy efficiency
- Cost-effectiveness and carbon mitigation

iv. Mechanistic Comparison

The comparison highlights how and why MPSS outperforms SPSS:

- Wick increases evaporation by thin-layer water distribution
- Coil enhances condensation by maintaining sub-dew-point temperatures

Greater vapor generation and improved condensation synergy yield higher productivity.

4.2 Solar Radiation and Meteorological Parameters

A precise understanding of the prevailing meteorological conditions is essential for evaluating the thermal performance of both the Simple Passive Solar Still (SPSS) and the Modified Passive Solar Still (MPSS). Solar radiation, ambient temperature, relative humidity, and wind speed collectively govern the evaporative and convective processes occurring within solar distillation systems. This section presents the variation in these parameters over the experimental period and discusses their relevance to heat and mass transfer mechanisms within the stills.

4.2.1 Hourly Solar Intensity Profile

Solar radiation is the principal driving force behind evaporation in solar stills. Figure 4.1 illustrates the variation in global solar irradiance from 09:00 AM to 06:00 PM for average data from several clear days, specifically 11th May, 12th May, and 15th May 2023.

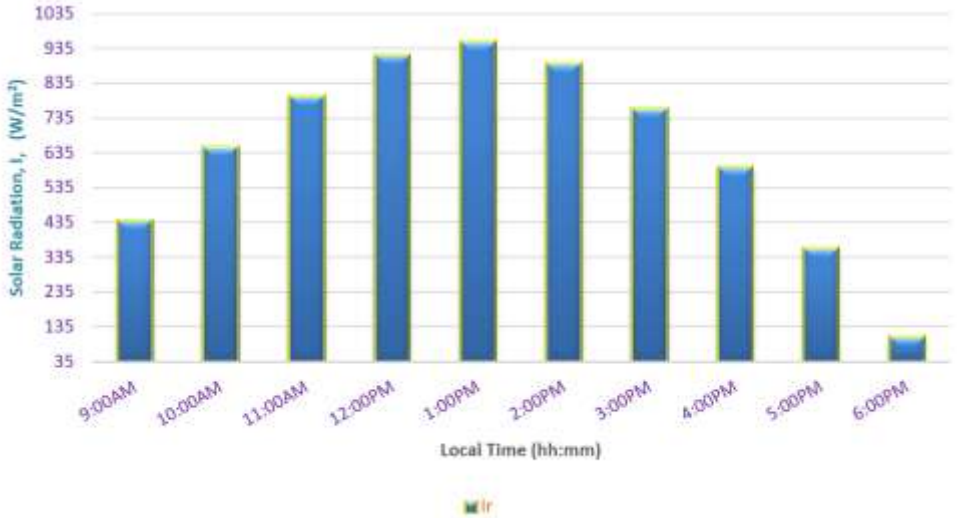

Figure 4.1 Hourly solar radiation

The radiation increases rapidly during the morning hours, peaking around 01:00 AM to 02:00 PM, and declines gradually toward the evening.

The profile resembles a typical bell-shaped curve consistent with average value for clear-sky days, and the peak intensity (950 W/m²) aligns well with experimental observations for similar climatic conditions. Higher midday irradiance increases basin water temperature, promoting greater evaporation in both stills. However, due to wick-assisted thin-film evaporation, MPSS benefits more significantly from this peak heating period.

4.2.2 Ambient Temperature and Relative Humidity Variations

The combined effect of ambient temperature and relative humidity (RH) strongly influences evaporation rates within MPSS. On a clear-sky day, Figure 4.2 presents the hourly variation of these two atmospheric parameters.

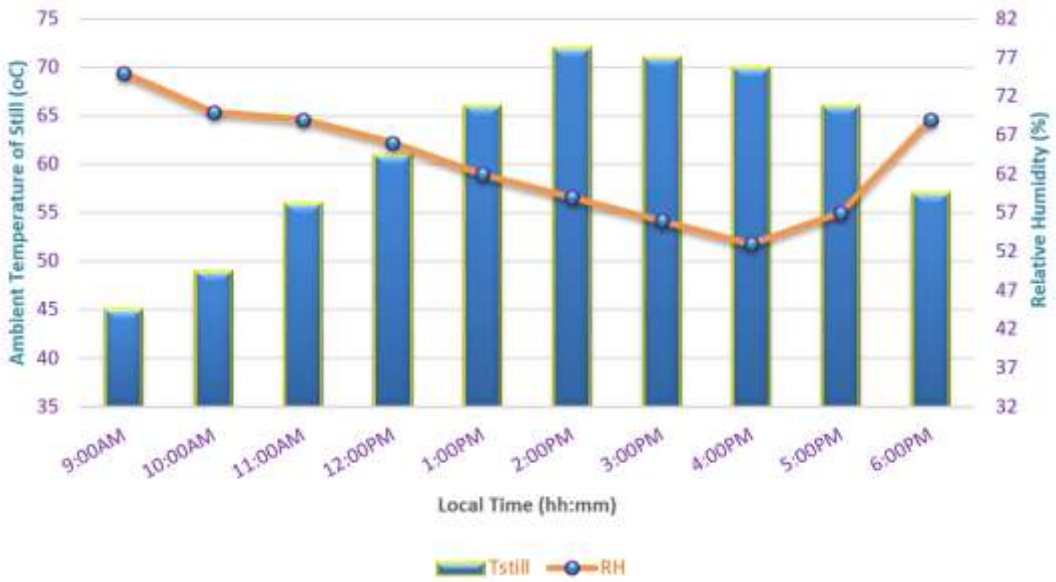

Figure 4.2 Ambient temperature and relative humidity profile

Ambient temperature rises steadily from early morning, reaching a maximum of about 72°C at 02:00 PM, then gradually decreases. This behavior increases water temperature in both stills during the day and increases vapor generation.

In contrast, RH exhibits an inverse relationship with temperature. It decreases from 75% in the morning to a minimum of 53% near 04:00 PM, then increases toward the

evening. Lower RH during high-temperature periods enhances vapor–air mass transfer, accelerating evaporation in the stills.

This atmospheric trend is particularly beneficial for MPSS because the wick surface evaporates water more efficiently under low humidity conditions.

4.2.3 Wind Speed and Atmospheric Influence on Heat Transfer

Wind speed affects the external convective heat-transfer coefficient at the outer glass surface. Higher wind velocity increases the rate at which heat is removed from the outer cover, facilitating condensation on the inner cover surface, an essential requirement for freshwater production.

Figure 4.3 shows the variation of wind speed throughout the experiment. Wind speed rises from 1.0 m/s in the morning to a peak of 1.4 m/s around 10:00 AM, then declines gradually.

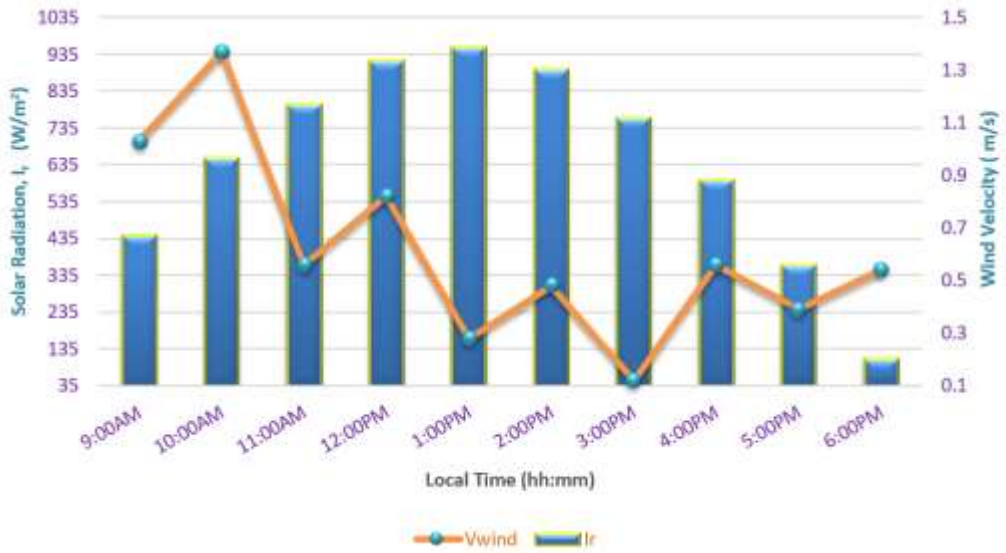

Figure 4.3 Wind speed variation during experimental

Implications of this behavior include:

- Enhanced condensation efficiency due to increased convective cooling of the glass surface.
- Reduced glass temperature**,** improving the temperature gradient between vapor and condensing surface.

- More effective condensation in MPSS**,** especially when combined with coil-assisted cooling.

Wind speed variations observed in this study align with reported meteorological patterns and contribute to improved condensation in both stills, with MPSS benefiting more due to its additional cooling mechanism.

4.3 Thermal Performance Analysis

Thermal performance of the simple passive solar still (SPSS) and the modified passive solar still (MPSS) was analyzed to evaluate the effectiveness of heat absorption, storage, and utilization under identical climatic conditions. The analysis primarily focuses on basin water temperature, inner glass temperature, evaporative heat transfer, and their combined influence on freshwater productivity.

Experimental observations indicate that the thermal behavior of both stills closely follows the average variation of solar radiation. However, MPSS consistently exhibits higher basin water and inner glass temperatures compared to SPSS. This improvement is attributed to the hanging black wick, which increases the effective evaporation surface area and promotes thin-film evaporation, thereby enhancing heat transfer from the basin to the moist air.

4.3.1 Basin Water Temperature profile (SPSS vs. MPSS)

Figure 4.4 illustrates the hourly variation of basin water temperature for the simple passive solar still (SPSS) and the modified passive solar still (MPSS) in relation to the incident solar radiation during the experimental period. As expected, the basin water temperature in both systems closely follows the trend of solar irradiance, confirming the dominant influence of solar irradiance on the stills' thermal behavior.

At the beginning of the observation period (09:00 AM), relatively low solar radiation results in lower basin water temperatures, recorded at approximately 33°C for SPSS and 35°C for MPSS. The slightly higher temperature in MPSS at this early stage indicates improved heat absorption, attributed to the presence of black-hanging wick surfaces that increase effective solar absorption and reduce reflective losses.

As shown in Figure 4.4, solar radiation intensity peaks around midday, and the basin water temperature in both systems increases steadily due to enhanced heat gain. Peak temperatures are observed around 03:00 PM, where the basin water temperature reaches about 52°C in SPSS and 53°C in MPSS. This time lag between maximum solar radiation (around noon) and peak water temperature is due to the thermal inertia of the basin water and its structural components. The consistently higher temperature of MPSS throughout this period demonstrates the effectiveness of the modified design in retaining and utilizing absorbed heat.

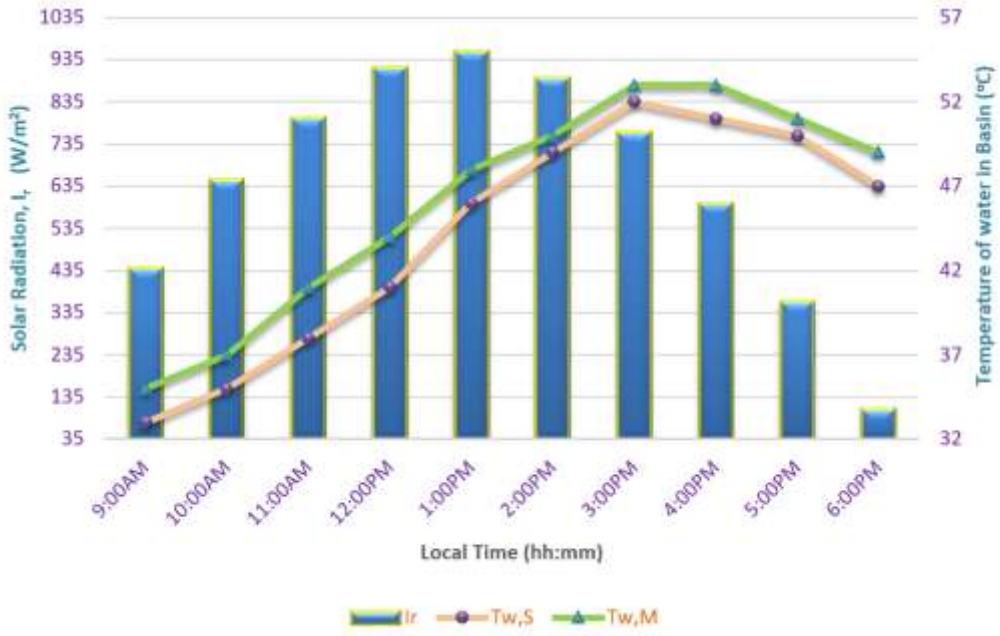

Figure 4.4 Variation of basin water temperature with respect to solar radiation in SPSS and MPSS

During late afternoon and evening, a decline in solar radiation leads to a gradual reduction in basin water temperature. By 06:00 PM, the temperature decreases to approximately 47°C for SPSS and 49°C for MPSS. Despite reduced solar input, MPSS maintains a higher basin water temperature than SPSS, indicating improved thermal storage and reduced heat loss. This behavior can be attributed to the combined effects of increased evaporative surface area provided by the wet hanging wick and enhanced internal heat retention.

Overall, the basin water temperature profile confirms that MPSS consistently operates at a higher thermal level than SPSS under identical climatic conditions. The elevated basin water temperature in MPSS directly increases evaporation rates, thereby enhancing freshwater productivity. These results clearly demonstrate that the design modifications incorporated in MPSS improve the thermal performance of the solar still, particularly during peak and post-peak solar radiation periods, which is crucial for sustained distillate production.

4.3.2 Glass Temperature Profiles

Figure 4.5 illustrates the hourly variation of incident solar radiation and the corresponding inner glass surface temperature (T_{ig}) for both the Simple Passive Solar Still (SPSS) and the Modified Passive Solar Still (MPSS) on clear sky day. Since both stills were installed under identical outdoor conditions, they received the same solar radiation throughout the day. The intensity of solar radiation increases steadily from 09:00 AM, reaches its maximum around 01:00 PM, and then decreases gradually until 06:00 PM, following a typical diurnal solar profile.

Inner surface temperature of the cover glass is governed by several interacting factors, including the intensity of incident solar radiation, convective and radiative heat losses from the outer glass surface to the ambient environment, thermal conductivity and thickness of the glass cover, and the magnitude of latent heat released during condensation. As solar radiation increases in the morning, the inner glass temperature of both stills rises due to increased absorption of solar energy and enhanced heat transfer from the humid air inside the chambers.

During the early morning period (09:00 AM to 11:00 AM), relatively low solar radiation results in lower inner glass temperatures for both stills. However, MPSS consistently exhibits a higher inner glass temperature than SPSS, indicating greater internal heat transfer caused by enhanced evaporation from the hanging wick surface. As the day progresses toward noon, the temperature difference between the two stills becomes more pronounced. The maximum temperature difference of approximately 10°C between MPSS and SPSS is observed around midday, highlighting the stronger thermal interaction between moist air and the glass surface in the modified system.

Peak inner glass temperatures are recorded at approximately 02:00 PM, with values of about 64°C for MPSS and 62°C for SPSS. This time lag between the peak solar radiation (around 01:00 PM) and the maximum glass temperature is attributed to the thermal inertia of the basin water and to the gradual accumulation of water vapour within the still. A higher inner glass temperature indicates greater absorption of incident solar energy and increased convective heat transfer from the moist air to the glass surface.

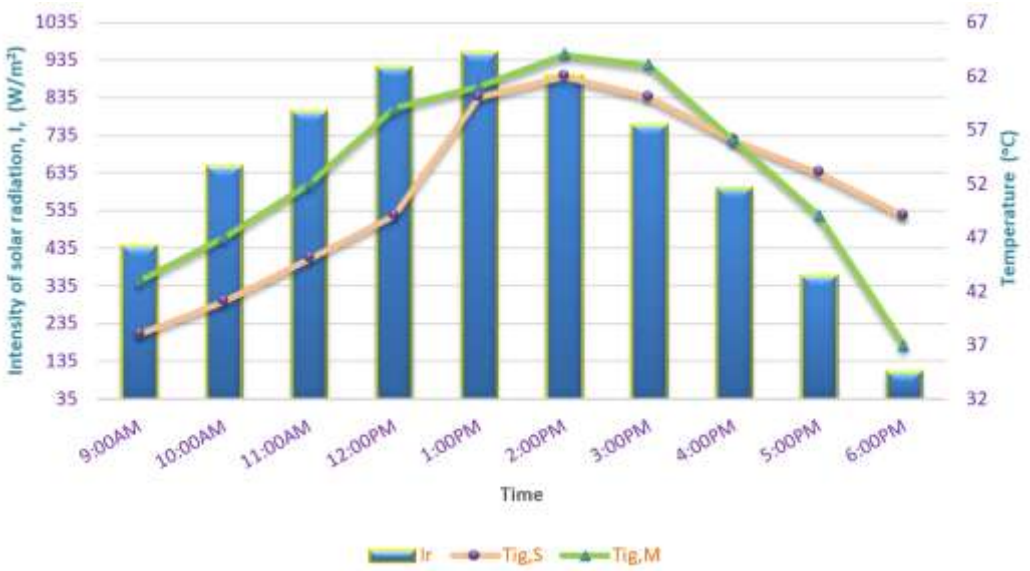

Figure 4.5 Temperature of inner surface of cover glass of SPSS and MPSS

From a condensation perspective, the glass temperature plays a critical role in determining freshwater productivity. Although higher inner glass temperatures indicate greater energy absorption, effective condensation requires the inner glass surface temperature to remain below the dew-point temperature of the moist air inside the chamber. Experimental observations confirm that, despite the higher glass temperature in MPSS, the inner glass surface temperature remains sufficiently lower than the dew-point temperature due to enhanced external cooling and latent heat removal through continuous condensation. This condition ensures sustained condensation throughout the operating period.

After 03:00 PM, solar radiation decreases significantly, leading to a corresponding decline in inner glass temperature for both stills. However, MPSS maintains a comparatively higher glass temperature for a longer duration, indicating improved heat retention and sustained evaporation–condensation interaction. The gradual decline in glass

temperature also enhances condensation efficiency by increasing the temperature difference between moist air and the glass surface, particularly during the late afternoon.

Overall, the glass temperature profiles show that MPSS exhibits higher inner-glass temperatures than SPSS throughout the day, reflecting intensified evaporation and vapor generation within the chamber. At the same time, effective condensation is maintained due to favorable psychrometric conditions. This balanced interaction between elevated evaporation and controlled condensation is a key factor in MPSS's superior freshwater productivity compared to SPSS.

4.3.3 Wick Surface Temperature Behavior

The wick surface temperature plays a crucial role in governing the evaporation–condensation mechanism in a Modified Passive Solar Still (MPSS). In the present study, the introduction of a vertically hanging wet cloth (wick) significantly alters the thermal behavior inside the still compared to the Simple Passive Solar Still (SPSS). The wick remains continuously wetted by strong capillary action and a passive water supply, creating a large free wet surface area exposed directly to incident solar radiation. As a result, the wick surface temperature increases rapidly during daylight hours, reaching a peak of 70 °C at 03:00 PM.

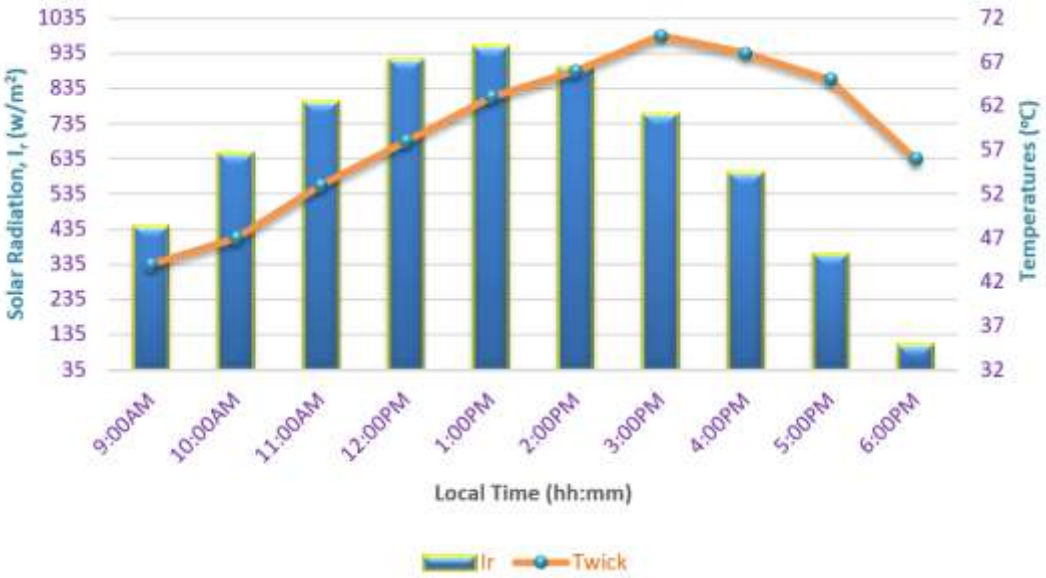

Figure 4.6 Temperature profile of wick surface MPSS

The elevated wick surface temperature enhances the evaporation rate by reducing the effective thermal resistance between the absorbed solar energy and the saline water film on the cloth. Unlike in a conventional basin, where evaporation is limited to a horizontal free surface, the hanging cloth provides a large vertical evaporative area, thereby intensifying heat and mass transfer. Experimental observations show that as solar radiation increases toward noon, the wick surface temperature rises proportionally, promoting higher vapor generation even when basin water temperature changes are marginal. This thermal behavior explains the sustained evaporation observed in MPSS during post-peak solar hours.

Furthermore, the higher wick temperature contributes to a greater temperature gradient between the evaporating surface and the condensing surfaces (the glass cover and the copper cooling coil). This gradient strengthens the vapor pressure difference inside the still chamber, which is the primary driving force for evaporation and condensation. Consequently, MPSS exhibits a higher moisture content within the enclosure, accelerating condensation and improving distillate yield. The decline in wick temperature during late afternoon is slower than that of basin water, supporting continued evaporation and explaining the enhanced productivity of MPSS even as solar radiation declines.

Overall, integrating a hanging wick into MPSS improves the thermal response of the evaporative surface, intensifies evaporation kinetics, and ensures better utilization of available solar energy. This favorable wick surface temperature behaviour directly translates into a substantial increase in freshwater yield, improved thermal efficiency, and superior overall performance of the still compared to SPSS, as demonstrated by the experimental findings.

4.3.4 Cooling Coil Temperature Behavior

Temperature behavior of the cooling coil in the Modified Passive Solar Still (MPSS) plays a decisive role in enhancing condensation and, consequently, the overall freshwater yield. In the present configuration, a copper cooling coil covered with a wet cloth is introduced as an auxiliary passive condenser. During operation, the coil temperature is observed to remain significantly lower than the moist air temperature inside the still chamber and close to the ambient dew point. This temperature difference

establishes a strong thermal and vapor-pressure gradient, which promotes effective condensation of water vapor on the coil surface.

Experimental observations reported in Figure 4.7 indicate that the cooling coil temperature in MPSS is typically maintained in the range of approximately 24°C to 32°C. In contrast, the moist air temperature inside the still often exceeds 50°C to 70°C during peak solar hours. A large temperature difference enhances latent heat transfer from the vapor phase, leading to rapid condensation on the coil surface. As condensation occurs, the partial pressure of water vapor in the vicinity of the coil decreases, thereby inducing additional vapor flow from the still chamber toward the cooling coil. This self-driven vapour-transport mechanism further increases the condensation rate without requiring any external energy input.

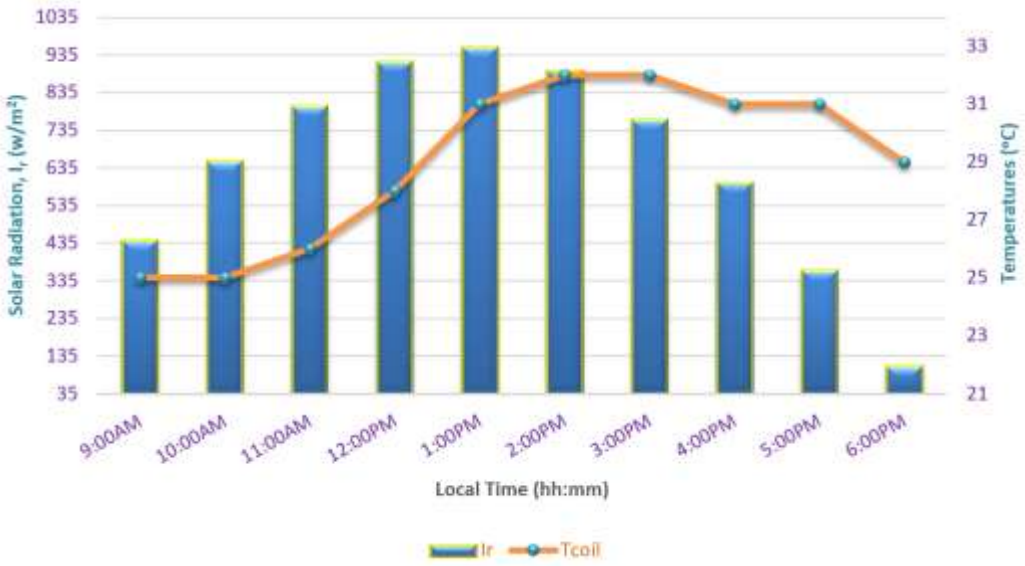

Figure 4.7 Temperature profile of coil surface in MPSS

Introduction of a hanging wet cloth (wick) synergistically enhances the cooling coil's effectiveness. The hanging cloth increases the evaporation rate by providing an enlarged free wet surface area and maintaining a higher moisture concentration within the still enclosure. As a result, the cooling coil experiences sustained condensation throughout the day, including during post-peak solar radiation hours when conventional stills typically exhibit reduced productivity. This balanced thermal behavior enhances both evaporation and condensation processes simultaneously, which is a key limitation in conventional SPSS designs.

In summary, the cooling coil temperature behavior in MPSS demonstrates that maintaining a condensing surface at or below the dew point temperature is highly effective for improving freshwater production. When integrated with a hanging wick, the cooling coil ensures rapid vapour condensation, sustained vapor flow, and reduced thermal losses. This integrated passive enhancement significantly improves the yield, thermal efficiency, and overall performance of the solar still, as demonstrated by experimental results.

4.3.5 Ambient Temperature of Still Profile

The variation of ambient temperature within the solar still for both Simple Passive Solar Still (SPSS) and Modified Passive Solar Still (MPSS) is presented in Figure 4.8 as a function of solar radiation intensity.

From 09:00 AM onward, solar radiation gradually increases, directly influencing the thermal environment inside both stills. At 09:00 AM, the ambient temperature inside SPSS and MPSS is 45 °C, which is relatively low and corresponds to lower solar radiation levels. However, even during the early hours, the ambient temperature inside MPSS is slightly higher than that of SPSS. This behavior is attributed to the presence of the hanging wet cloth in MPSS, which absorbs and retains a greater fraction of incident solar energy due to its blackened surface and increased effective heat transfer area.

As solar radiation steadily increases and peaks around 01:00–02:00 PM, the ambient temperature in both stills also rises significantly. The MPSS consistently exhibits a higher ambient temperature than the SPSS, with a noticeable difference during peak hours. This enhancement is primarily due to the combined effect of increased evaporative surface area provided by the hanging cloth and improved absorption of solar radiation by the wetted vertical surfaces. The cloth acts as a thermal absorber and an evaporative medium, increasing the enthalpy of moist air inside the chamber.

After 02:00 PM, although solar radiation begins to decline, the ambient temperature inside the stills remains relatively high until about 04:00 PM. This thermal lag is more pronounced in MPSS, indicating better heat retention and sustained evaporation. The hanging cloth continues to release stored thermal energy and moisture into the chamber, maintaining a higher internal temperature compared to SPSS. In

contrast, SPSS shows a relatively faster reduction in ambient temperature due to the absence of additional heat-absorbing and moisture-retaining surfaces.

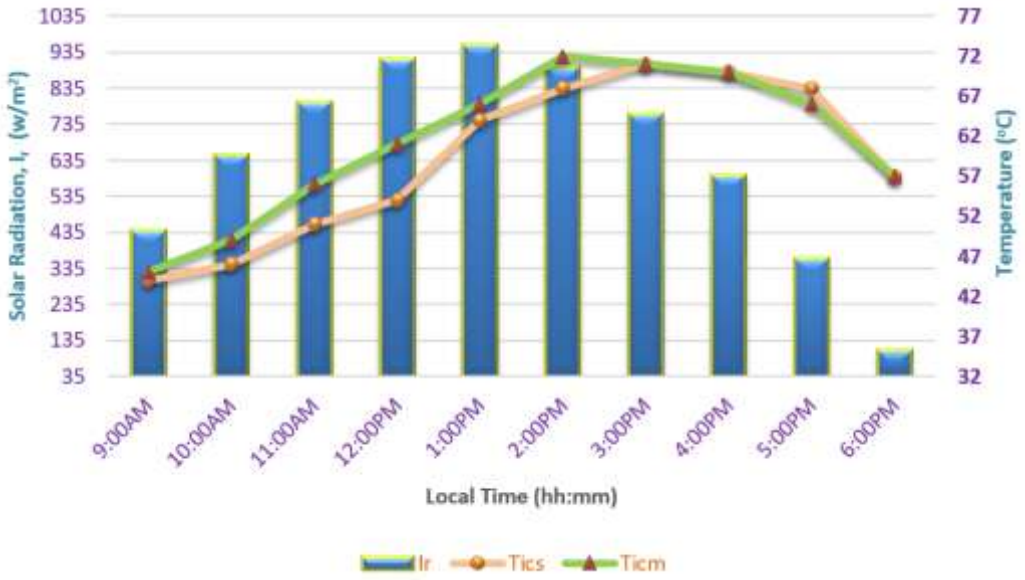

Figure 4.8 Inside temperature of SPSS and MPSS

During the late afternoon (05:00 PM to 06:00 PM), a sharp decrease in solar radiation results in a corresponding drop in ambient temperature in both systems. However, MPSS still maintains a marginally higher internal temperature than SPSS, which supports continued evaporation and condensation even under reduced solar input. This behavior explains the higher late-hour distillate yield observed in MPSS.

Overall, the results clearly demonstrate that the ambient temperature within the solar still is strongly governed by solar radiation intensity and internal design features. The introduction of a hanging wet cloth in MPSS significantly enhances the internal thermal environment by increasing heat absorption, moisture availability, and thermal inertia. This elevated, sustained ambient temperature leads to greater vapor generation, improved condensation potential, and ultimately superior freshwater yield in MPSS compared to SPSS.

4.4 Psychrometric Behavior of Moist Air inside Still

Psychrometric behavior of moist air within the solar still chamber plays a fundamental role in controlling evaporation, condensation, and freshwater productivity. Unlike conventional thermal analyses that rely primarily on temperature gradients,

psychrometric analysis incorporates parameters such as relative humidity, specific humidity, dew-point temperature, and moist-air enthalpy, which collectively govern phase-change phenomena. In the present study, these parameters were experimentally investigated under both clear blue-sky and full-haze conditions to understand their influence on condensation dynamics and distillate yield.

Inside the solar still, evaporation of basin water continuously increases the moisture content of the confined air, converting it into humid air. As solar radiation intensifies during the day, heat transfer from the basin water raises the dry-bulb temperature of the moist air, increasing specific humidity. This process establishes a transient thermodynamic state in which evaporation from the basin water and condensation on the cover glass coexist, governed by psychrometric equilibrium.

4.4.1 Moist-Air Temperature Profiles

Figure 4.9 illustrates the variation in incident solar radiation temperature on average data recorded for clear-sky days (I_{csd}) and hazy days (I_{hzd}) during the experimental observation period. Solar radiation incident on the glass cover varies continuously throughout the day, increasing progressively after sunrise, reaching a maximum around 01:00 PM, and then declining toward sunset. This trend is characteristic of clear-sky conditions and confirms the dominant role of solar radiation as the primary energy source driving the solar distillation process.

Solar radiation significantly influences the thermal and psychrometric conditions inside the solar still. Variations in incident radiation directly affect basin water temperature, inner glass surface temperature, and ambient air temperature within the chamber. In addition, psychrometric parameters of the enclosed moist air, such as relative humidity, specific enthalpy, dew-point temperature, and dry-bulb temperature, exhibit noticeable dependence on the intensity of incoming solar radiation.

Experimental observations show that the dry-bulb temperature of moist air inside the chamber continues to increase until approximately 03:00 PM, even as solar radiation begins to decline after 01:00 PM. This delayed thermal response is attributed to the basin water's thermal inertia and the gradual accumulation of water vapour in the still, which increases both the specific humidity and the specific enthalpy of the moist air.

Figure 4.9 further presents the variation in the dry-bulb temperature of moist air (chamber temperature) for SPSS, using average data for selected clear-sky and hazy days. For each observation day, all measured temperatures exhibit a similar trend: initially increasing with time, reaching peak values around 03:00 PM, and then gradually decreasing toward evening. This behaviour demonstrates that the system's maximum thermal response occurs after the peak solar radiation period, highlighting the combined influence of heat storage, evaporation dynamics, and psychrometric evolution within the solar still chamber.



Figure 4.9 Variation of chamber temperature for SPSS

4.4.2 Variation of Relative Humidity and Specific Humidity

Figure 4.10 presents the hourly variation in relative humidity and specific humidity of moist air inside the solar still chamber, with average values for a clear blue sky day and a fully hazy day. On both experimental days, the relative humidity is initially high in the morning, while the specific humidity remains comparatively low. This behavior is attributed to lower air temperatures and limited evaporation during the early hours of operation.

As the day progresses, the relative humidity of the moist air gradually decreases, reaching its minimum around 03:00 PM. During the same period, the specific humidity shows an opposite trend, increasing continuously as enhanced evaporation driven by rising

basin water temperatures increases. After 03:00 PM, the trend reverses: relative humidity begins to increase, while specific humidity decreases, reflecting reduced evaporation rates and the onset of condensation as solar input declines.

Psychrometric analysis, assuming atmospheric pressure within the chamber, indicates that specific enthalpy does not vary directly with incident solar radiation intensity. Although solar radiation reaches its peak around 01:00 PM and then decreases, both the specific humidity and the specific enthalpy of the moist air continue to increase until approximately 03:00 PM. This delayed response is associated with the basin water's thermal inertia and the gradual accumulation of water vapor within the enclosure.

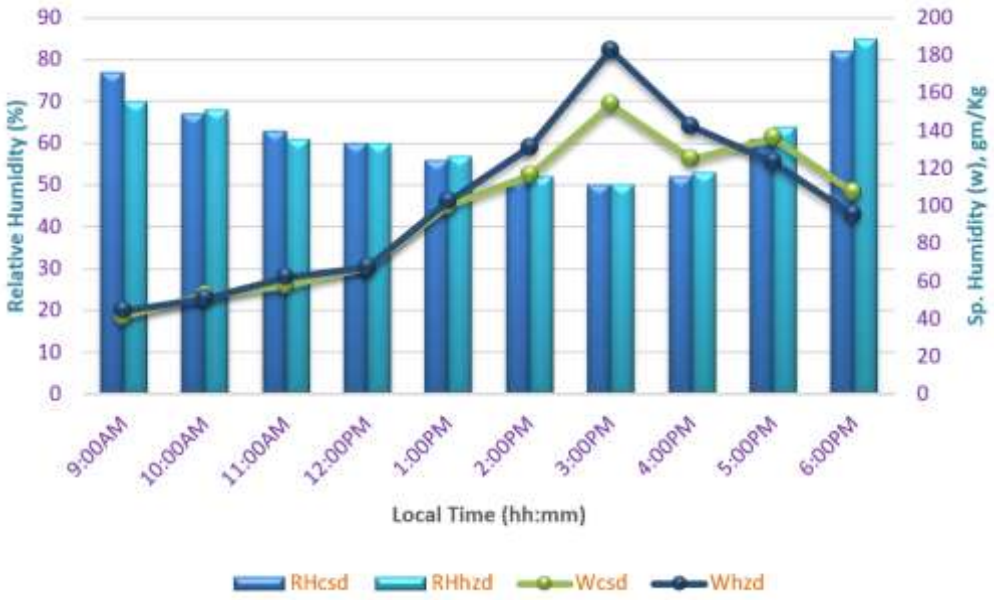

Figure 4.10 Hourly variation in relative humidity and specific humidity

Furthermore, experimental observations show that the maximum specific humidity attained during fully hazy conditions (183 gm/kg) is higher than that during clear-sky conditions (158 gm/kg), as illustrated in Figure 4.10. This behavior is attributed to reduced convective heat losses and lower glass temperatures during hazy days, which promote moisture retention within the chamber. Overall, the results confirm an inverse relationship between relative humidity and specific humidity and demonstrate that psychrometric parameters are primarily governed by internal moisture dynamics rather than by instantaneous solar radiation intensity.

4.4.3 Dew-Point Temperature and Condensation Feasibility

Figure 4.11 illustrates the temporal variation in the inner glass surface temperature, the dew-point temperature of moist air within the chamber, specific humidity, and potable water productivity on a hazy day during the SPSS experimental observation period. Data acquisition commenced at 09:00 AM, when the temperatures of the enclosed moist air (DBT, 45 °C) and the internal surfaces of the glass (32 °C) were relatively low. With the increase in solar heating, all temperature-related parameters exhibited a gradual rise and reached their peak values at approximately 03:00 PM, including 77 °C dry bulb temperature, 62 °C dew point temperature, and 51 °C inner glass surface temperature, as illustrated in Figure 4.11.

A combination of interacting parameters, including incident solar radiation, basin and surface temperatures, the temperature difference between the moist air and the inner glass surface, the thermal conductivity of the glass cover, convective heat-transfer coefficients, and ambient wind velocity, governs potable water productivity. The synergistic influence of these parameters determines the rate of vapor generation, condensation, and freshwater collection.

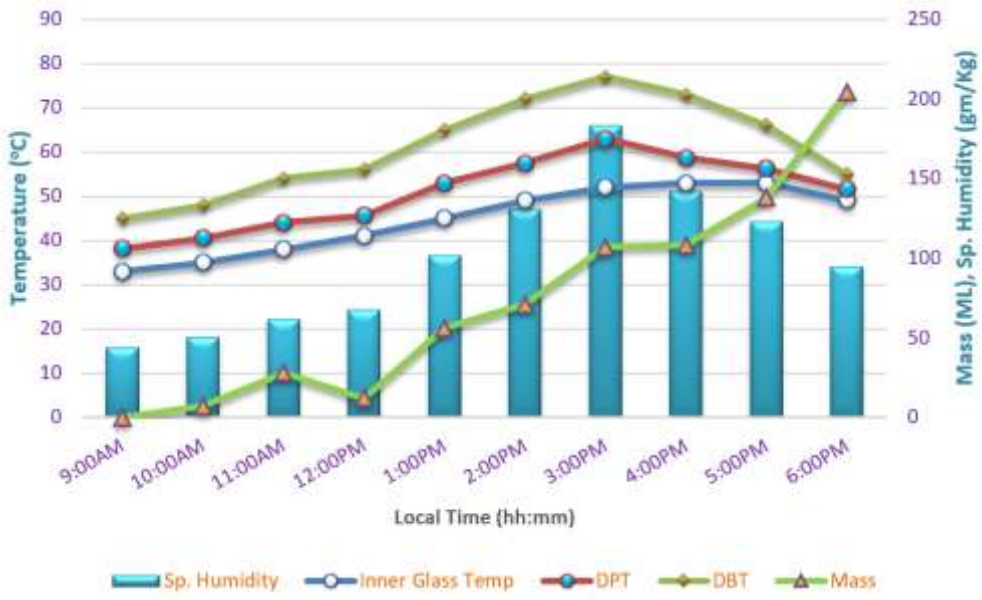

Figure 4.11 Variation in glass temperatures, dew point temperature, RH

According to psychrometric principles, the dry-bulb temperature of moist air is always higher than its corresponding dew-point temperature, as shown in Figure 4.11. For

effective condensation to occur, the inner surface of the cover glass must remain below the dew-point temperature (DPT) of the enclosed humid air throughout the experiment. Experimental observations confirm that this condition is satisfied throughout the entire observation period, as the measured inner glass temperature consistently remains below the evaluated dew-point temperature.

During solar still operation, evaporation of basin water increases the specific humidity of the enclosed air in the chamber from 16 to 172 gm/kg, peaking at 03:00 PM and then decreasing steadily until evening. Moist air accumulates on the inner surface of the glass cover, where water vapour condenses due to heat loss by convection and conduction, and is collected as distillate. The specific humidity of the moist air increases with the addition of thermal energy in the chamber and decreases as condensation progresses. This behavior confirms the strong coupling between psychrometric conditions and freshwater productivity within the solar still.

4.4.4 Key Psychrometric Findings

The conclusions from the recorded observation acquired from the experimental work are:

i. Regular distillate output of the designed still is higher on a fully hazy day than on a clear-sky day, due to a higher condensation rate.
ii. Inner cover glass surface temperature is always lower than the dew point temperature of moist air.
iii. Variation in relative humidity and specific humidity of moist air is inversely related.

4.5 Energy Analysis and Comparison for SPSS and MPSS

Figure 4.12 illustrates the variation of hourly distillate yield and cumulative freshwater production for the Single-Slope Passive Solar Still (SPSS) and the Modified Passive Solar Still (MPSS) during the experimental observation period. The hourly yield profiles of both systems closely follow the thermal behavior, which is governed by solar radiation intensity, basin water temperature, and internal heat-transfer mechanisms.

At the initial monitoring hours (09:00 AM to 11:00 AM), both stills exhibit relatively low hourly yield due to insufficient basin water temperature and limited evaporation. As solar intensity increases toward midday, the hourly distillate output rises sharply for both systems. The maximum hourly yield is observed at approximately 02:00 PM, with peak values of about 210 ml for SPSS and 280 ml for MPSS. This represents an enhancement of nearly 33.30% in the hourly yield for MPSS compared to SPSS, demonstrating the effectiveness of the design modifications in accelerating evaporation and condensation.

Beyond the peak period, the hourly yield gradually decreases as solar radiation and basin water temperature decline. However, MPSS maintains a higher hourly output in the late afternoon, indicating improved thermal retention and sustained evaporation, driven by the increased effective evaporative surface area provided by the hanging wick arrangement.

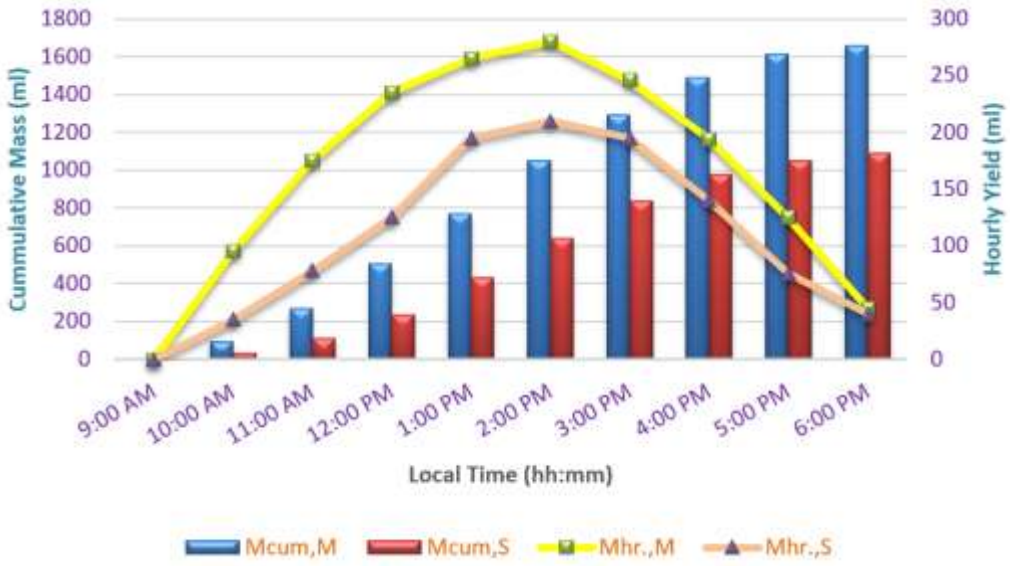

Figure 4.12 Cumulative and hourly yield for SPSS and MPSS

The cumulative yield curves further highlight MPSS's superior performance over SPSS throughout the entire operational period. By the end of the experiment (06:00 PM), the total freshwater production reaches approximately 1094 ml for SPSS and 1660 ml for MPSS. This corresponds to an enhancement of about 51.73% in cumulative yield for MPSS. The consistent divergence between the cumulative yield curves confirms that the

modified configuration improves freshwater productivity not only during peak solar hours but also over extended operating periods.

The observed improvement in both hourly and cumulative yields for MPSS is primarily attributed to enhanced evaporation and condensation rates, resulting from increased effective evaporation surface area and improved internal heat and mass transfer characteristics. These results clearly demonstrate that the MPSS offers a significant advantage over conventional SPSS in freshwater production efficiency under identical climatic conditions.

Efficiency trends of both systems are strongly influenced by solar intensity, evaporation dynamics, and condensation effectiveness, as shown in Figure 4.13. From the commencement of observations, MPSS consistently exhibits higher thermal efficiency than SPSS. This improvement is primarily attributed to the increased free wet surface area in MPSS, provided by the hanging wick arrangement, which enhances the evaporation rate of basin water. An increased evaporation rate directly increases latent heat utilization, thereby improving the system's overall thermal efficiency. In addition to evaporation, effective condensation of water vapour on the inner surface of the glass cover is crucial for maintaining higher efficiency.

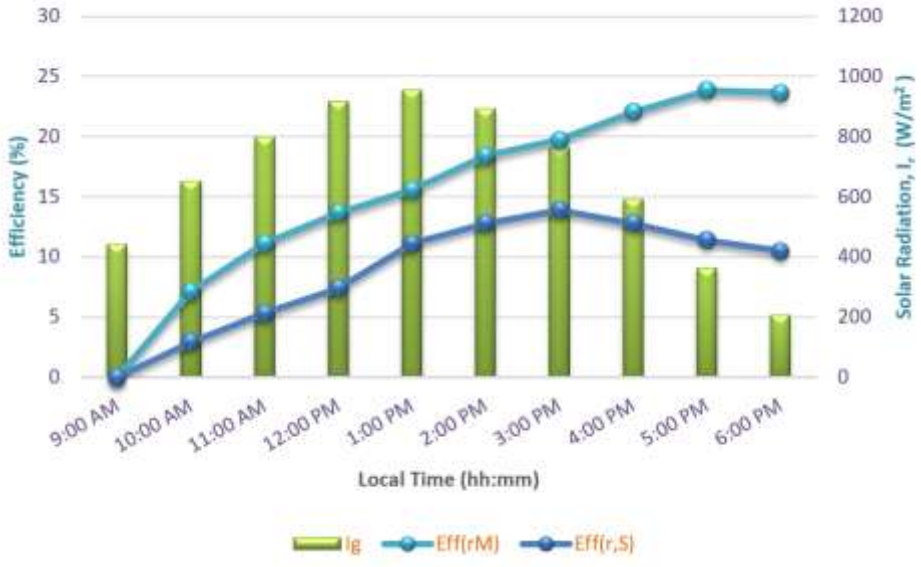

Figure 4.13 Efficiency of SPSS and MPSS

During the morning and early afternoon hours, thermal efficiency of both stills increases steadily with rising solar radiation. The efficiency of SPSS reaches its maximum

value of approximately 13.89% at 03:00 PM, corresponding to the period of high basin water temperature and favorable evaporation conditions. Beyond this time, a noticeable decline in SPSS efficiency is observed, associated with the continuous reduction in solar radiation intensity, resulting in a decrease in evaporation rate and available water vapor within the chamber.

In contrast, MPSS demonstrates a different efficiency trend during the post-peak solar period. Although solar radiation begins to decline after 03:00 PM, the MPSS efficiency continues to increase, reaching a peak of approximately 23.84% around 05:00 PM. This delayed peak efficiency indicates that the modified still effectively utilizes stored thermal energy and retains a higher moisture content within the chamber. The enhanced free-evaporation surface ensures the availability of water vapor for condensation even under reduced solar input, allowing the system to maintain higher efficiency during late afternoon.

Overall, the results clearly demonstrate that MPSS not only achieves higher peak thermal efficiency but also maintains superior performance over a longer period than SPSS. The combined effects of increased evaporative surface area, improved heat and mass transfer, and sustained condensation make MPSS thermally more efficient than the conventional SPSS under identical climatic conditions.

4.6 Exergy-based Assessment for SPSS and MPSS

Figure 4.14 illustrates the hourly variation of useful exergy output and exergy efficiency for the Single-Slope Passive Solar Still (SPSS) and the Modified Passive Solar Still (MPSS) during the experimental period. Exergy analysis provides insight into the quality of energy conversion by quantifying the maximum useful work obtainable from the absorbed solar energy.

In both still configurations, the useful exergy output increases steadily from the morning hours onward. It attains its maximum values of 2.98% and 2.23% at approximately 02:00 PM for MPSS and SPSS, respectively, on blue-sky days. This peak occurs after the maximum solar radiation intensity, which is observed around 01:00 PM. The observed time lag is attributed to the thermal storage effect within the basin water and

the internal chamber, which allows stored energy to continue driving evaporation and condensation even after solar radiation begins to decline.

The MPSS consistently exhibits higher exergy output than the SPSS throughout the operating period. This improvement is primarily due to enhanced evaporation driven by increased free wetted surface area and improved heat and mass transfer within the chamber. As a result, a larger fraction of the absorbed thermal energy is converted into useful latent heat of vaporization, thereby increasing exergy utilization.

Peak exergy efficiency of MPSS is significantly higher than that of SPSS, indicating superior thermodynamic performance of the modified system. The decline in exergy efficiency after the peak period is mainly due to reduced solar input, lower temperature gradients, and increased irreversibilities from heat losses to the surroundings.

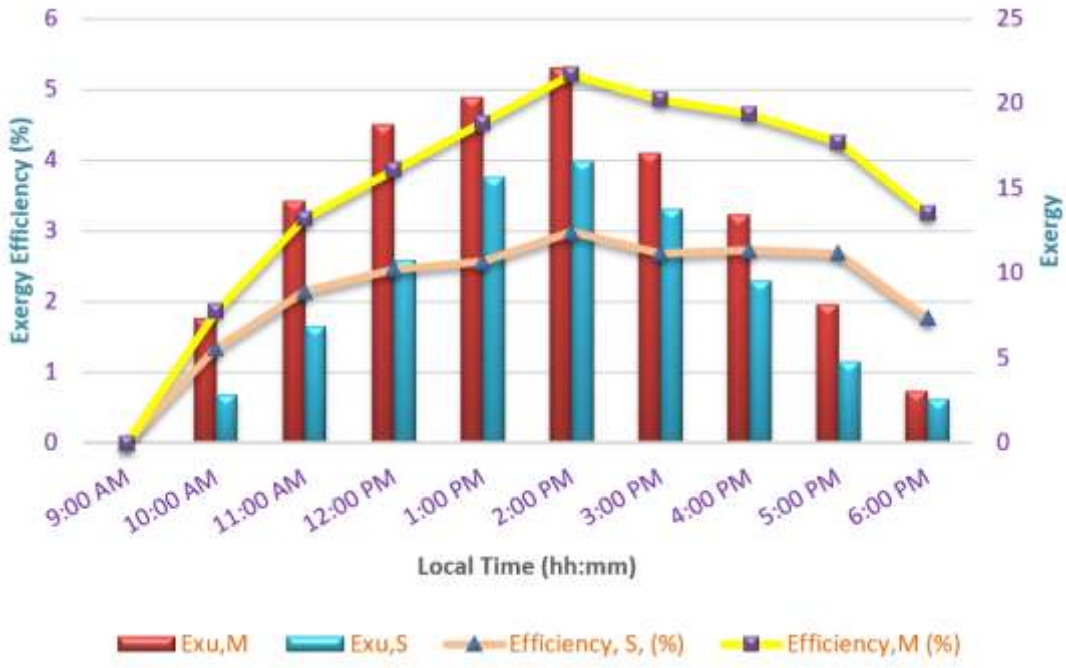

Figure 4.14 Exergy and exergy efficiency for SPSS and MPSS

Overall, the results confirm that the MPSS exhibits higher exergy efficiency and greater useful exergy output than the conventional SPSS. The presence of thermal storage within the system and improved evaporation–condensation dynamics enables the MPSS to utilize stored energy more effectively, thereby reducing irreversibilities and improving overall system performance.

4.7 Economic analysis

Table 4.1 presents the detailed capital investment and cost components associated with the Single-Slope Passive Solar Still (SPSS) and the Modified Passive Solar Still (MPSS). The uniform annual cost (UAC) is considered the primary economic parameter for comparative evaluation of both systems. Since the MPSS design modification is limited to the inclusion of a cotton hanging wick and a black surface coating, the total initial investment for both solar stills remains nearly identical.

Consequently, the calculated uniform annual costs for SPSS and MPSS are also comparable. However, a substantial difference is observed in the cost per liter (CPL) of distilled water, reflecting the significantly higher annual freshwater production achieved by MPSS. The enhanced evaporation and condensation mechanisms in MPSS lead to improved productivity without a proportional increase in cost.

As a result, the CPL for MPSS is approximately 50.52% lower than that for SPSS, at ₹0.85 per liter (USD 0.0097 per liter). This outcome clearly demonstrates the economic advantage of the modified configuration, confirming that performance enhancements from simple design modifications yield substantial cost benefits without increasing capital investment.

Table 4.1 Cost analysis of water per liter for SPSS and MPSS

Parameters (Unit)	**SPSS**	**MPSS**
Total Initial Cost	6290	7330
Interest Rate, I (%)	7	7
Life of Still, n (years)	25	25
Capital recovery factor (CRF)	0.08	0.08
First Annual Cost, FAC	498.06	580.41
Shrinking Fund Factor, SFF	0.009183	0.009183
Annual Maintenance Cost (AMC)	943.50	1099.50
Annual Salvage Value (ASV)	11.55	13.46
Uniform Annual Cost (UAC), INR	1430.01	1666.45

Annual Production, AP (Lit.)	832	1174
Cost per liter, (CPL), INR	1.72	1.42

4.8 Exergoeconomic based analysis for SPSS and MPSS

Exergo-economic analysis integrates thermodynamic performance with economic considerations to evaluate the feasibility of the Single-Slope Passive Solar Still (SPSS) and the Modified Passive Solar Still (MPSS). Table 4.2 summarizes the key exergo-economic indicators obtained for both desalination systems. The results clearly demonstrate that MPSS outperforms SPSS from an exergo-economic standpoint.

The calculated energo-economic parameters for SPSS and MPSS are found to be 15.20 kWh/US$ and 23.28 kWh/US$, respectively, indicating a higher useful energy output per unit cost for the modified system. Similarly, the exergo-economic performance parameters for SPSS and MPSS are evaluated as 0.51 kWh/US$ and 0.77 kWh/US$, respectively. These higher values associated with MPSS reflect improved utilization of available exergy relative to economic investment.

Table 4.2. Exergo economic Parameter for SPSS and MPSS

Parameters	**SPSS**	**MPSS**
Annual $E_{n,o}$ (kWh)	250.88	380.67
Annual $E_{x,o}$ (kWh)	8.46	12.65
Uniform Annual Cost, UA (US$)	16.50	16.34
R_{en} (kWh/US$)	15.20	23.28
R_{ex} (kWh/US$)	0.51	0.77

Overall, the exergo-economic assessment confirms that the MPSS configuration offers a more favorable balance between thermodynamic efficiency and economic viability. The improved exergo-economic indicators highlight the desirability of the modified system for practical desalination applications, as enhanced performance is achieved without a significant increase in capital cost.

4.9 Environmental-based Assessment for SPSS and MPSS

Table 4.3 presents the estimated carbon dioxide (CO_2) emissions and mitigation potential associated with the Single-Slope Passive Solar Still (SPSS) and the Modified Passive Solar Still (MPSS) over their projected operational lifespan of 25 years. Although MPSS is associated with marginally higher embodied CO_2 emissions due to its enhanced configuration, it demonstrates substantially greater CO_2 mitigation potential owing to its higher freshwater productivity and improved energy utilization.

Using the energy-based assessment approach, the total CO_2 mitigation achieved by SPSS is estimated at 12.54 tonnes. In contrast, MPSS attains a significantly higher mitigation value of 19.03 tonnes, corresponding to an improvement of approximately 51.75% compared to SPSS. Similarly, exergetic-based analysis indicates CO_2 mitigation values of 0.42 tonnes for SPSS and 0.63 tonnes for MPSS, reflecting an enhancement of about 50.00% for the modified system.

Table 4.3. Environmental parameters for SPSS and MPSS

Parameters	**SPSS**	**MPSS**
E_{emb} (kWh)	627.18	630.51
Annual E_{no} (kWh)	250.88	380.67
Annual E_{xo} (kWh)	8.46	12.64
CO_2emissions (tons) over life span	1.25	1.26
CO_2 Mitigation (E_n, CO_2)	12.54	19.03
CO_2 Mitigation(E_x,CO_2)	0.42	0.63
Net CO_2 Mitigation (Tonnes)	11.28	17.77
Net Earnings from Carbon Credit (US$)	361.26	568.72

The higher CO_2 mitigation capability of MPSS is primarily attributed to its superior energy and exergy outputs, which enable greater displacement of conventional fossil-fuel-based freshwater production. In addition, the total carbon credit earned by SPSS is estimated at USD 361.26, while the same earned by MPSS is USD 568.72.

Overall, the environmental assessment confirms that MPSS offers greater sustainability benefits than SPSS. The enhanced freshwater yield and better thermodynamic efficiency of MPSS result in greater long-term CO_2 mitigation, reinforcing the environmental advantages of the proposed modification for solar desalination applications.

4.10 Enviroeconomic parameters

Environmental and enviro-economic indicators for the Single-Slope Passive Solar Still (SPSS) and the Modified Passive Solar Still (MPSS) were evaluated using both energy- and exergy-based assessment approaches, as shown in Table 4.4. The enviroeconomic parameters for SPSS and MPSS based on the energy method were 401.41 and 609.08 US dollars, respectively. The comparable values of enviro-economic parameters using the exergetic technique were 13.54 and 20.23 US dollars for SPSS and MPSS, respectively. The maximum carbon credits earned were 609.08 for MPSS through energetic and exergetic techniques.

Table 4.4. Enviroeconomic parameters for SPSS and MPSS based on energy and exergy perspectives

Parameter	**SPSS**	**MPSS**
CO_2 Mitigation (Tonnes), $\emptyset en,CO_2$	12.54	19.03
CO_2 Mitigation (Tonnes), $\emptyset ex,CO_2$	0.42	0.63
ZCO_2,en (US$)	401.41	609.08
ZCO_2,ex (US$)	13.54	20.23

Among the two systems, MPSS achieves the highest carbon credit value of USD 609.08, as estimated using the energy-based approach, reflecting its enhanced freshwater productivity and improved thermodynamic efficiency. Overall, the enviro-economic analysis demonstrates that the proposed modifications to MPSS yield greater environmental benefits and higher economic returns through carbon credit mechanisms than conventional SPSS.

Chapter 5

CONCLUSION AND FUTURE SCOPE

5.1 Conclusions

This research experimentally investigated a modified passive slope solar still (MPSS) over simple passive solar still (SPSS) by incorporating the following two parameters:

- A black hanging wick attached to all vertical surfaces to increase the effective free water surface area for evaporation, and
- A helical copper cooling coil wrapped in a wet cloth, maintained near the dew-point temperature, to intensify condensation.

The MPSS was benchmarked against a simple passive solar still (SPSS) under identical climatic conditions. The major conclusions drawn from the integrated energy, exergy, economic, exergoeconomic, environmental, and psychrometric analyses are summarised as follows:

5.1.1 Significant enhancement in freshwater yield

The MPSS consistently outperformed the SPSS, achieving 41.10% higher annual productivity (1174 L vs. 832 L). The hanging wick increased the wetted evaporative area, while the cooled coil created an additional low-temperature condensation surface, jointly improving the evaporation–condensation cycle.

5.1.2 Improved thermal and exergy performance

The MPSS attained a peak thermal efficiency of 23.84%, significantly higher than that of SPSS at 13.89%. The maximum exergy efficiency achieved by the MPSS (2.98%) was higher than that obtained for the SPSS (2.23%)**,** reflecting a greater proportion of useful work potential captured from solar energy. This enhancement is attributed to faster moisture generation at the wick surface and stronger condensation potential created by dew-point–driven cooling.

5.1.3 Superior psychrometric behavior

The modified design maintained a greater temperature differential between the basin water, moist air, and condensing surfaces. Psychrometric observations showed:

- The inner glass surface temperature remained consistently below the dew-point temperature, ensuring continuous condensation, and
- Relative humidity and specific humidity showed inverse variation, validating moisture-saturation dynamics within the chamber.

These findings establish the critical role of moist-air properties in distillation behaviour.

5.1.4 Enhanced economic

Despite similar fabrication costs, the MPSS demonstrated far better economic performance due to higher annual water output.

Cost per liter of yield in MPSS is 17.44% lower than that in the SPSS (₹1.42 vs. ₹1.72).

5.1.5 Improved environmental and carbon-mitigation potential

Higher freshwater output directly translated into greater CO_2 avoidance. MPSS achieved: 19.03 tonnes CO_2 mitigation over its lifetime (51.75% higher than SPSS), and highest carbon-credit earnings (US$609.08 using the energy-based method). Thus, the MPSS design demonstrates superior sustainability benefits.

This confirms the suitability of wick-based systems as an economical and scalable solution.

Overall Outcome

Integration of a hanging wick and low-temperature copper coil has proven to be a highly effective, low-cost, and sustainable intervention for improving the performance of passive solar stills. The MPSS design significantly enhances the thermal, psychrometric, economic, and environmental attributes of desalination systems. It offers a robust solution for decentralized water purification, particularly in rural and water-scarce regions.

5.2 Future Scope

Future scope of this research includes further enhancing productivity through the integration of advanced wick materials, phase change materials (PCMs) for thermal energy storage, and nanofluid-based absorbers to extend operational hours. Incorporating hybrid configurations, such as solar collectors, photovoltaic-thermal (PVT) systems, or waste heat recovery, can further enhance system performance. Additionally, large-scale field deployment, long-term reliability studies, and socio-economic impact assessments are recommended to facilitate commercialization and policy adoption. Optimization using artificial intelligence and techno-economic modeling for different climatic zones can also support widespread implementation of this sustainable desalination technology. Based on the outcomes and limitations observed in the experimental and analytical phases, the following avenues are recommended for future research:

i. Advanced wick material and geometry optimization

Investigate alternative wick materials (composite fibers, nano-coated fabrics, layered wicks) with improved porosity, durability, and thermal response. Evaluate wick geometry (curved, stepped, or multi-layered surfaces) for maximized evaporation.

ii. Development of a detailed 5E numerical model

Create an integrated simulation framework encompassing Energy–Exergy–Economic–Exergoeconomic–Enviroeconomic (5E) assessment for predictive optimization and multi-parameter design analysis.

iii. Hybridization with renewable subsystems

Investigate coupling with solar PV, thermoelectric coolers, heat pumps, or flat-plate collectors to improve hybrid freshwater and energy co-generation.

iv. Scaling, commercialization, and lifecycle assessment

Evaluate large-scale designs (multi-basin MPSS, cascade systems, community-scale modules) and perform full LCA to support commercialization and policy adoption.

v. Psychrometric–AI based control models

Apply machine learning to predict evaporation-condensation behavior based on moist-air parameters (dew point, humidity ratio, glass temperature) for adaptive optimization.

REFERENCES

[1] M. Jobrane, A. Kopmeier, A. Kahn, H. M. Cauchie, A. Kharroubi, and C. Penny, "Internal and external improvements of wick type solar stills in different configurations for drinking water production– A review," *Groundw. Sustain. Dev.*, vol. 12, p. 100519, Feb. 2021, doi: 10.1016/j.gsd.2020.100519.

[2] "UNICEF, 'Press releases,' Unicef.org, 2016," 2016. [Online]. Available: https://www.unicef.org/sites/default/files/press-releases/glo-media-UNICEF_Early_Moments_Matter_for_Every_Child_report.pdf

[3] World Health Organisation, "Facts and Figures: Water, Sanitation and Hygiene Links to Health," no. March, p. 2, 2004, [Online]. Available: http://www.who.int/water_sanitation_health/publications/factsfigures04/en/

[4] A. E. Kabeel and S. A. El-Agouz, "Review of researches and developments on solar stills," *Desalination*, vol. 276, no. 1–3, pp. 1–12, 2011, doi: 10.1016/j.desal.2011.03.042.

[5] P. Burek *et al.*, "Water Futures and Solution," 2016. [Online]. Available: http://pure.iiasa.ac.at/id/eprint/13008/1/WP-16-006.pdf

[6] A. Tiwari and G. Tiwari, *Solar distillation practice for water desalination systems*. 2007.

[7] M. Freire-Gormaly and A. M. Bilton, "Design of photovoltaic powered reverse osmosis desalination systems considering membrane fouling caused by intermittent operation," *Renew. Energy*, vol. 135, pp. 108–121, 2019, doi:

10.1016/j.renene.2018.11.065.

[8] G. Tiwari and L. Sahota, *Advanced Solar-Distillation Systems: Basic Principles, Thermal Modeling, and Its Application*. 2017. doi: 10.1007/978-981-10-4672-8.

[9] P. Pandey, O. Prakash, and A. Kumar, *Solar Desalination Technology*. 2019. [Online]. Available: http://link.springer.com/10.1007/978-981-13-6887-5

[10] A. K. Singh, "An inclusive study on new conceptual designs of passive solar desalting systems," *Heliyon*, vol. 7, no. 2, 2021, doi: 10.1016/j.heliyon.2020.e05793.

[11] K. K. Murugavel, S. Sivakumar, J. R. Ahamed, K. K. S. K. Chockalingam, and K. Srithar, "Single basin double slope solar still with minimum basin depth and energy storing materials," *Appl. Energy*, vol. 87, no. 2, pp. 514–523, 2010, doi: 10.1016/j.apenergy.2009.07.023.

[12] T. Rajaseenivasan and K. Kalidasa Murugavel, "Theoretical and experimental investigation on double basin double slope solar still," *Desalination*, vol. 319, pp. 25–32, 2013, doi: 10.1016/j.desal.2013.03.029.

[13] T. Abderachid and K. Abdenacer, "Effect of orientation on the performance of a symmetric solar still with a double effect solar still (comparison study)," *Desalination*, vol. 329, pp. 68–77, 2013, doi: 10.1016/j.desal.2013.09.011.

[14] M. M. Belhadj, H. Bouguettaia, Y. Marif, and M. Zerrouki, "Numerical study of a double-slope solar still coupled with capillary film condenser in south

Algeria," *Energy Convers. Manag.*, vol. 94, pp. 245–252, 2015, doi: 10.1016/j.enconman.2015.01.069.

[15] A. K. Singh, "Mathematical analysis of optimized requisites for novel combination of solar distillers," *J. Eng. Res.*, vol. 11, no. 4, pp. 515–525, 2023, doi: 10.1016/j.jer.2023.100121.

[16] A. E. Kabeel, "Performance of solar still with a concave wick evaporation surface," *Energy*, vol. 34, no. 10, pp. 1504–1509, 2009, doi: 10.1016/j.energy.2009.06.050.

[17] R. Sathyamurthy, H. J. Kennady, P. K. Nagarajan, and A. Ahsan, "Factors affecting the performance of triangular pyramid solar still," *Desalination*, vol. 344, pp. 383–390, 2014, doi: 10.1016/j.desal.2014.04.005.

[18] A. K. Tiwari and G. N. Tiwari, "Effect of cover inclination and water depth on performance of a solar still for indian climatic conditions," *J. Sol. Energy Eng. Trans. ASME*, vol. 130, no. 2, pp. 0245021–0245024, 2008, doi: 10.1115/1.2844450.

[19] A. A. El-Sebaii, "Effect of wind speed on some designs of solar stills," *Energy Convers. Manag.*, vol. 41, no. 6, pp. 523–538, 2000, doi: 10.1016/S0196-8904(99)00119-3.

[20] A. A. El-Sebaii, "Effect of wind speed on active and passive solar stills," *Energy Convers. Manag.*, vol. 45, no. 7–8, pp. 1187–1204, 2004, doi: 10.1016/j.enconman.2003.09.036.

[21] A. A. El-Sebaii, “On effect of wind speed on passive solar still performance based on inner/outer surface temperatures of the glass cover,” *Energy*, vol. 36, no. 8, pp. 4943–4949, 2011, doi: 10.1016/j.energy.2011.05.038.

[22] R. Sathyamurthy, A. E. Kabeel, M. Balasubramanian, M. Devarajan, S. W. Sharshir, and A. M. Manokar, “Experimental study on enhancing the yield from stepped solar still coated using fumed silica nanoparticle in black paint,” *Mater. Lett.*, vol. 272, p. 127873, Aug. 2020, doi: 10.1016/j.matlet.2020.127873.

[23] N. K. Dhiman, “Transient analysis of a spherical solar still,” *Desalination*, vol. 69, no. 1, pp. 47–55, Jan. 1988, doi: 10.1016/0011-9164(88)80005-5.

[24] B. I. Ismail, “Design and performance of a transportable hemispherical solar still,” *Renew. Energy*, vol. 34, no. 1, pp. 145–150, 2009, doi: 10.1016/j.renene.2008.03.013.

[25] T. Arunkumar *et al.*, “An experimental study on a hemispherical solar still,” *Desalination*, vol. 286, pp. 342–348, 2012, doi: 10.1016/j.desal.2011.11.047.

[26] B. S. Kumar, S. Kumar, and R. Jayaprakash, “Performance analysis of a ‘V’ type solar still using a charcoal absorber and a boosting mirror,” *Desalination*, vol. 229, no. 1–3, pp. 217–230, 2008, doi: 10.1016/j.desal.2007.09.009.

[27] A. E. Kabeel *et al.*, “Effect of water depth on a novel absorber plate of pyramid solar still coated with TiO 2 nano black paint,” *J. Clean. Prod.*, vol. 213, pp. 185–191, 2019, doi: 10.1016/j.jclepro.2018.12.185.

[28] V. Dimri, B. Sarkar, U. Singh, and G. N. Tiwari, “Effect of condensing cover

material on yield of an active solar still: an experimental validation," *Desalination*, vol. 227, no. 1–3, pp. 178–189, Jul. 2008, doi: 10.1016/j.desal.2007.06.024.

[29] O. Prakash, B. Bhushan, A. Kumar, and A. Ahmed, "Thermal analysis of domestic type single Slope-Basin solar still under two different water depths," *Mater. Today Proc.*, vol. 46, pp. 5482–5489, 2020, doi: 10.1016/j.matpr.2020.09.239.

[30] S. Shoeibi *et al.*, "A review on evaporation improvement of solar still desalination using porous material," *Int. Commun. Heat Mass Transf.*, vol. 138, p. 106387, Nov. 2022, doi: 10.1016/j.icheatmasstransfer.2022.106387.

[31] S. Saravanavel, K. Vijayakumar, G. B. SathishKumar, M. Meignanamoorthy, and M. Ravichandran, "WITHDRAWN: Performance on single basin square pyramid solar still," *Mater. Today Proc.*, 2020, doi: 10.1016/j.matpr.2020.10.943.

[32] P. K. Srivastava and S. K. Agrawal, "Winter and summer performance of single sloped basin type solar still integrated with extended porous fins," *Desalination*, vol. 319, pp. 73–78, Jun. 2013, doi: 10.1016/j.desal.2013.03.030.

[33] V. Velmurugan and K. Srithar, "Performance analysis of solar stills based on various factors affecting the productivity - A review," *Renew. Sustain. Energy Rev.*, vol. 15, no. 2, pp. 1294–1304, 2011, doi: 10.1016/j.rser.2010.10.012.

[34] S. K. Suraparaju and S. K. Natarajan, "Experimental investigation of single-basin solar still using solid staggered fins inserted in paraffin wax PCM bed for

enhancing productivity," *Environ. Sci. Pollut. Res.*, vol. 28, no. 16, pp. 20330–20343, Apr. 2021, doi: 10.1007/s11356-020-11980-w.

[35] H. Panchal and I. Mohan, "Various methods applied to solar still for enhancement of distillate output," *Desalination*, vol. 415, pp. 76–89, Aug. 2017, doi: 10.1016/j.desal.2017.04.015.

[36] V. Velmurugan, M. Gopalakrishnan, R. Raghu, and K. Srithar, "Single basin solar still with fin for enhancing productivity," *Energy Convers. Manag.*, vol. 49, no. 10, pp. 2602–2608, 2008, doi: 10.1016/j.enconman.2008.05.010.

[37] S. K. Suraparaju and S. K. Natarajan, "Sustainability assessment of single slope solar still with glass cover cooling using naturally available fibers," *Environ. Prog. Sustain. Energy*, vol. 41, no. 4, 2022, doi: 10.1002/ep.13840.

[38] W. An, L. Chen, T. Liu, and Y. Qin, "Enhanced solar distillation by nanofluid-based spectral splitting PV/T technique: Preliminary experiment," *Sol. Energy*, vol. 176, pp. 146–156, 2018, doi: 10.1016/j.solener.2018.10.029.

[39] C. Suresh and S. Shanmugan, "Effect of water flow in a solar still using novel materials," *J. Therm. Anal. Calorim.*, vol. 150, no. 16, pp. 12199–12212, Aug. 2025, doi: 10.1007/s10973-019-08449-5.

[40] S. K. Suraparaju, R. Dhanusuraman, and S. K. Natarajan, "Performance evaluation of single slope solar still with novel pond fibres," *Process Saf. Environ. Prot.*, vol. 154, pp. 142–154, Oct. 2021, doi: 10.1016/j.psep.2021.08.011.

[41] S. K. Suraparaju and S. K. Natarajan, “Augmentation of freshwater productivity in single slope solar still using Luffa acutangula fibres,” *Water Sci. Technol.*, vol. 84, no. 10–11, pp. 2943–2957, Nov. 2021, doi: 10.2166/wst.2021.298.

[42] S. K. Suraparaju and S. K. Natarajan, “Performance analysis of single slope solar desalination setup with natural fiber,” *Desalin. Water Treat.*, vol. 193, pp. 64–71, Jul. 2020, doi: 10.5004/dwt.2020.25679.

[43] A. K. Kaviti, A. Yadav, and A. Shukla, “Inclined solar still designs: A review,” *Renew. Sustain. Energy Rev.*, vol. 54, pp. 429–451, Feb. 2016, doi: 10.1016/j.rser.2015.10.027.

[44] V. S. V. Bapeshwararao, U. Singh, and G. N. Tiwari, “Transient analysis of double basin solar still,” *Energy Convers. Manag.*, vol. 23, no. 2, pp. 83–90, Jan. 1983, doi: 10.1016/0196-8904(83)90065-1.

[45] G. N. Tiwari and G. A. Mohamed Selim, “Double slope fibre reinforced plastic (FRP) multiwick solar still,” *Sol. Wind Technol.*, vol. 1, no. 4, pp. 229–235, Jan. 1984, doi: 10.1016/0741-983X(84)90018-3.

[46] A. Kumar and J. D. Anand, “Modelling and performance of a tubular multiwick solar still,” *Energy*, vol. 17, no. 11, pp. 1067–1071, Nov. 1992, doi: 10.1016/0360-5442(92)90023-S.

[47] A. Ahsan, M. Imteaz, A. Rahman, B. Yusuf, and T. Fukuhara, “Design, fabrication and performance analysis of an improved solar still,” *Desalination*, vol. 292, pp. 105–112, Apr. 2012, doi: 10.1016/j.desal.2012.02.013.

[48] T. Arunkumar, R. Velraj, D. C. Denkenberger, R. Sathyamurthy, K. V. Kumar, and A. Ahsan, "Productivity enhancements of compound parabolic concentrator tubular solar stills," *Renew. Energy*, vol. 88, pp. 391–400, 2016, doi: 10.1016/j.renene.2015.11.051.

[49] T. Arunkumar and A. E. Kabeel, "Effect of phase change material on concentric circular tubular solar still-Integration meets enhancement," *Desalination*, vol. 414, pp. 46–50, Jul. 2017, doi: 10.1016/j.desal.2017.03.035.

[50] J. Hou, J. Yang, Z. Chang, H. Zheng, and Y. Su, "The mass transfer coefficient assessment and productivity enhancement of a vertical tubular solar brackish water still," *Appl. Therm. Eng.*, vol. 128, pp. 1446–1455, Jan. 2018, doi: 10.1016/j.applthermaleng.2017.09.129.

[51] A. K. Singh and G. N. Tiwari, "Performance study of double effect distillation in a multiwick solar still," *Energy Convers. Manag.*, vol. 33, no. 3, pp. 207–214, Mar. 1992, doi: 10.1016/0196-8904(92)90127-I.

[52] J. T. Mahdi, B. E. Smith, and A. O. Sharif, "An experimental wick-type solar still system: Design and construction," *Desalination*, vol. 267, no. 2–3, pp. 233–238, Feb. 2011, doi: 10.1016/j.desal.2010.09.032.

[53] P. Pal, P. Yadav, R. Dev, and D. Singh, "Performance analysis of modified basin type double slope multi–wick solar still," *Desalination*, vol. 422, pp. 68–82, Nov. 2017, doi: 10.1016/j.desal.2017.08.009.

[54] P. Pal and R. Dev, "Experimental Study on Modified Double Slope Solar Still and Modified Basin Type Double Slope Multiwick Solar Still," *Int. Sch. Sci.*

Res. Innov., vol. 10, no. 1, 2016, [Online]. Available: https://publications.waset.org/10003580/experimental-study-on-modified-double-slope-solar-still-and-modified-basin-type-double-slope-multiwick-solar-still

[55] P. Pal, R. Dev, D. Singh, and A. Ahsan, "Energy matrices, exergoeconomic and enviroeconomic analysis of modified multi–wick basin type double slope solar still," *Desalination*, vol. 447, pp. 55–73, Dec. 2018, doi: 10.1016/j.desal.2018.09.006.

[56] S. K. Suraparaju and S. K. Natarajan, "Combined enhancement of evaporation and condensation rates in the solar still for augmenting the freshwater productivity using energy storage and natural fibres," *J. Water Supply Res. Technol.*, vol. 71, no. 5, pp. 628–641, May 2022, doi: 10.2166/aqua.2022.017.

[57] G. Ni, S. H. Zandavi, S. M. Javid, S. V. Boriskina, T. A. Cooper, and G. Chen, "A salt-rejecting floating solar still for low-cost desalination," *Energy Environ. Sci.*, vol. 11, no. 6, pp. 1510–1519, 2018, doi: 10.1039/C8EE00220G.

[58] T. A. Cooper *et al.*, "Contactless steam generation and superheating under one sun illumination," *Nat. Commun.*, vol. 9, no. 1, p. 5086, Dec. 2018, doi: 10.1038/s41467-018-07494-2.

[59] V. Kashyap *et al.*, "Capture and conversion of carbon dioxide by solar heat localization," *Sustain. Energy Fuels*, vol. 3, no. 1, pp. 272–279, 2019, doi: 10.1039/C8SE00546J.

[60] A. K. Singh and S. Gautam, "Optimum techno-eco performance requisites for

vacuum annulus tube collector–assisted double-slope solar desaltification unit integrated modified parabolic concentrator," *Environ. Sci. Pollut. Res.*, vol. 29, no. 23, pp. 34379–34405, 2022, doi: 10.1007/s11356-021-18426-x.

[61] K. Fukuia, T. Nosoko, H. Tanaka, and T. Nagata, "A new maritime lifesaving multiple-effect solar still design," *Desalination*, vol. 160, no. 3, pp. 271–283, Jan. 2004, doi: 10.1016/S0011-9164(04)90029-X.

[62] B. Bouchekima, B. Gros, R. Ouahes, and M. Diboun, "Performance study of the capillary film solar distiller," *Desalination*, vol. 116, no. 2–3, pp. 185–192, Sep. 1998, doi: 10.1016/S0011-9164(98)00194-5.

[63] K. Ohshiro, T. Nosoko, and T. Nagata, "A compact solar still utilizing hydrophobic poly(tetrafluoroethylene) nets for separating neighboring wicks," *Desalination*, vol. 105, no. 3, pp. 207–217, Jul. 1996, doi: 10.1016/0011-9164(96)00078-1.

[64] S. Toyama, T. Aragaki, H. M. Salah, and K. Murase, "Dynamic characteristics of a multistage thermal diffusion type solar distillator," *Desalination*, vol. 67, pp. 21–32, Dec. 1987, doi: 10.1016/0011-9164(87)90228-1.

[65] R. Ouahes, C. Ouahes, P. Le Goff, and J. Le Goff, "A hardy, high-yield solar distiller of brackish water.," *Desalination*, vol. 67, pp. 43–52, Dec. 1987, doi: 10.1016/0011-9164(87)90230-X.

[66] M. M. Elsayed, "Parametric study of a direct solar-operated, multiple-effect, diffusion still," *Sol. Wind Technol.*, vol. 3, no. 2, pp. 95–101, Jan. 1986, doi: 10.1016/0741-983X(86)90020-2.

[67] S. Toyama, T. Aragaki, K. Murase, and K. Tsumura, “Simulation of a multieffect solar distillator,” *Desalination*, vol. 45, no. 2, pp. 101–108, Jan. 1983, doi: 10.1016/0011-9164(83)87013-1.

[68] H. Tanaka, “Experimental study of vertical multiple-effect diffusion solar still coupled with a flat plate reflector,” *Desalination*, vol. 249, no. 1, pp. 34–40, Nov. 2009, doi: 10.1016/j.desal.2008.10.022.

[69] T.-L. Chong, B.-J. Huang, P.-H. Wu, and Y.-C. Kao, “Multiple-effect diffusion solar still coupled with a vacuum-tube collector and heat pipe,” *Desalination*, vol. 347, pp. 66–76, Aug. 2014, doi: 10.1016/j.desal.2014.05.023.

[70] B.-J. Huang, T.-L. Chong, P.-H. Wu, H.-Y. Dai, and Y.-C. Kao, “Spiral multiple-effect diffusion solar still coupled with vacuum-tube collector and heat pipe,” *Desalination*, vol. 362, pp. 74–83, Apr. 2015, doi: 10.1016/j.desal.2015.02.011.

[71] H. Tanaka, “Theoretical analysis of a vertical multiple-effect diffusion solar still coupled with a tilted wick still,” *Desalination*, vol. 377, pp. 65–72, Jan. 2016, doi: 10.1016/j.desal.2015.09.013.

[72] H. Tanaka and K. Iishi, “Experimental study of a vertical single-effect diffusion solar still coupled with a tilted wick still,” *Desalination*, vol. 402, pp. 19–24, Jan. 2017, doi: 10.1016/j.desal.2016.09.031.

[73] H. Tanaka, “Parametric investigation of a vertical multiple-effect diffusion solar still coupled with a tilted wick still,” *Desalination*, vol. 408, pp. 119–126, Apr. 2017, doi: 10.1016/j.desal.2017.01.019.

[74] T. Rajaseenivasan, K. K. Murugavel, T. Elango, and R. S. Hansen, “A review of different methods to enhance the productivity of the multi-effect solar still,” *Renew. Sustain. Energy Rev.*, vol. 17, pp. 248–259, Jan. 2013, doi: 10.1016/j.rser.2012.09.035.

[75] A. K. Kaushal, M. K. Mittal, and D. Gangacharyulu, “An experimental study of floating wick basin type vertical multiple effect diffusion solar still with waste heat recovery,” *Desalination*, vol. 414, pp. 35–45, Jul. 2017, doi: 10.1016/j.desal.2017.03.033.

[76] A. K. Kaushal, M. K. Mittal, and D. Gangacharyulu, “Productivity correlation and economic analysis of floating wick basin type vertical multiple effect diffusion solar still with waste heat recovery,” *Desalination*, vol. 423, pp. 95–103, Dec. 2017, doi: 10.1016/j.desal.2017.09.016.

[77] S. B. Sadineni, R. Hurt, C. K. Halford, and R. F. Boehm, “Theory and experimental investigation of a weir-type inclined solar still,” *Energy*, vol. 33, no. 1, pp. 71–80, Jan. 2008, doi: 10.1016/j.energy.2007.08.003.

[78] F. F. Tabrizi, M. Dashtban, and H. Moghaddam, “Experimental investigation of a weir-type cascade solar still with built-in latent heat thermal energy storage system,” *Desalination*, vol. 260, no. 1–3, pp. 248–253, Sep. 2010, doi: 10.1016/j.desal.2010.03.033.

[79] H. Aghaei Zoori, F. Farshchi Tabrizi, F. Sarhaddi, and F. Heshmatnezhad, “Comparison between energy and exergy efficiencies in a weir type cascade solar still,” *Desalination*, vol. 325, pp. 113–121, Sep. 2013, doi:

10.1016/j.desal.2013.07.004.

[80] F. Sarhaddi, F. Farshchi Tabrizi, H. Aghaei Zoori, and S. A. H. S. Mousavi, "Comparative study of two weir type cascade solar stills with and without PCM storage using energy and exergy analysis," *Energy Convers. Manag.*, vol. 133, pp. 97–109, Feb. 2017, doi: 10.1016/j.enconman.2016.11.044.

[81] S. K. Natarajan, S. K. Suraparaju, R. M. Elavarasan, R. Pugazhendhi, and E. Hossain, "An experimental study on eco-friendly and cost-effective natural materials for productivity enhancement of single slope solar still," *Environ. Sci. Pollut. Res.*, vol. 29, no. 2, pp. 1917–1936, 2022, doi: 10.1007/s11356-021-15764-8.

[82] S. A. El-Agouz, "Experimental investigation of stepped solar still with continuous water circulation," *Energy Convers. Manag.*, vol. 86, pp. 186–193, Oct. 2014, doi: 10.1016/j.enconman.2014.05.021.

[83] A. E. Kabeel, A. Muthu Manokar, R. Sathyamurthy, D. Prince Winston, S. A. El-Agouz, and A. J. Chamkha, "A Review on Different Design Modifications Employed in Inclined Solar Still for Enhancing the Productivity," *J. Sol. Energy Eng.*, vol. 141, no. 3, Jun. 2019, doi: 10.1115/1.4041547.

[84] B. C. Nakra and K. K. Chaudhry, *Instrumentation, Measurement and Analysis*. Tata McGraw-Hill Education Pvt. Ltd., 2018.

[85] R. Kant and A. Kumar, "Thermodynamic analysis of solar assisted steam distillation system for peppermint oil extraction," *J. Food Process Eng.*, vol. 46, no. 2, Feb. 2023, doi: 10.1111/jfpe.14228.

[86] N. M. Shatar, M. F. M. Sabri, M. F. M. Salleh, and M. H. Ani, “Energy, exergy, economic, environmental analysis for solar still using partially coated condensing cover with thermoelectric cover cooling,” *J. Clean. Prod.*, vol. 387, p. 135833, Feb. 2023, doi: 10.1016/j.jclepro.2022.135833.

[87] A. A. El-Sebaii and M. El-Naggar, “Year round performance and cost analysis of a finned single basin solar still,” *Appl. Therm. Eng.*, vol. 110, pp. 787–794, Jan. 2017, doi: 10.1016/j.applthermaleng.2016.08.215.

[88] N. Abbasi, M. H. Khoshgoftar Manesh, and M. Yazdi, “Dynamic Analysis of a Novel Quadruple Combined Cycle Based on Integrated Solar Tower-Gas Turbine-Supercritical CO2 and Organic Rankine Cycles,” *J. Energy Resour. Technol.*, vol. 144, no. 5, May 2022, doi: 10.1115/1.4051743.

[89] S. Vijayan, T. V. Arjunan, and A. Kumar, “Exergo-environmental analysis of an indirect forced convection solar dryer for drying bitter gourd slices,” *Renew. Energy*, vol. 146, pp. 2210–2223, Feb. 2020, doi: 10.1016/j.renene.2019.08.066.

[90] R. Kant, A. Kumar, and M. K. Dubey, “Energetic, exergetic, exergoeconomic, and enviroeconomic analysis of solar dish-integrated water desalination system with various nanofluids,” *Groundw. Sustain. Dev.*, vol. 26, p. 101207, Aug. 2024, doi: 10.1016/j.gsd.2024.101207.

[91] A. Saxena, E. Cuce, A. E. Kabeel, M. Abdelgaied, and V. Goel, “A thermodynamic review on solar stills,” *Sol. Energy*, vol. 237, pp. 377–413, May 2022, doi: 10.1016/j.solener.2022.04.001.

[92] D. B. Singh, N. Kumar, S. Kumar, V. K. Dwivedi, J. K. Yadav, and G. N. Tiwari, “Enhancement in Exergoeconomic and Enviroeconomic Parameters for Single Slope Solar Still by Incorporating N Identical Partially Covered Photovoltaic Collectors,” *J. Sol. Energy Eng.*, vol. 140, no. 5, Oct. 2018, doi: 10.1115/1.4039632.

DELHI TECHNOLOGICAL UNIVERSITY

(Formerly Delhi College of Engineering)

Shahbad Daulatpur, Main Bawana Road, Delhi-42

PLAGIARISM VERIFICATION

Title of the Thesis: Impact of Free Water Surface on Single Slope Solar Still Yield

Total Pages: 131

Name of the Scholar: Maneesh Kumar Shivhare

Supervisor (s)

(1) Dr. Anil Kumar

(2) Dr. Samsher

Department of Mechanical Engineering

This is to report that the above thesis was scanned for similarity detection. Process and outcome is given below:

Software used: _____Similarity Index: _____, Total Word Count: _____

Date: _____

Candidate's Signature **Signature of Supervisor(s)**

Brief Bio-Data

Mr. Maneesh Kumar Shivhare

manishkrshivhare@gmail.com

Mailing/Permanent Address:

3rd Floor, BQ-108, Shalimar Bagh, New Delhi, INDIA

Contact No: **+91-9818346488**, +91-7303015135,

ACADEMIC QUALIFICATION

- Pursuing **Ph. D. (Thermal Engg.)** from **July 2018**, **Delhi Technological University**, Delhi 110042, INDIA.
- **M.Tech.** (CFD & HT), June **2011**, **NIT Hamirpur,** Hamirpur, Himachal Pradesh-177005, INDIA.
- **B.Tech. (Mech. Engg)**, June **2009**, **BBDNITM,** Lucknow, U.P.-226028, INDIA.
- 12th June 2003, U.P. Board, INDIA, with Physics, Chemistry, English and Hindi.
- 10th June 2001, U.P. Board, INDIA, with Science, Math, English, Drawing and Hindi.

Expertise in Professional Associations and Publications:

- Analysis and submission of Tender with technical & financial evaluation.
- Review & Preparation of Technical Due Diligence, Energy Yield Assessment (EYA), Plant performance and Detailed Project Report etc.
- EPC contracts, Tender documentation, BOQ preparation
- Identification, selection, and coordination of contractors for execution of the projects.
- Conduct technical lectures on technical discussion.

PUBLICATION

A. From Present Study

Indian Patent

1. Maneesh Kumar Shivhare, Samsher, and Anil Kumar, 2024, Solar Still Apparatus, Indian Patent Application No. 202411056840, Published by the Indian Patent Office, Government of India.

International Journal

1. Maneesh Kumar Shivhare, Samsher, and Anil Kumar, 2024, Impact of various design parameters on solar still systems performance: a review, AQUA—Water Infrastructure, Ecosystems and Society 73, no. 2: 239-265, **SCI-E,** Impact factor 2.3, https://doi.org/10.2166/aqua.2024.290.

2. Maneesh Kumar Shivhare, Anil Kumar, and Samsher, 2026, Productivity and sustainability enhancement in solar still using wick and copper cooling coil, Environmental Progress & Sustainable Energy: e70160, **SCI-E,** Impact factor 2.3, DOI:10.1002/ep.70160.
3. Maneesh Kumar Shivhare, Anil Kumar and Samsher, Performance Assessment of Single-Slope Solar Still Integrated with Hanging Cotton Wick, Thermal Science: International Scientific Journal, SCI Impact Factor 1.45. https://doi.org/10.2298/TSCI251113033S.

International Conference

1. Shivhare, Maneesh Kumar, Samsher, and Anil Kumar, 2024, Enhanced Single Slope Solar Still Using Novel Technology than Nanoparticles with More Economical and Efficient, In *Biennial International Conference on Future Learning Aspects of Mechanical Engineering*, pp. 115-124. Singapore: Springer Nature Singapore.
2. Shivhare, Maneesh Kumar, Samsher, and Anil Kumar, 2023, Performance of Solar Still with Effects of Psychometric Terms for Developed Moist Air, In International Conference on Mechanical and Energy Technologies, pp. 41-49. Singapore: Springer Nature Singapore.

B. Others Publication

Indian Patent

1. Shivhare, Maneesh Kumar, and Anil Kumar, 2026, Fruit & Vegetable Plucker Stick with Storage Bag, Indian Patent ID 446340-001, Published by the Indian Patent Office, Government of India.

International Journal

1. Ashok Kumar, Manessh Kumar Shivhare, N.S. Thakur, 2011, Optimization of Tilt Angle for Photovoltaic Array, International Journal of Engineering Science and Technology (IJEST), ISSN: 0975-5462 Vol. 3 No. 4.

International Conference

1. Muttumthala, N.L., Singh, A., Pillai, S.R., Yadav, A. and Shivhare, M.K., 2025. IoT and Computer Vision-based Real-time Solar PV Soiling Monitoring System. In *EPJ Web of Conferences* (Vol. 343, p. 04001). EDP Sciences.
2. Muttumthala, N.L., Yadav, A., Pillai, S.R. and Shivhare, M.K., 2025. Design and Simulation of Vertical-Axis Wind Turbine for Urban Environment. In *EPJ Web of Conferences* (Vol. 343, p. 04008). EDP Sciences.
3. Yadav, Apurv, Harsha Yadav, Vineet Kumar Vashishtha, and Maneesh Kumar Shivhare, 2021, Comparative Performance Evaluation of Si and Ge Solar Cell

Using PC1D Modelling, In *Recent Advances in Mechanical Engineering*, pp. 199-205. Springer, Singapore.

4. Yadav, Apurv, Manish Kumar Shivhare, Vineet Kumar Vashishtha, and Harsha Yadav, 2021, Nanofuels: An Advancement in Biodiesel Applications, In Recent Advances in Mechanical Engineering, pp. 509-514. Springer, Singapore.
5. Shivhare, Maneesh Kumar, Apurv Yadav, Swaroop Ramaswamy Pillai, Vineet Kumar Vashishtha, and Manish Kumar, 2020, Prediction of Anti-reflection Coating Thickness of a Solar Cell using Artificial Neural Network." In 2020 IEEE 15th International Conference on Industrial and Information Systems (ICIIS), pp. 28-33. IEEE.
6. Yadav, Apurv, and Maneesh Kumar Shivhare, 2020, Nanoparticle enhanced PCM for solar thermal energy storage, In 2020 Advances in Science and Engineering Technology International Conferences (ASET), pp. 1-3. IEEE.

National Conference

1. Sunil Verma, Vineet Kumar Vashishtha, Maneesh Kumar Shivhare, 2012, Study of Autoignition delay period on variation of equivalence ratio for PRF (i-octane) and n-pentane, Proceedings of the International Conference on Innovative Technologies in Mechanical Engineering held at KIET, Ghaziabad, 24-25.

FDP/Seminar/workshop

1. E-Workshop: on “Modelling and Simulation in Thermal Engineering” at National Institude of Technology, Hamirpur, H.P. during Oct 30 to Nov 03, 2020.
2. Webinar: On “Rethinking Innovation in Product Development” organised by AKGEC-SIEMENS, on 23rd May, 2020, AKGEC Skills Foundation, Ghaziabad.
3. Webinar: On “Future of Welding Journey Towards Industry 4.0” organised by AKGEC-FRONIUS, on 16th May, 2020, AKGEC Skills Foundation, Ghaziabad.
4. Faculty Development Programme: On "Advances in Surface Engineering", Mechanical Engineering Dept, DTU, Delhi, 01-05 May, 2018.
5. Short Term Course: On "Indoor Air Quality of Buildings: Theory and Simulations" at National Institute of Technology Hamirpur, H.P., June 27 to July 01, 2016

Place: Delhi, INDIA
Date: 09/04/2026 **(Maneessh Kumar Shivhare)**

Google Scholar ID: https://shorturl.at/bVBdg
Orcid ID**:** 0009-0006-6860-0987
Research Gate: https://www.researchgate.net/profile/Maneesh-Shivhare